PHOSPHOLIPID REQUIREMENTS FOR MITOCHONDRIAL RESPIRATORY CHAIN FUNCTION

A Dissertation

by

CHARLI D. BAKER

Submitted to the Office of Graduate and Professional Studies of
Texas A&M University
in partial fulfillment of the requirements for the degree of

DOCTOR OF PHILOSOPHY

Chair of Committee,	Vishal M. Gohil
Committee Members,	Robert S. Chapkin
	Craig D. Kaplan
	Paul A. Lindahl
Head of Department,	Gregory D. Reinhart

May 2017

Major Subject: Biochemistry

ABSTRACT

The mitochondrial respiratory chain (MRC) consists of four large protein complexes that catalyze redox reactions driving cellular energy production. These complexes assemble into supra-molecular structures called supercomplexes in the mitochondrial inner membrane. Mitochondrial membrane phospholipid composition is unique and highly conserved, with the bilayer-forming phosphatidylcholine (PC) and non-bilayer forming phosphatidylethanolamine (PE) and cardiolipin (CL) being the most abundant phospholipids. Previous studies highlighted the critical role of CL in MRC supercomplex formation, however, the roles of PE and PC, remained poorly understood. To address this gap in our knowledge, I utilized the yeast *Saccharomyces cerevisiae* as a model organism to dissect the role of PE and PC in MRC biogenesis.

By performing biochemical analysis of yeast mutants of PC, PE and CL biosynthesis, I discovered a specific requirement for non-bilayer forming phospholipids in MRC biogenesis. Specifically, I showed that PE is required for MRC complex III and IV activities, whereas the loss of the most abundant phospholipid PC does not affect MRC function. Unlike CL, neither PE nor PC is required for MRC supercomplex formation. Furthermore, I found that the loss of mitochondrial PE biosynthesis could be compensated by exogenous supplementation of ethanolamine, a PE precursor, suggesting the existence of a mitochondrial PE import pathway.

The non-bilayer phospholipids PE and CL have been proposed to have overlapping functions, raising an intriguing possibility that elevating mitochondrial PE may compensate for CL deficiency. To test this hypothesis, I utilized an ethanolamine

supplementation strategy and demonstrated that ethanolamine rescues the respiratory growth of CL deficient cells by promoting MRC supercomplexes. Surprisingly, the rescue was independent of PE biosynthesis and was solely dependent on ethanolamine. This exciting finding has important biomedical implications in the treatment of Barth syndrome, a rare genetic disorder characterized by CL deficiency.

Finally, I describe how the inhibition of non-mitochondrial PE biosynthesis by meclizine, an over-the-counter anti-nausea drug, attenuates respiration by elevating phosphoethanolamine, a PE precursor. Together, the research presented in this dissertation uncovers the specific roles of phospholipids in MRC biogenesis and describes novel approaches for manipulating MRC function that can be utilized for the treatment of mitochondrial disorders.

ACKNOWLEDGEMENTS

I would like to thank my advisor, Dr. Gohil, for all of his constant guidance, care, and support throughout the course of this research. Also, I would like to thank my committee members, Dr. Chapkin, Dr. Kaplan, and Dr. Lindahl, for their advice and direction regarding my project. I would also like to thank Dr. Writoban Basu Ball for his experimental guidance and for our daily scientific discussions regarding mitochondrial phospholipid biology. Thanks also go to Dr. Prachi Trivedi for her constant support in and out of the lab. In addition, thanks to all the members of the Gohil lab for their helpful discussions and suggestions. Finally, I want to thank to my husband and my girls for their unwavering understanding, patience, encouragement, and love throughout this process.

CONTRIBUTORS AND FUNDING SOURCES

This work was supported by a dissertation committee consisting of my advisor Dr. Vishal M. Gohil of the Department of Biochemistry and Biophysics, Dr. Craig D. Kaplan of the Department of Biochemistry and Biophysics, Dr. Paul A. Lindahl of the Department of Biochemistry and Biophysics as well as the Department of Chemistry, and Robert S. Chapkin of the Departments of Nutrition and Food Science, Biochemistry and Biophysics, Veterinary Medicine and Biomedical Sciences, and Microbial and Molecular Pathogenesis at Texas A&M Health Science Center. The head of the Biochemistry and Biophysics department, Dr. Gregory D. Reinhart, also supported this work.

Chapter II is a reprint of a publication for which I am the first author. I performed all the experimental work described in this chapter except for the transmission electron micrographs (Fig. 2.3) which were performed by Erin N. Pryce at Integrated Imaging Center, Department of Biology, Johns Hopkins University, and the respiration measurements (Fig. 2.5C and D), performed by Dr. Writoban Basu Ball of the Department of Biochemistry and Biophysics at Texas A&M University. I also greatly appreciate Dr. Writoban Basu Ball's help in performing mitochondrial isolation and phospholipid measurements (Fig. 2.2). We thank Dr. Miriam L. Greenberg (Wayne State University) for yeast strains as well as Dr. Sharon Ackerman (Wayne State University), Dr. Dennis Winge (University of Utah), and Dr. Vincenzo Zara (Università del Salento) for their generous gift of antibodies. We are also thankful to Dr. Craig Kaplan, Dr. Steve Lockless, Dr. Jean-Philippe Pellois, and the members of the Gohil lab for valuable

discussions and comments. We also thank Mary Casillas and Shrishiv Timbalia for artwork and John Neff for technical help. The research reported in this chapter was supported by the Welch Foundation grant [A-1810] and the National Institutes of Health award [R01GM111672] to Vishal M. Gohil. The content is solely the responsibility of the authors and does not necessarily represent the official views of the National Institute of Health.

The manuscript describing the work in Chapter III is in preparation for submission to the journal *Molecular Biology of the Cell*. I am co-first author, and I did all the experiments described in this chapter except for the ones reported in Fig. 3.2, 3.3, 3.5, 3.6, 3.8, 3.14, and 3.15, which were performed by Dr. Writoban Basu Ball, John K. Neff, and Gabriel L. Apfel of the Department of Biochemistry and Biophysics at Texas A&M University. We thank Miriam L. Greenberg (Wayne State University) for yeast strains and Dennis Winge (University of Utah), and Vincenzo Zara (Università del Salento) for their generous gift of antibodies. We also thank members of the Gohil lab, including Ashley Adams and Donna Iadarola, for their valuable comments in the preparation of this manuscript. This work was supported by the Welch Foundation Grant (A-1810), the American Heart Association Award (16GRNT31020028), and the National Institutes of Health award (R01GM111672) to Vishal M. Gohil. The content is solely the responsibility of the authors and does not necessarily represent the official views of the National Institutes of Health.

The work described in Chapter IV comprises a reprint of a publication to which I contributed as a third author. The authors include Vishal M. Gohil (Center for Human

Genetic Research, Massachusetts General Hospital, Boston; Broad Institute; Harvard Medical School; Texas A&M University), Lin Zhu (University of Guelph), Charli D. Baker (Texas A&M University), Valentin Cracan (Center for Human Genetic Research, Massachusetts General Hospital; Broad Institute; Harvard Medical School), Abbas Yaseen (Center for Human Genetic Research, Massachusetts General Hospital), Mohit Jain (Center for Human Genetic Research, Massachusetts General Hospital; Broad Institute; Harvard Medical School), Clary B. Clish (Broad Institute), Paul S. Brookes (University of Rochester Medical Center), Marica Bakovic (University of Guelph), Vamsi K. Mootha (Center for Human Genetic Research, Massachusetts General Hospital; Broad Institute; Harvard Medical School). I contributed to the following figures in this publication: Fig. 4.1D, Fig. 4.4E, Fig. 4.6, and Fig. 4.7. We thank Michelle Yu for assistance with measurements of bioenergetics. We thank Eric Shoubridge and Marcy MacDonald for providing MCH58 and mouse striatal cell lines, respectively. This work was supported by a grant from the American Diabetes Association/Smith Family Foundation to Vamsi K. Mootha. Charli D. Baker and Vishal M. Gohil were supported by the Welch Foundation Grant (A-1810) and discretionary funds from Texas A&M University. Mohit Jain was supported by NIH 5K08HL107451. Lin Zhu and Marica Bakovic were supported by grants from the Canadian Institutes of Health Research and Ontario President Research Excellence Award that was awarded to Marica Bakovic.

NOMENCLATURE

MRC	Mitochondrial Respiratory Chain
ATP	Adenosine Triphosphate
ADP	Adenosine Diphosphate
PE	Phosphatidylethanolamine
CL	Cardiolipin
PC	Phosphatidylcholine
PI	Phosphatidylinositol
PS	Phosphatidylserine
PA	Phosphatidic Acid
PG	Phosphatidylglycerol
PP	Phosphatidylpropanolamine
PDME	Phosphatidyldimethylethanolamine
PMME	Phosphatidylmonomethylethanolamine
MLCL	Monolysocardiolipin
Etn	Ethanolamine
PEtn	Phosphoethanolamine
Cho	Choline
PCho	Phosphocholine
Prn	Propanolamine
BTHS	Barth Syndrome

TABLE OF CONTENTS

Page

LIST OF FIGURES

Page

LIST OF TABLES

Page

CHAPTER I

INTRODUCTION AND LITERATURE REVIEW

Mitochondria are ancient organelles that are a defining feature of the eukaryotic cell, performing many important cellular functions including energy production. The mitochondria are double membrane bound structures consisting of a highly permeable outer membrane and an ion impermeable inner membrane. The inner membrane is characterized by the presence of distinctive folds called cristae; customized structures that house and influence the function of the mitochondrial respiratory chain (MRC) (Cogliati et al., 2013). The MRC consists of four protein complexes that perform essential redox reactions by transferring electrons from nutrients to molecular oxygen and, in the process, generates the electrochemical gradient that drives ATP synthesis. While mitochondrial bioenergetics has been studied for decades, the role of the native membrane environment in MRC function and formation has not been investigated in a systematic manner (Schug et al., 2012).

Mitochondrial Energy Production

The MRC is composed of four multimeric protein complexes that are assembled within the inner mitochondrial membrane (Fig. 1.1). In humans complex I, or nicotinamide adenine dinucleotide (NADH) dehydrogenase, is composed of 46 protein subunits (Scarpulla, 2008), whereas in yeast three single polypeptide enzymes replace this massive protein complex (Fig. 1.1) (Joseph-Horne et al., 2001). However, across evolution, the function of NADH dehydrogenase remains the same, to transfer electrons

from NADH to ubiquinone, or Coenzyme Q, reducing this two-electron carrier to ubiquinol. Complex II consists of four subunits in both yeast and humans and, like complex I, also donates electrons to ubiquinone, but does so through the oxidation of succinate. Ubiquinol diffuses readily through the membrane and delivers electrons to complex III. The function of complex III, or cytochrome *c* reductase, is to accept electrons from ubiquinol and reduce cytochrome *c*, a single electron carrier. Cytochrome *c* delivers electrons to complex IV, where they are ultimately accepted by molecular oxygen reducing it to water. Together the activities of MRC complexes I-IV result in oxygen consumption, or respiration, a parameter that is measured to assess MRC function.

The activity of the MRC results in the translocation of protons across the inner mitochondrial membrane, which generates an electrochemical gradient that drives the activity of complex V, or ATP synthase. In higher eukaryotes, the redox reactions performed by complexes I, III, and IV result in the pumping of protons into the mitochondrial intermembrane space - whereas, in yeast, only complexes III and IV pump protons (Fig. 1.1). Complex V is able to harness the energy from the difference in membrane potential to synthesize ATP by transporting protons from the intermembrane space back into the mitochondrial matrix. Thus, ATP synthase couples respiration to energy production by harnessing the electrochemical gradient. Any disruption in MRC biogenesis results in reduced respiration, decreased membrane potential, and diminished ATP production, parameters that are often measured to assess MRC function. Perturbation in MRC function occasionally results in electron leakage and is frequently

associated with elevated reactive oxygen species and increased oxidative stress (Willems et al., 2015).

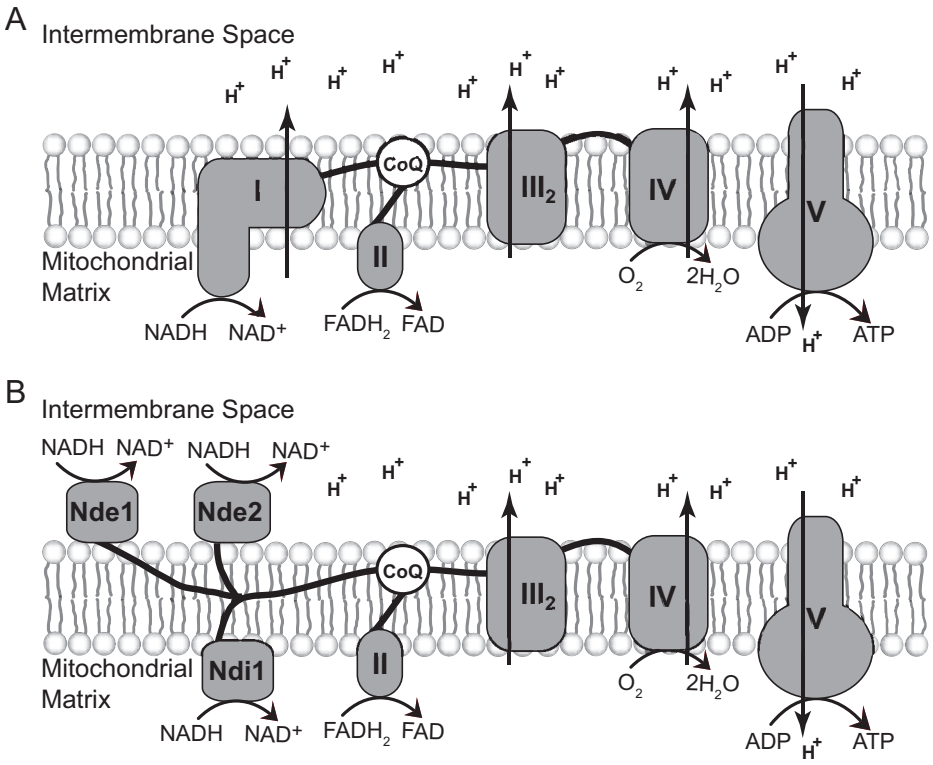

Figure 1.1 Mitochondrial respiratory chain is the main site of cellular respiration and ATP production.

(A) Depiction of mammalian and (B) yeast mitochondrial respiratory chain complexes embedded in the inner mitochondrial membrane.

Within the mitochondrial inner membrane, MRC complexes interact in different stoichiometries and assemble into supra-molecular structures known as supercomplexes (Dudkina et al., 2011; Schagger and Pfeiffer, 2000). Schagger and colleagues first described supercomplexes through their employment of blue native polyacrylamide gel electrophoresis (Schagger and Pfeiffer, 2000). Although initially the presence of supercomplexes *in vivo* was controversial, later studies demonstrated their existence in a variety of organisms across evolution (Table 1.1). Recently, cryo-electron microscopy

was utilized to determine the structures of supercomplexes, thus, unequivocally proving their existence (Althoff et al., 2011; Dudkina et al., 2011; Wu et al., 2016; Letts et al., 2016).

Table 1.1 Identified respiratory supercomplexes by EM (O) and BN-page (X)
(Data obtained from personal communication with Dudkina and Dudkina et al., 2006)

		$I+III_2$	III_2+IV_{1-2}	$I+III_2+IV_{1-4}$	V_2
Plants	Arabidopsis	O, X	-	-	O
	Barley	X	-	-	-
	Bean	X	-	-	-
	Potato	O, X	O, X	O, X	O, X
	Spinach	X	X	X	X
	Tobacco	X	-	-	-
	Pea	X	-	-	-
	Sunflower	-	X	-	-
	Maize	O	-	-	O
	Asparagus	X	-	-	X
Algae	Chlamydomonas	-	-	-	X
	Polytomella	O, X	-	-	O, X
Fungi	S. cerevisiae	-	O, X	-	O, X
	Yarrowia lipolytica	X	X	X	X
	Podospora anserina	X	-	X	X
Protists	Tetrahymena	O	-	-	O
Animals	Bovine	O, X	X	O, X	O, X
	Homo sapiens	X	-	X	-

While the existence of supercomplexes is now well established, their function is not as well defined (Blaza et al., 2014; Genova and Lenaz, 2014). The prevailing view is that supercomplex formation offers a kinetic advantage by increasing the efficiency of electron transfer through spatial restriction of electron carrier diffusion, a process known as substrate channeling (Acin-Perez et al., 2008). The structure of the Bovine $I_1III_2IV_1$ supercomplex revealed potential pathways that could be used to channel electrons between these three complexes, providing evidence that supports substrate channeling

(Althoff et al., 2011). However, a similar study by Dudkina et al. doubted whether a 13 nm gap between the Coenzyme Q binding sites of complex I and complex III would support substrate channeling (2011). Furthermore, additional work concluded that supercomplexes do not have a dedicated Q pool and do not trap cytochrome *c*, suggesting supercomplexes do not play a substantial kinetic role in catalysis (Blaza et al., 2014; Trouillard et al., 2011). Alternatively, Blaza et al. proposed that supercomplexes form out of spatial necessity, as the inner mitochondrial membrane has to maintain an extremely high protein concentration while avoiding nucleation and aggregation (2014). Although the functional significance of supercomplex formation is still murky, it is well established that the disruption in the function of MRC supercomplexes perturbs mitochondrial bioenergetics, and that the loss of supercomplex formation is associated with a rare genetic disorder called Barth syndrome (McKenzie et al., 2006). Notably, perturbations in MRC function have been associated with many common disorders including diabetes (Szendroedi et al., 2012), cancer (Hanahan and Weinberg, 2011; Wallace, 2012), neurodegenerative disorders (Nunnari and Suomalainen, 2012), cardiovascular diseases (Huss and Kelly, 2005) as well as rare inborn errors of metabolism (Vafai and Mootha, 2012; Koopman et al., 2012).

Interestingly, significant amounts of phospholipids were found bound to purified supercomplexes (Althoff et al., 2011), suggesting that phospholipids play a vital role in supercomplex biogenesis. The specific phospholipid requirement for MRC supercomplex formation is discussed further in Chapter II of this dissertation.

Supercomplex formation has also been suggested to play a role in reducing oxidative stress, a relationship that has been examined in a variety of model systems (Maranzana et al., 2013; Lenaz et al., 2010; Baracca et al., 2010; Strogolova et al., 2012; Chen et al., 2008). These studies support a link between supercomplex disassociation and enhanced reactive oxygen species (ROS) production. Specifically, Maranzana et al. suggested that ROS produced by complex I is reduced when this complex is incorporated into supercomplexes (2013). However, a recent review notes that many functional studies investigating the relationship between supercomplex formation and ROS generation fail to distinguish causality (Genova and Lenaz, 2014). A better understanding of the requirement for supercomplex formation in mediating oxidative stress will shed light on the molecular basis underlying the mitochondrial pathogenesis associated with the loss of supercomplex formation (Schlame, 2013)

MRC Function and Mitochondrial Membrane Phospholipid Composition

The lipid matrix of biological membranes determines generic physical properties, such as membrane surface charge, thickness, fluidity, and curvature (de Kroon et al., 2013). Each membrane is a complex assembly of different lipid molecules, with a lipid composition tailored to the function of the particular membrane (de Kroon et al., 2013). Mitochondrial membranes consist predominantly of phospholipids, which make up 75-95% of total mitochondrial membrane lipids in yeast and higher eukaryotes (Horvath and Daum, 2013). Mitochondrial membranes mainly comprise three types of phospholipids, including phosphatidylcholine (PC), phosphatidylethanolamine (PE), and cardiolipin (CL), along with the less abundant phosphatidylinositol (PI),

phosphatidylserine (PS), and phosphatidic acid (PA). These phospholipids can be further categorized, based on their overall shape, as bilayer or non-bilayer forming phospholipids. According to the shape-structure concept of lipid polymorphism, bilayer-forming phospholipids, like PC, are cylindrical in shape and can self assemble into a phase similar to a biological membrane (Fig. 1.2). Whereas, non-bilayer phospholipids, like PE and CL, are cone-shaped and promote membrane curvature when introduced into biological membranes (Fig 1.2) (Holthuis and Menon, 2014). As our understanding of membrane biology deepens, it is becoming clear that these phospholipids are more than just membrane building blocks. Non-bilayer forming phospholipids have been shown to influence the function of both peripheral (Li et al., 2003; Attard et al., 2000) and integral (van der Does et al., 2000; Botelho et al., 2002; Schwarz et al., 1997) membrane proteins. The non-bilayer phospholipids may mediate their effects through direct protein-lipid interaction or by alterations in bulk properties, such as membrane surface charge, thickness, fluidity, and curvature (van Meer et al., 2008).

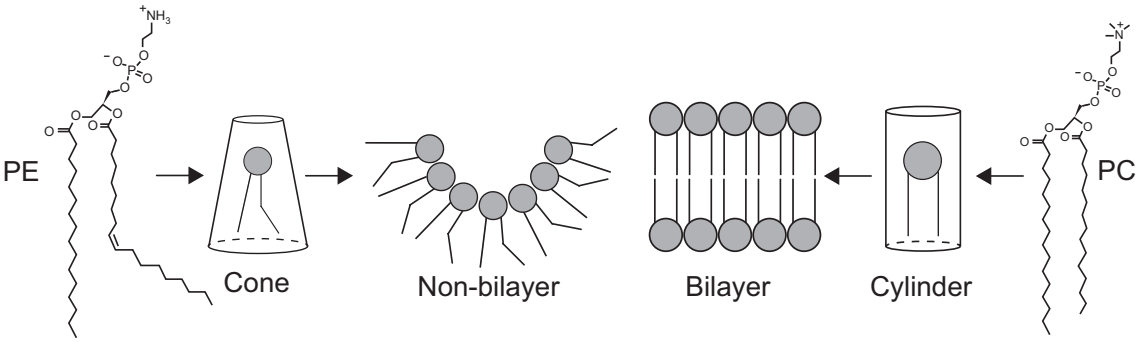

Figure 1.2 The shape-structure concept of phospholipid polymorphism.
PE is cone-shaped non-bilayer forming phospholipid that promotes membrane curvature, whereas PC is cylindrical in shape that forms membrane bilayers.

The biological significance of bilayer and non-bilayer forming phospholipids was eluded to by early studies showing that their ratio is tightly regulated (Morein et al., 1996), and that they are essential for cell viability (Rietveld et al., 1993). As far as mitochondrial phospholipid composition is concerned, the ratio of non-bilayer to bilayer forming phospholipids is highly conserved (Fig 1.3A) (Daum, 1985), suggesting their importance in mitochondrial membrane structure and function. When compared to other cellular membranes, the curved inner mitochondrial membrane is enriched in non-bilayer forming phospholipids (Fig. 1.3B) (Zinser et al., 1991), suggesting these cone-shaped phospholipids play an important role in the function of the proteins embedded in this membrane. Together, PC, PE and CL comprise 80-90% of total mitochondrial phospholipids in yeast and humans, respectively (Horvath and Daum, 2013). However, the specific contribution of these phospholipids versus their contribution to bulk membrane properties in MRC function and formation is not well defined. Determining how alterations in the non-bilayer to bilayer ratio affect MRC function and formation as well as the ability of similarly shaped phospholipids to compensate for one another will further our understanding of the relationship between the MRC and its phospholipid membrane environment.

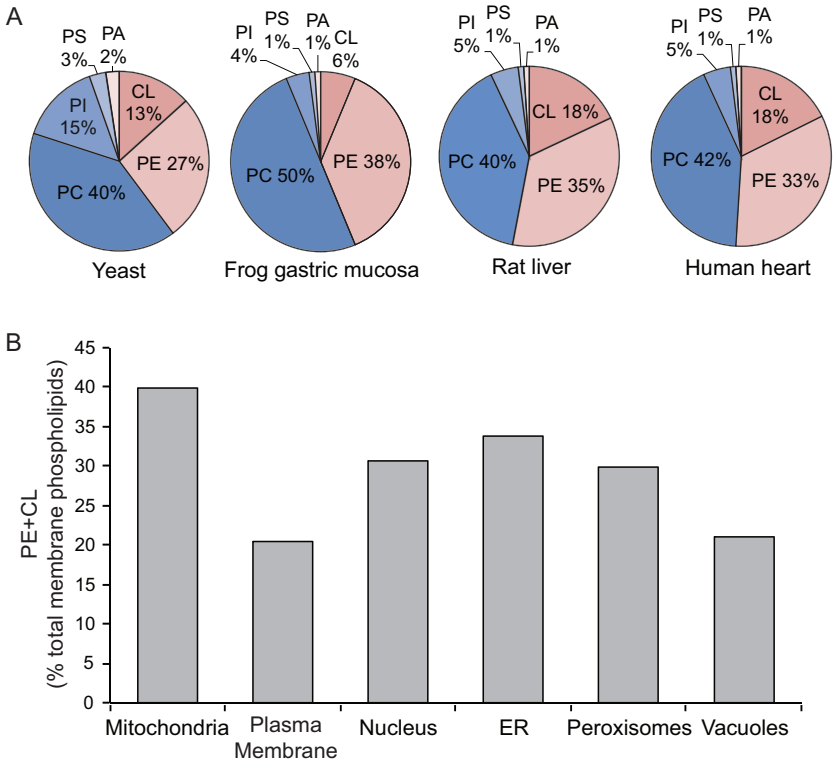

Figure 1.3 Mitochondrial membrane phospholipid composition is highly conserved.
(A) Pie charts depicting the distribution of mitochondrial membrane phospholipids in eukaryotes (Data from Daum, 1985). (B) Proportion of non-bilayer forming phospholipids in different organellar membrane fractions (Data from Zinser et al., 1992).

Phospholipid Synthesis

Phospholipid biosynthetic pathways are well conserved from yeast to humans, and these pathways are compartmentalized into various subcellular organelles, including the endoplasmic reticulum (ER), endosome, and mitochondria. Only the non-bilayer phospholipids PE and CL are synthesized within the mitochondria, suggesting these phospholipids are important for mitochondrial function (Gohil and Greenberg, 2009). CL is exclusively synthesized in the mitochondria from its precursor PA, which must be imported from the ER. Once imported, PA is converted to phosphatidylglycerol (PG) by

the sequential action of the mitochondrial Pgs1 and Gep4 enzymes. A diacylglycerol moiety is further added to PG via cytidinediphospho-diacylglycerol (CDP-DAG) by CL synthase, or Crd1, to form premature CL. The acyl chain composition of newly formed CL species is remodeled by the sequential action of a cardiolipin-specific deacylase, Cld1, and a transacylase, Taz1, to generate mature CL. Unlike CL, which is exclusively synthesized within the mitochondria, PE can be synthesized both inside and outside of the mitochondria. Within the mitochondrial inner membrane, PE is synthesized by decarboxylation of PS via phosphatidylserine decarboxylase, or Psd1. Psd1 accounts for 80% of PS decarbolxylase activity in yeast and is the primary source of cellular PE. A second PS decarboxylase, Psd2, is a yeast specific enzyme that is localized to an endosomal compartment (Gulshan et al., 2010). PE synthesized by Psd2 is mainly used as a substrate for PC (Bürgermeister et al. 2004a). The de novo biosynthesis of PC proceeds through three sequential methylations of PE catalyzed by two ER-localized phosphatidylethanolamine methyltransferases, Pem1 and Pem2. In addition to the de novo biosynthetic pathways, PE and PC can be synthesized from their precursors ethanolamine (Etn) or choline (Cho), respectively, through the non-mitochondrial Kennedy pathway (Kennedy and Weiss, 1956). The Kennedy pathway consists of three enzymatic steps. First Etn or Cho is phosphorylated by ethanolamine kinase (Eki1) or choline kinase (Cki1), respectively. The second step is considered the rate-limiting step of this pathway and is catalyzed by ethanolamine-phosphate cytidylyltransferase (Ect1) or phosphocholine cytidylyltransferase (Pct1). These enzymes utilize phosphoethanolamine or phosphocholine and cytidine-5-triphosphate (CTP) to form the

high-energy intermediate CDP-ethanolamine or CDP-choline, respectively. Finally, ethanolamine phosphotransferase (Ept1) and choline phosphotransferase (Cpt1) form PE and PC, respectively, by incorporation of the lipid anchor diacylglycerol (DAG). Interestingly, the Kennedy pathway and de novo synthesis produce unique phospholipid species defined by the composition of their acyl chains (Bleijerveld et al., 2007; Boumann et al., 2003). However, the significance of this phenomenon in not well understood. The contribution of these pathways to cellular phospholipid composition differs among organisms and is influenced by growth conditions. In yeast, the Etn-Kennedy pathway is only essential in the absence of the PS decarboxylase enzymes, and its activity can be regulated by the composition of the growth media (Birner et al., 2001). Disruption of the Kennedy pathway in mammals is embryonic lethal or results in severe deformities (Vance and Vance, 2009), and the contribution of the Kennedy pathway to cellular PE content is tissue specific (Gibellini and Smith, 2010). Because disruptions in phospholipid homeostasis are associated with several human diseases (Lu and Claypool 2015), understanding the relative contribution of the phospholipid biosynthetic pathways will play a crucial role in understanding the mechanism of disease pathogenesis as well as in devising potential therapeutic approaches for these newly emerging disorders for which no therapies currently exists.

Phospholipid Transport

As discussed in the previous section, phospholipid biosynthesis is compartmentalized in different subcellular organelles from where they are transported to other subcellular membranes. Our current understanding of phospholipid transport is

limited, especially when compared to protein transport (Tamura et al., 2014; Scharwey et al., 2013). However, recent studies have begun to provide intriguing insights into phospholipid exchange between the ER and mitochondria as well as between the mitochondrial outer and inner membranes (Kornmann et al., 2009; Elbaz-Alon et al., 2014; Aaltonen et al., 2016; Connerth et al., 2012). These studies have proposed two distinct mechanisms of phospholipid transport. One model is based on the close apposition of donor and recipient membranes and the other involves a phospholipid-binding transport protein. One of the major unanswered questions in mitochondrial membrane biogenesis is how the phospholipid substrates PS and PA are transported to mitochondria. Most of the mitochondrial PE requirement is met by PE synthesized within, therefore whether non-mitochondrial PE, synthesized by Psd2 or by the Kennedy pathway, can be imported into mitochondria remains controversial (Bürgermeister et al., 2004a; Chan and McQuibban, 2012; Wang et al., 2014). Results from Bürgermeister et al. are consistent with equilibrium transport of PE and PC between mitochondrial and microsomal membranes (Bürgermeister et al., 2004a; Bürgermeister et al., 2004b). However, subsequent studies showed that PE synthesized by the Kennedy pathway is not able to restore mitochondrial respiration (Chan and McQuibban, 2012; Wang et al., 2014) implying that either PE transport from ER to mitochondria is insufficient to functionally compensate for a lack of mitochondrial PE biosynthesis or that the non-mitochondrial PE species cannot substitute for mitochondrial PE species. By elucidating the mechanisms underlying phospholipid transport we can design approaches to

manipulate mitochondrial membrane composition to control mitochondrial function. Mitochondrial PE import is further described in Chapter II of this dissertation.

Cardiolipin

CL is a unique dimeric phospholipid that is almost exclusively located in membranes that house energy-transducing machinery, including the bacterial plasma membrane and the mitochondrial inner membrane. Therefore, its role in MRC function and formation has been examined more extensively than other more abundant mitochondrial phospholipids, like PE and PC. Within the inner mitochondrial membrane, CL is required for the optimal activities of complex I (Fry and Green, 1981; Paradies et al., 2002; Drose et al., 2002), complex III (Fry and Green, 1981; Gomez Jr and Robinson, 1999; Lange et al., 2001), complex IV (Robinson, 1993), and complex V (Eble et al., 1990). Furthermore, the crystal structures of complex III (Lange et al., 2001) and complex IV (Ozawa et al., 1982) revealed tightly bound CL molecules in conserved binding sites, suggesting CL as an integral component of these complexes. Respiratory supercomplexes containing complex III and complex IV are destabilized in mitochondria lacking CL (Pfeiffer et al., 2003; Zhang et al., 2002). Specifically, CL is thought to neutralize a positively charged region of complex III that allows for interaction with complex IV and stabilizes supercomplex formation (Wenz et al., 2009). The requirement for CL in supercomplex formation was further elucidated when CL was found to be absolutely required for the *in vitro* reconstitution of the yeast tetrameric supercomplex, III_2IV_2 (Bazan et al., 2013). However, it is not clear if the *in vivo* requirement of CL in

supercomplex formation is specific or if any perturbations in membrane phospholipid composition disrupt supercomplex formation.

In addition to the MRC, CL interacts with several different transporter proteins. For example, the activity of the essential ADP/ATP carrier (AAC) protein also requires CL (Jiang et al., 2000, Claypool, 2009). Moreover, CL associates with and is required for the activity of carrier proteins for phosphate (Kadenbach et al., 1982), pyruvate (Nalecz et al., 1986), carnitine (Indiveri et al., 1991), and adenine nucleotides (Beyer and Klingenberg, 1985). In addition, its interaction with cytochrome *c* has implicated CL in the process of apoptosis (Petrosillo et al., 2001; Gonzalvez and Gottlieb, 2007; Huttemann et al., 2011). The peroxidation of CL bound to cytochrome *c* is an essential step in its release during apoptosis (Kagan et al., 2005). CL contains a high proportion of unsaturated acyl chains, which are particularly susceptible to ROS-induced oxidation (Paradies et al., 2014). Interestingly, exogenously added CL-liposomes prevented ROS mediated inactivation of MRC complexes while PE, PC, and oxidized CL were unable to prevent this effect (Paradies et al., 2001; Paradies et al., 2000). Due to its multiple roles, disruptions in CL biosynthesis have a broad impact on mitochondrial function and cellular physiology.

Barth Syndrome

The importance of CL in mitochondrial function is underscored by the fact that genetic mutation of a CL remodeling enzyme TAZ leads to the debilitating disorder known as Barth syndrome (BTHS) (Bione et al., 1996; Schlame and Ren, 2006). BTHS is an X-linked genetic disorder characterized by cardiomyopathy, skeletal muscle

myopathy, neutropenia, growth-delay, and exercise intolerance (Barth et al., 1983). Studies from BTHS patient cells - as well as a number of model systems, including the yeast *Saccharomyces cerevisiae* - have shown that mitochondrial dysfunction caused by perturbation of mitochondrial membrane phospholipid composition is the primary cause of BTHS pathology (Vreken et al., 2000; Schlame et al., 2003; Gu et al., 2004). Specifically, BTHS mitochondria contain elevated monolysocardiolipin (MLCL), no tetralinoleoyl-CL, and an overall decrease in CL levels. The downstream consequences of the altered mitochondrial phospholipid composition in BTHS cells are the destabilization of the MRC supercomplexes and increased oxidative stress (McKenzie et al., 2006). Similarly, the destabilization of MRC supercomplexes and increased oxidative stress were observed in a yeast model of BTHS (Brandner et al., 2005; Chen et al., 2008). Interestingly, these phenotypes are not observed in yeast cells where MLCL accumulation is prevented. These results suggest MLCL build-up is the major contributor to mitochondrial dysfunction, not alterations in CL species or overall levels (Ye et al., 2014; Baile et al., 2014; Tyurina et al., 2017). These recent findings highlight the potential for targeting mitochondrial membrane phospholipid composition in correcting the pathophysiology associated with BTHS.

Phosphatidylethanolamine and Phosphatidylcholine

Mitochondrial PE is critically important during the development of a multicellular organism, as indicated by the study showing that the elimination of the mitochondrial PE biosynthetic enzyme PISD1/Psd1 in mice is embryonic lethal (Steenbergen et al., 2005). PE is not just a membrane constituent, it is essential for

protein biogenesis (Becker et al., 2013), folding (Bogdanov and Dowhan 1998; Bogdanov and Dowhan, 1999), and function (Bogdanov and Dowhan, 1995) as well as a variety of important cellular processes, including autophagy (Ichimura et al., 2000), membrane fusion (Verkleij et al., 1984), and mitochondrial function (Birner et al., 2001; Storey et al., 2001). Two groups have recently examined the role of PE in mitochondrial bioenergetics, but the results from their studies have painted a conflicting picture. In a study performed on Chinese hamster ovary cells, in which Pisd activity is reduced by 62%, a variety of mitochondrial defects, including aberrant mitochondrial morphology, reduced respiration, increased mitochondrial membrane potential, reduced level and activity of complex IV, and destabilization of complex IV-containing supercomplexes (Tasseva et al., 2013) were observed. However, these results are in direct contrast to a recent study in yeast *psd1Δ* cells, where mitochondrial membrane potential was reduced and a higher order complex IV-containing supercomplex was observed (Bottinger et al., 2012). The conflicting phenotypes observed in these studies could be due to use of different model systems or different growth conditions. Even within the same model system, it has been long known that phospholipid composition is influenced by the growth conditions (Storey et al., 2001; Gohil et al., 2005). For example, the reduction in respiratory growth of *psd1Δ* cells is much more pronounced in synthetic lactate medium devoid of Etn (Birner et al., 2001) when compared to complex lactate medium (Bottinger et al., 2012), which presumably contains enough Etn to drive PE synthesis by Kennedy pathway (Storey et al., 2001). Therefore, the question remains: Does mitochondrial PE play a specific role in MRC function and formation? Chapter II of this dissertation

addresses this question by characterizing MRC function in yeast mutants where PE is depleted.

PE also serves as the phospholipid substrate for PC, which constitutes 40-50% of phospholipids in most organelles (Vance, 2015). The prevailing view is that PC simply serves as a membrane building block (Choi et al., 2004). However, this idea overlooks earlier studies showing that PC functions as storage for arachidonoyl fatty acids (Kramer and Deykin, 1983; Ziboh and Lord, 1979). Recent work has revealed different PC species that function as protein ligands and influence gene expression (Kersten, 2014; Lee et al., 2011). In addition, PC may play a role in insulin signaling (Ersoy et al., 2013; Sakai et al., 2014). Interestingly, PC depleted mice, lacking the PE methyltransferase enzyme, were protected against diet-induced obesity and insulin resistance (Jacobs et al., 2010). Mitochondria from these mice revealed increased activities of cytochrome *c* oxidase and succinate reductase. Accordingly, ATP levels in hepatocytes from PC depleted mice were double that of control mice (van der Veen et al., 2014). In addition to increased mitochondrial respiration, this study noted a strong correlation between an increased mitochondrial PE-to-PC ratio and increased cellular ATP levels in PC depleted hepatoma cells (van der Veen et al., 2014). Despite these recent advances, the precise role of PC in MRC function and formation has not been examined. It is not well understood how cells tolerate a loss in what normally comprises ~50% of mitochondrial membrane phospholipids, but a study in yeast suggests that upon PC depletion, the fatty acid chains of PE are remodeled rendering a more bilayer-like phospholipid species that can compensate for the loss of PC (Boumann et al., 2006). These findings raise the

following questions: Do disruptions in PC biosynthesis result in a loss of the absolute amount of phospholipids or simply alterations in phospholipid ratios, without decreasing total phospholipid content? How does the loss of the most abundant mitochondrial phospholipid affect MRC function and formation? Chapter II of this dissertation addresses these questions by characterizing MRC function in a yeast mutant where PC is depleted.

Overlapping Functions of Mitochondrial PE and CL

Owing to their similar biophysical properties, PE and CL have been proposed to have overlapping functions. For example, the simultaneous loss of mitochondrial PE and CL biosynthetic enzymes leads to synthetic lethality (Gohil et al., 2005; Osman et al., 2009). Several studies have implicated the involvement of CL and PE in the maintenance of mitochondrial morphology (Osman et al., 2009; Kuroda et al., 2011). Furthermore, both PE and CL are required for mitochondrial fusion, protein import, and MRC activities (Jiang et al., 2000; Bottinger et al., 2012; Joshi et al., 2012; Becker et al., 2013). In an *Escherichia coli* strain lacking PE, there is a three to five fold elevation of CL (Rietveld et al., 1993). Conversely, the disruption of CL biosynthesis in yeast results in increased mitochondrial PE (Zhong et al., 2004; Tuller et al., 1998), suggesting a compensatory mechanism in which the loss of one non-bilayer forming phospholipid is compensated by an increase in the other. Based on these observations, I have examined the ability of elevated mitochondrial PE to compensate for CL deficiency in BTHS yeast cells in Chapter III of this dissertation.

Yeast as a Model System

Since phospholipid biosynthetic pathways are essential in mammals, it has been difficult to definitively dissect their precise role in MRC function. Therefore, the genetically tractable model organism *Saccharomyces cerevisiae*, where phospholipid biosynthetic mutants are viable, is ideal to dissect the role phospholipids play in MRC structure and function. In addition, the yeast lipidome only contains a few-hundred lipid species (Guan and Wenk, 2006; Ejsing et al., 2009), whereas mammalian cells have thousands (Sampaio et al., 2011; Yetukuri et al., 2008). The simplicity of the yeast lipidome simplifies the task of studying lipid homeostasis. Furthermore, unlike mammalian cells that require serum for growth, yeast can be cultured in media with defined compositions. This is especially important because phospholipid composition is influenced by growth conditions (Storey et al., 2001; Gohil et al., 2005; Santos and Riezman, 2012). Notably, the average concentration of Etn in the serum of an adult human is ~2 μM (Kume et al., 2006), which could affect PE levels. Both yeast and mammalian cells can take up molecules that influence phospholipid synthesis and composition. These include small phospholipid precursors like Etn, Cho, and inositol, as well as free fatty acids and lyso-phospholipids (Santos and Riezman, 2012). These molecules are abundant in serum or yeast extract containing media, therefore the phenotypic interpretation of phospholipid mutants becomes difficult when cells are cultivated in lipid-rich conditions. A primary example of this is the different phenotypes observed when PE mutants are grown in rich versus synthetic growth media (Birner et al., 2001; Chan and McQuibban, 2012). In yeast extract containing, rich media it is much

more difficult to elevate mitochondrial PE through Etn supplementation, presumably because the presence of choline in rich media reduces levels of the Etn importer, Hnm1 (Fernández-Murray et al., 2013). Importantly, all the experiments in this dissertation were performed in synthetic defined medium to reproducibly control phospholipid levels.

S. cerevisiae also serves as an excellent model organism for studying mitochondrial biology. Yeast can survive on a fermentable carbon source, like glucose, in the absence of mitochondrial respiration. This allows for the identification of genes required for mitochondrial function through a simple comparison of growth in fermentable media with that in non-fermentable media. Mutants of essential mitochondrial genes that are not viable in higher organisms can be characterized in yeast because of this ability to produce sufficient energy via glycolysis in glucose-containing medium. Finally, the high conservation of the mitochondrial proteome and phospholipids between yeast and humans make yeast ideal for dissecting fundamental mitochondrial processes, as well as furthering our understanding of mitochondrial diseases.

CHAPTER II

SPECIFIC REQUIREMENTS OF NON-BILAYER PHOSPHOLIPIDS IN MITOCHONDRIAL RESPIRATORY CHAIN FUNCTION AND FORMATION*

Disclaimer

Chapter II is a reprint of a publication for which I am the first author. In this chapter, I describe my work utilizing yeast phospholipid mutant strains to define the function of the three most abundant mitochondrial phospholipids in MRC activity and assembly. The summary section of this chapter is the abstract of the publication, and the rest is as published. I performed all the experimental work described in this chapter except for the transmission electron micrographs (Fig. 2.3) and the respiration measurements (Fig. 2.5C and D), which were performed by Erin N. Pryce and Dr. Writoban Basu Ball. I also greatly appreciate Dr. Writoban Basu Ball's help in performing mitochondrial isolation and phospholipid measurements (Fig. 2.2).

---

* Republished with permission of Molecular Biology of the Cell, from Special Requirements of Nonbilayer Phospholipids in Mitochondrial Respiratory Chain Function and Formation, Baker CD, Basu Ball W, Pryce EN, Gohil VM, 27(14) 2016; Permission conveyed through Copyright Clearance Center, Inc.

Summary

Mitochondrial membrane phospholipid composition impacts mitochondrial function by influencing the assembly of the mitochondrial respiratory chain (MRC) complexes into supercomplexes. For example, the loss of cardiolipin (CL), a signature non-bilayer forming phospholipid of mitochondria, results in disruption of MRC supercomplexes. However, the functions of the most abundant mitochondrial phospholipids, bilayer-forming phosphatidylcholine (PC) and non-bilayer forming phosphatidylethanolamine (PE) are not clearly defined. Using yeast mutants of PE and PC biosynthetic pathways, we show a specific requirement for mitochondrial PE in MRC complex III and IV activities but not for their formation, whereas loss of PC does not affect MRC function or formation. Unlike CL, mitochondrial PE or PC are not required for MRC supercomplex formation emphasizing the specific requirement of CL in supercomplex assembly. Interestingly, PE biosynthesized in the endoplasmic reticulum (ER) can functionally substitute for the lack of mitochondrial PE biosynthesis, suggesting the existence of PE transport pathway from ER to mitochondria. To understand the mechanism of PE transport, we disrupted ER-mitochondrial contact sites formed by the ERMES complex and show that, though not essential for PE transport, ERMES facilitates the efficient rescue of mitochondrial PE deficiency. Our work highlights specific roles of non-bilayer-forming phospholipids in MRC function and formation.

Introduction

The mitochondrial respiratory chain (MRC) consists of four multimeric protein complexes (complex I-IV) that generate an electrochemical proton gradient across the mitochondrial inner membrane driving adenosine triphosphate (ATP) synthesis via ATP synthase (complex V). MRC complexes are embedded within the inner mitochondrial membrane, where they interact in different stoichiometries and assemble into supra-molecular structures known as supercomplexes (Dudkina et al., 2011; Schagger and Pfeiffer, 2000). Supercomplex formation increases the efficiency of electron transfer by spatial restriction of electron carrier diffusion (Acín-Pérez et al., 2008). Disruption in the function or formation of MRC complexes or supercomplexes perturbs mitochondrial bioenergetics manifesting clinically in a wide range of metabolic disorders (Koopman et al., 2012; Nunnari and Suomalainen, 2012; Vafai and Mootha, 2012). Thus, manipulating the function of the MRC complexes has been proposed as a possible therapeutic avenue for the treatment and prevention of these diseases (Walters et al., 2012; Weinberg and Chandel, 2015).

Traditionally, the functions of MRC complexes have been studied in isolation from their native membrane environment, often overlooking the contribution of membrane lipids (Gohil and Greenberg, 2009). Phospholipids constitute a large proportion of mitochondrial membrane lipid milieu where they specify MRC function by influencing physical properties of the membrane and by specific phospholipid:protein interactions (Horvath and Daum, 2013; Ren et al., 2014). Mitochondrial membranes contain all of the major classes of phospholipids found in cell membranes, including

phosphatidylcholine (PC), phosphatidylethanolamine (PE), phosphatidylinositol (PI), phosphatidylserine (PS), and phosphatidic acid (PA), as well as cardiolipin (CL), which is predominantly, if not exclusively, found in the mitochondria (Horvath and Daum, 2013). PC is the most abundant mitochondrial phospholipid, accounting for almost 50% of total phospholipids (Horvath and Daum, 2013). The cylindrical shape of PC promotes bilayer formation. PE is the second most abundant mitochondrial phospholipid and has a cone-shape structure that imposes negative curvature stress on the membrane, increasing its tendency to form non-bilayer structures (Holthuis and Menon, 2014). Like PE, CL is the other major cone-shaped mitochondrial phospholipid with the tendency to induce negative membrane curvature to the lipid bilayer. These 'non-bilayer' forming phospholipids are proposed to facilitate membrane fusion and influence the binding and activity of membrane proteins (van Meer et al., 2008). The ratio of bilayer to non-bilayer-forming phospholipids in the mitochondria is roughly equal and highly conserved suggesting both coordinate regulation of their biosynthesis and their importance in mitochondrial function (Daum, 1985).

Phospholipid biosynthesis in eukaryotes is compartmentalized into various subcellular organelles, including the endoplasmic reticulum (ER), endosome, and mitochondria. Mitochondria are able to synthesize PE and CL in situ, whereas all the other phospholipids are imported (Gohil and Greenberg, 2009) (Fig. 2.1). CL is synthesized from phosphatidylglycerol (PG) and cytidinediphospho-diacylglycerol (CDP-DAG) in the inner mitochondrial membrane, by CL synthase, Crd1. The acyl chain composition of newly formed CL species is remodeled by the sequential action of

cardiolipin-specific deacylase, Cld1, and a transacylase, Taz1, to generate mature CL. PE is synthesized by decarboxylation of PS via phosphatidylserine decarboxylase 1, Psd1, which is localized to the inner mitochondrial membrane and is the primary source of cellular PE (Bürgermeister et al., 2004a). The yeast specific enzyme Psd2 is localized to an endosomal compartment (Gulshan et al., 2010) and contributes to the cellular PE content to a lesser extent (Bürgermeister et al., 2004a). The de novo biosynthesis of PC proceeds through three sequential methylations of PE catalyzed by phosphatidylethanolamine methyltransferases, Pem1 and Pem2. In addition to these de novo biosynthetic pathways, PE and PC can be synthesized from their precursors ethanolamine (Etn) or choline (Cho), respectively, through the non-mitochondrial Kennedy pathway (Fig. 2.1). Currently, the functional contribution of the Kennedy pathway phospholipids to mitochondrial membranes is not clear. Results from Bürgermeister et al. are consistent with equilibrium transport of PE and PC between mitochondrial and microsomal membranes (Bürgermeister et al., 2004a; Bürgermeister et al., 2004b). However, subsequent studies showed that PE synthesized by the Kennedy pathway is not able to restore mitochondrial respiration (Chan and McQuibban, 2012; Wang et al., 2014) implying that either PE transport from ER to mitochondria is insufficient to functionally compensate for the lack of mitochondrial PE biosynthesis or that the non-mitochondrial PE species cannot substitute for mitochondrial PE species.

Although the role of CL in MRC function and formation has been extensively studied (Joshi et al., 2009; Mileykovskaya and Dowhan, 2014), the roles of more abundant mitochondrial phospholipids including PE and PC are incompletely

understood. Recently, depletion of mitochondrial PE in mammalian cells was shown to result in reduced respiratory capacity, ATP production and destabilization of complex IV-containing supercomplexes (Tasseva et al., 2013). In contrast, yeast cells lacking mitochondrial PE biosynthesis was shown to contain higher order supercomplexes (Bottinger et al., 2012). While these studies suggest conflicting roles of PE in MRC assembly, the role of PC in mitochondrial bioenergetics has not been investigated at all. Therefore, it is not clear whether MRC defects are exclusive to alterations in non-bilayer mitochondrial phospholipids, like PE and CL, or simply the result of any perturbation in mitochondrial phospholipid composition.

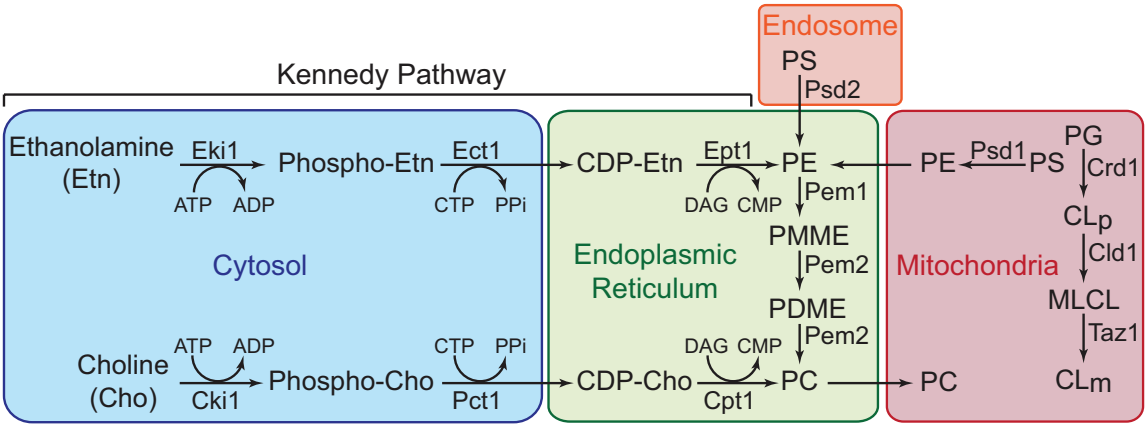

Figure 2.1 Aminoglycerophospholipids and CL biosynthetic pathways in yeast.

PE biosynthesis in yeast is accomplished by three major pathways: 1) Psd1-catalyzed decarboxylation of PS in the mitochondria, 2) Psd2-catalyzed decarboxylation of PS in endosomal compartments, and 3) incorporation of Etn via the cytosolic/ER Kennedy pathway. PC is produced by two major pathways: 1) formation of Pem1 and Pem2 PC by successive methylation of PE, and 2) incorporation of choline via the Kennedy pathway. CL biosynthesis occurs exclusively in the mitochondria, where premature cardiolipin (CLp) is synthesized from phosphatidylglycerol (PG) by Crd1. The resulting CLp is deacylated by the phospholipase Cld1 to produce monolysocardiolipin (MLCL) and reacylated by Taz1 to form mature cardiolipin (CLm). CDP, cytidine diphosphate; CTP, cytidine triphosphate; CMP, cytidine monophosphate; DAG, diacylglycerol; PA, phosphatidic acid; PI, phosphatidylinositol; PDME, phosphatidyldimethylethanolamine; PP_i, inorganic pyrophosphate.

To address these gaps in our knowledge, in this report, we have used isogenic yeast mutants of PE and PC biosynthetic enzymes to systematically dissect their roles in MRC biogenesis. We show that the disruption of mitochondrial PE biosynthesis causes diminished activities of fully assembled MRC complex III and IV containing supercomplexes. Surprisingly, the most abundant mitochondrial phospholipid, PC, is not required for MRC function or formation. In contrast to the prevailing model of inter-organelle phospholipid trafficking (Lahiri et. al, 2015; Osman et al., 2011), we demonstrate that PE synthesized in the ER via the Kennedy pathway can be transported into mitochondria, where it can fully substitute for the loss of mitochondrial PE biosynthesis. Our work thus, identifies specific roles of the two most abundant mitochondrial phospholipids in MRC biogenesis and provides means for manipulating mitochondrial phospholipid composition by stimulating non-mitochondrial Kennedy pathway.

Results

Deletion of Psd1 and Pem2 Dramatically Alters Mitochondrial PE/PC Ratio

In order to dissect the roles of the two most abundant mitochondrial phospholipids, PE and PC, in MRC function and formation in vivo, we focused on *psd1Δ* and *pem2Δ* cells, which lack key enzymes for PE and PC biosynthesis, respectively (Fig. 2.1). Previous studies have shown that phospholipid composition and mitochondrial biogenesis is dependent upon carbon source used in the growth medium (Tuller et al., 1999). Therefore, we analyzed the phospholipid composition of yeast cells

grown in glucose-containing fermentable (SC glucose) or lactate-containing non-fermentable (SC lactate) carbon sources. Whole cell phospholipid analysis of glucose-grown *psd1Δ* cells revealed a three-fold reduction in PE with a concomitant increase in PC (Fig. 2.2A). Conversely, *pem2Δ* cells showed a 15-fold reduction in PC with a two-fold increase in PE and its precursor, phosphatidylmonomethylethanolamine (PMME), which could not be separated by the thin layer chromatography used in this study (Fig. 2.2A). Similar PE and PC changes were observed when *psd1Δ* and *pem2Δ* cells were grown in a medium containing lactate (Fig. 2.2B). To analyze mitochondrial phospholipid composition, we obtained highly purified mitochondria with minimal contamination from other cellular organelles (Fig. 2.2C). Consistent with whole cell phospholipid composition, the levels of PE decreased by ~six-fold in *psd1Δ* mitochondria (Fig. 2.2D). The decrease in PE in *psd1Δ* mitochondria was accompanied by alterations in other phospholipids, including a significant increase in PC and PA and a decrease in CL (Fig. 2.2D). In *pem2Δ* mitochondria, PC levels decreased by five-fold while the PE/PMME content doubled (Fig. 2.2D). We also observed a significant accumulation of phosphatidyldimethylethanolamine (PDME) in *pem2Δ* mitochondria (Fig. 2.2D). In both glucose and lactate-containing media, the absolute phospholipid levels in whole cells and in isolated mitochondria did not change in either mutant relative to the wild type (WT) cells (Fig. 2.2E-G). These results suggest that in yeast cells a homeostatic mechanism exists which buffers cells against the loss of the absolute amount of membrane phospholipids, such that the depletion in PE is compensated by an increase in PC, and vice-versa. Therefore, *psd1Δ* and *pem2Δ* cells have a significantly

altered PE/PC ratio, without any change in their absolute amount of membrane phospholipids. We noted that the mitochondrial PE/PC ratio in WT was 0.503, which was reduced to 0.065 in *psd1Δ* cells and increased to 6.02 in *pem2Δ* cells. Despite these dramatic deviations in the mitochondrial PE/PC ratios in *psd1Δ* and *pem2Δ* cells, the gross cellular and mitochondrial morphology remained unaltered, with only a small reduction in the average length of mitochondrial cristae and outer membrane in *psd1Δ* cells (Fig. 2.3B). There was no change in mitochondrial cristae length of *pem2Δ* cells, but we did observe a slight reduction in the average outer membrane length (Fig. 2.3C). Collectively, these results demonstrate that yeast cells can tolerate extensive alteration in mitochondrial PE/PC ratios and that a decrease in the PE level is countered by an increase in PC, and vice-versa.

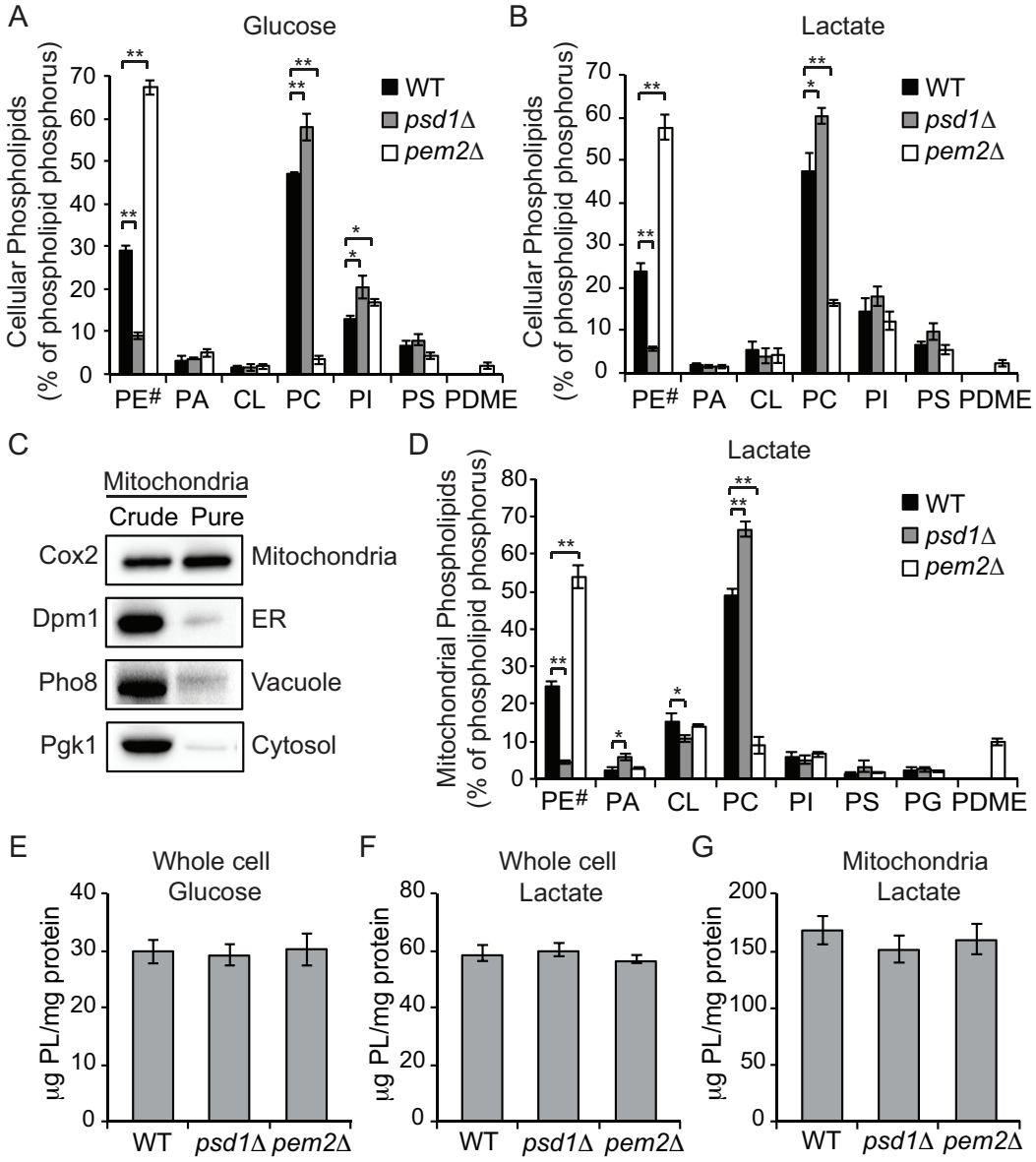

Figure 2.2 Cellular and mitochondrial phospholipid composition of *psd1Δ* and *pem2Δ* cells.

The whole-cell phospholipid composition of WT, *psd1Δ*, and *pem2Δ* cells grown in (A) SC glucose and (B) SC lactate. Phospholipid levels are expressed as the percentage of total phospholipid phosphorus in each phospholipid class. PE# represents the sum of PE and PMME in *pem2Δ* cells. Data are expressed as mean ± SD (n = 3); **p < 0.005, *p < 0.05. (C) Western blot analysis of crude and sucrose-gradient purified mitochondria from WT cells. Cox2, Dpm1, Pho8, and Pgk1 are used as markers of the yeast mitochondria, ER, vacuole, and cytoplasm, respectively. (D) Phospholipid composition of sucrose gradient–purified mitochondria from WT, *psd1Δ*, and *pem2Δ* cells grown in SC lactate. Data are expressed as mean ± SD (n = 3); **p < 0.005, *p < 0.05. (E, F) Total phospholipid content of whole-cell homogenates of WT, *psd1Δ*, and *pem2Δ* cells grown in (E) SC glucose or (F) SC lactate. (G) Total phospholipid content of mitochondria from SC lactate-grown cells. Data are expressed as mean ± SD (*n* = 3).

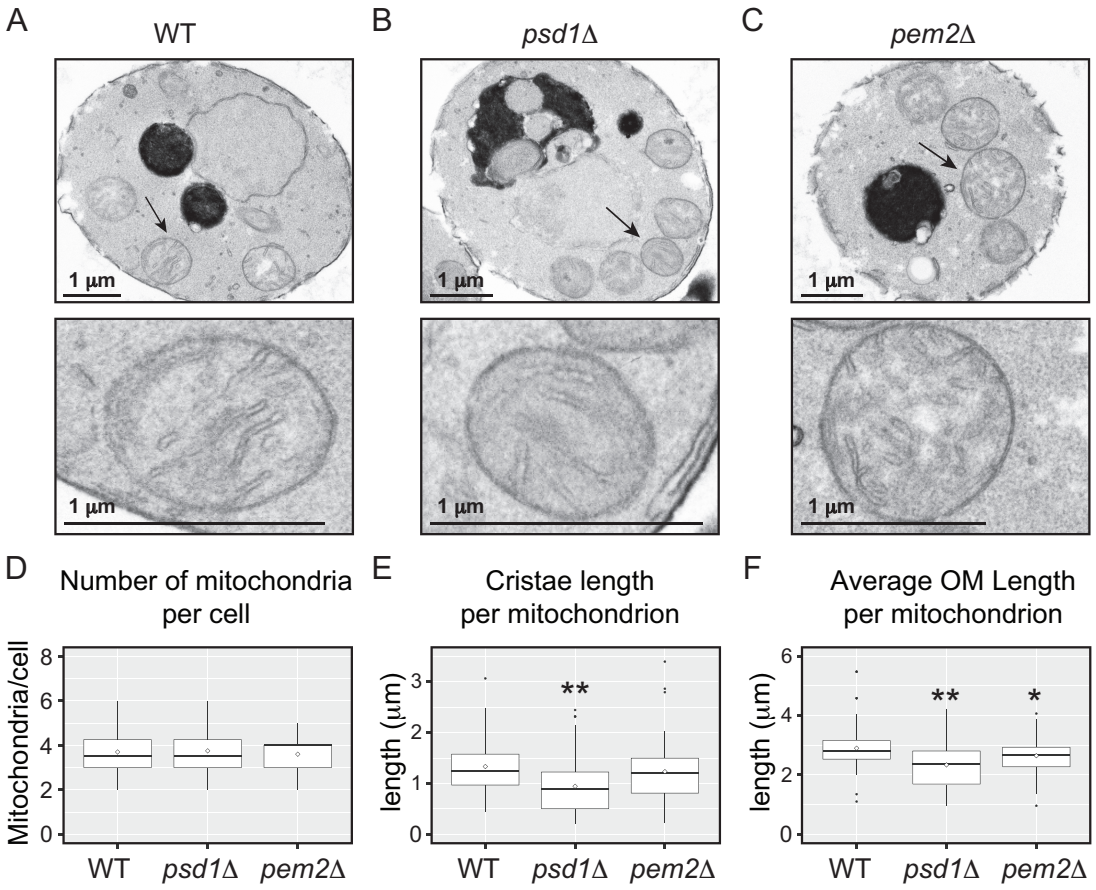

Figure 2.3 Cellular and mitochondrial morphology of PE and PC depleted cells.

(A) Representative transmission electron micrographs from the total of 20 different images of WT, (B) *psd1Δ*, and (C) *pem2Δ* cells are shown. Top panel shows yeast cells and bottom panel shows mitochondria (scale bars, 1 μm). Arrows in top panel indicate mitochondria shown in bottom panel. (D) Box plots depicting the average number of mitochondria per cell, (E) average cristae length per mitochondrion, and (F) average outer mitochondrial membrane (OM) length. Box plots shown in (D), (E), and (F) show median, first and third quartiles, greatest values within 1.5 inter-quartile range, and outliers, *$p < 0.05$ and **$p < 0.005$.

Decreased Mitochondrial PE/PC Ratio Results in Reduced Respiration and ATP Levels

To dissect the specific roles of PC and PE in MRC function, we performed extensive growth characterization of *psd1Δ* and *pem2Δ* cells in different carbon sources. The growth of *psd1Δ* and *pem2Δ* cells in fermentable SC glucose medium was comparable to WT cells (Fig. 2.4A and 2.5A). Consistent with a previous report (Birner

et al., 2001), the growth of *psd1Δ* cells in non-fermentable SC lactate medium was severely compromised, whereas *pem2Δ* cells were able to grow albeit with slightly reduced rate (Fig. 2.4B and 2.5B). The growth defects in non-fermentable medium suggested respiratory deficiency.

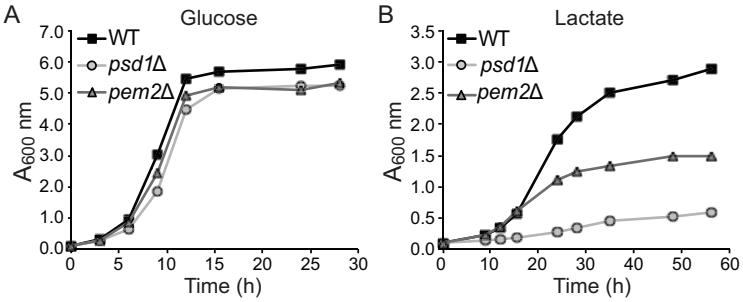

Figure 2.4 Growth of PE and PC depleted cells in liquid media.
(A) Growth of WT, *psd1Δ*, and *pem2Δ* cells in SC glucose or (B) SC lactate liquid medium at 30°C was monitored by measuring absorbance at 600 nm. Data are representative of at least three independent measurements.

To directly assess respiration, we measured oxygen consumption in WT, *psd1Δ*, and *pem2Δ* cells. Consistent with the severely diminished respiratory growth, the *psd1Δ* cells had a ~60% reduction in oxygen consumption compared to WT cells (Fig. 2.5C and D). Oxygen consumption in *pem2Δ* cells was comparable to WT cells in SC lactate and even slightly elevated in SC glucose media (Fig. 2.5C and D). The reduced growth of *pem2Δ* cells could be due to defects in mitochondrial protein import machinery as reported recently (Schuler et al., 2015) and not due to defects in respiration per se. In accordance with reduced respiration in *psd1Δ* cells, we observed a significant 50% reduction in ATP levels, while the ATP levels in the respiratory competent *pem2Δ* cells remained unaltered (Fig. 2.5E and F). These results suggest that mitochondrial PE, but not PC, is essential for maintaining normal respiration.

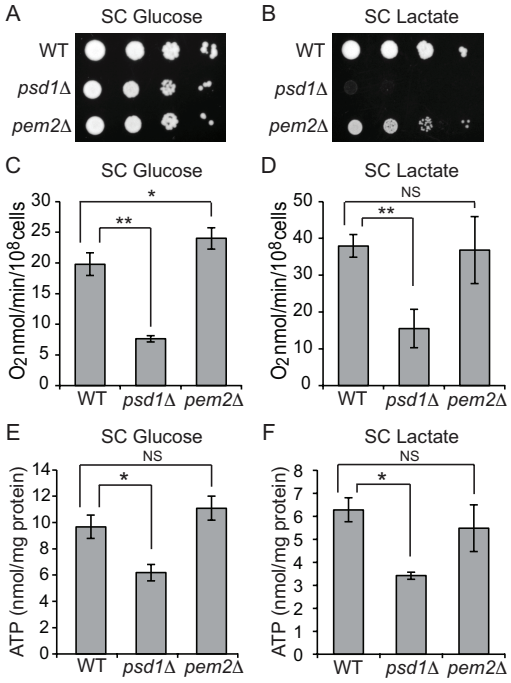

Figure 2.5 Mitochondrial respiration is dependent on PE but not PC levels.

Tenfold serial dilutions of WT, *psd1Δ*, and *pem2Δ* cells were spotted onto (A) SC glucose and (B) SC lactate plates, and images were captured after 2 (SC glucose) or 5 d (SC lactate) of growth at 30°C. Data are representative of at least three independent experiments. (C, D) WT, *psd1Δ*, and *pem2Δ* cells were grown in (C) SC glucose or (D) SC lactate to late log phase, and the rate of oxygen consumption was measured. Data are expressed as mean ± SD (n = 6); *p < 0.05, **p < 0.005. (E, F) Cellular ATP levels of WT, *psd1Δ*, and *pem2Δ* cells cultured in (E) SC glucose or (F) SC lactate. Data are expressed as mean ± SD (n = 3); *p < 0.05.

Decreased Mitochondrial PE/PC Ratio Reduces MRC Supercomplex Activities without Affecting Supercomplex Formation

To ascertain the biochemical basis for reduced respiration in PE depleted cells, we analyzed the levels of native and denatured MRC complexes in the mitochondrial lysate from WT, *psd1Δ* and *pem2Δ* cells grown in SC lactate medium. There was no change in the steady-state levels of individual MRC subunits (Fig. 2.6) or their incorporation into fully assembled MRC complexes in either of the mutant cells (Fig. 2.7A and B). As reported previously, MRC supercomplexes containing complex III and IV were disrupted in CL-lacking crd1Δ cells (Zhang et al., 2002; Pfeiffer et al., 2003).

These results imply that reduced PE and accompanying 33% decrease in CL levels in *psd1Δ* is insufficient to disrupt supercomplex formation. We noticed that *pem2Δ* cells, which exhibit an increased PE/PC ratio, showed an enhanced formation of a larger supercomplex (III_2IV_2) at the expense of the smaller supercomplex (III_2IV) (Fig. 2.7A). The lack of alterations in the amount and assembly of the MRC complexes cannot explain the respiratory deficiency of *psd1Δ* cells, suggesting that the reduced respiration could be due to a decrease in MRC activity. Therefore, we measured the enzymatic activities of MRC complexes and observed a four-fold and a two-and-half-fold reductions in complex III and complex IV activities, respectively, in *psd1Δ* cells (Fig. 2.7C and D). The specific reduction in complex III and complex IV activities could, in part, explain the respiratory defects observed in *psd1Δ* cells. The activities of MRC complexes were comparable in WT and *pem2Δ* cells (Fig. 2.7C and D), which is consistent with the normal respiratory phenotype of *pem2Δ* cells. Together, these results demonstrate specific requirement of CL for MRC supercomplex formation and PE for MRC complex III and IV activities, whereas PC is redundant for these functions.

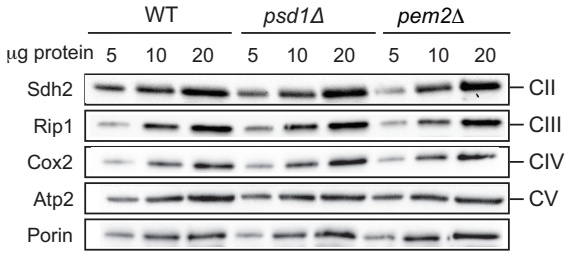

Figure 2.6 Steady-state levels of MRC subunits are unaltered in PE and PC depleted cells. Mitochondria from SC lactate grown WT, *psd1Δ*, and *pem2Δ* cells were subjected to SDS-PAGE and immunoblotted using complex II, III, IV, and V specific antibodies Sdh2, Rip1, Cox2, and Atp2, respectively. Porin was used as a loading control. Data are representative of at least three independent experiments.

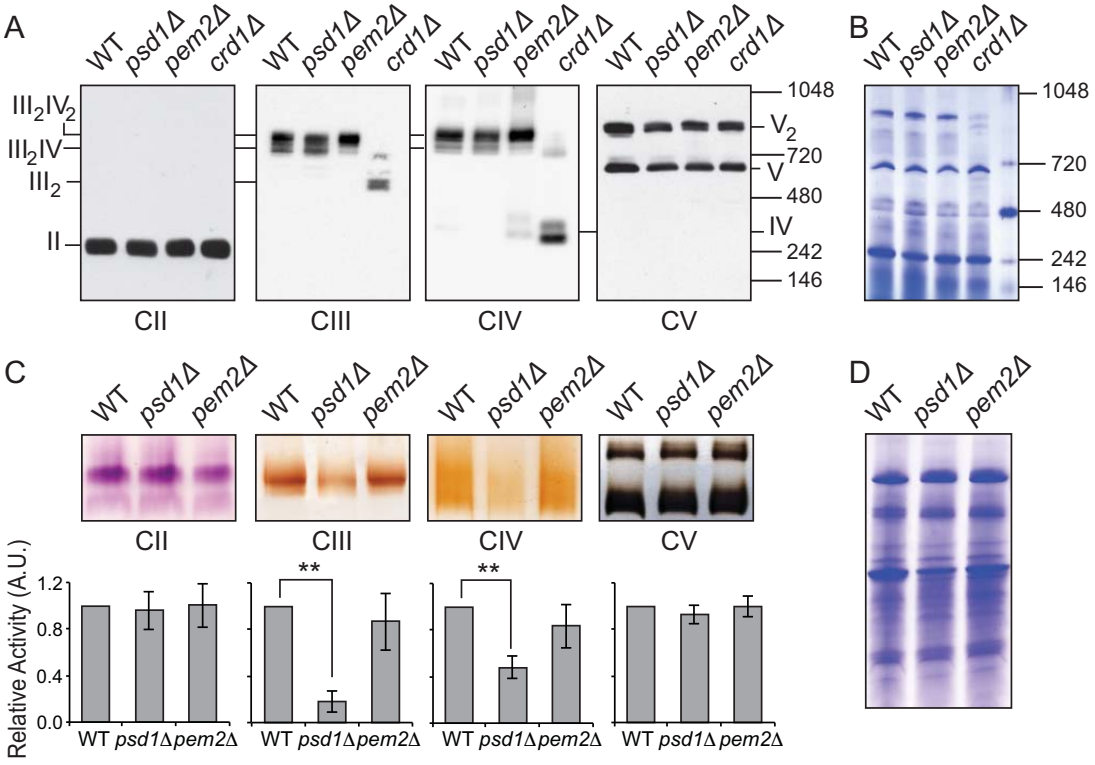

Figure 2.7 Mitochondrial PE is required for MRC complex III and IV activities but not MRC supercomplex formation.

(A) Mitochondria from SC lactate–grown cells were solubilized by 1% digitonin and subjected to BN–PAGE/Western blot, and complexes II–V were detected by Sdh2, Rip1, Cox2, and Atp2 antibodies, respectively. Mitochondria from CL-deficient *crd1Δ* cells were used as positive control to demonstrate loss of supercomplexes (III_2IV_2, large supercomplex; III_2IV, small supercomplex) under identical conditions. (B) Samples from A were stained with Coomassie blue to demonstrate equal loading. (C) Digitonin-solubilized mitochondrial complexes from WT, *psd1Δ*, and *pem2Δ* cells were separated by CN-PAGE, followed by in-gel activity staining for complexes II–V. In-gel activities of MRC complexes were quantified by densitometric analysis, and relative activities were plotted for complexes II–V. Data were normalized to WT cells and expressed as mean ± SD (n = 3); **p < 0.005. (D) Samples from C were stained with Coomassie blue, and total protein, quantified using densitometric analysis, was used to normalize activity staining.

Depletion of PE Results in a Specific Loss of Mitochondrial DNA-Encoded MRC Subunits

In contrast to previous studies (Tasseva et al., 2013; Bottinger et al., 2012), which reported aberrant formation of MRC supercomplexes in PE depleted cells, we did not find any alterations in the MRC supercomplexes in *psd1Δ* cells. We reasoned that

this discrepancy could be related to use of different growth conditions and carbon sources in these studies. Indeed, we found reduced levels of MRC supercomplexes (III_2IV_2 and III_2IV) in glucose grown *psd1Δ* cells (Fig. 2.8A). These carbon source-dependent differences in MRC supercomplex assembly might be due to increased petite formation in *psd1Δ* cells as reported previously (Birner et al., 2001). The petite phenotype results from mutations in the mitochondrial genome or loss of mitochondrial DNA (mtDNA), which leads to the loss of mtDNA-encoded MRC subunits. Consistent with the previous report, we found a significant increase in the number of petite colonies in the *psd1Δ* mutant (Fig. 2.9). Accordingly, SDS-PAGE/western blot analysis of MRC subunits showed a specific decrease in the steady-state levels of mtDNA-encoded subunits Cox1, Cox2, and Cox3 (Fig. 2.8B) without affecting the levels of the nuclear-encoded subunits Sdh2, Rip1, Cox4, and Atp2 (Fig. 2.8C). Unlike PE depleted *psd1Δ* cells, loss of PC in *pem2Δ* cells did not result in any alterations in the assembly or steady-state levels of MRC complexes or petite formation (Figs. 2.8 and 2.9). Collectively, these results suggest that the decrease in the MRC supercomplex levels in glucose-grown *psd1Δ* cells results from the loss of mtDNA-encoded subunits.

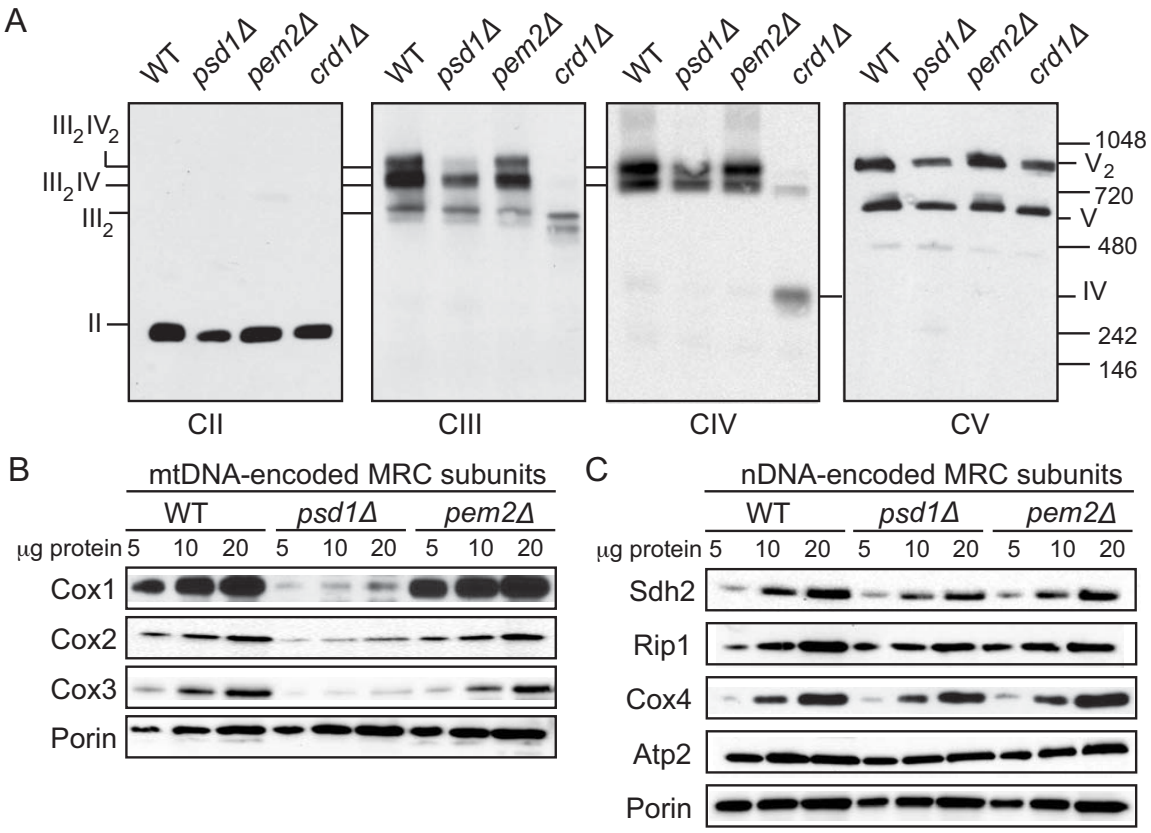

Figure 2.8 Depletion of mitochondrial PE in glucose-grown *psd1Δ* cells results in a specific loss of mtDNA-encoded MRC subunits.

(A) Digitonin-solubilized mitochondria from SC glucose–grown WT, *psd1Δ*, and *pem2Δ* cells were subjected to BN–PAGE/Western blot. Complexes II–V were detected by Sdh2, Rip1, Cox2, and Atp2 antibodies, respectively. Data are representative of at least three independent experiments. (B) Mitochondria from SC glucose–grown WT, *psd1Δ*, and *pem2Δ* cells were subjected to SDS–PAGE, and mtDNA-encoded subunits were probed using Cox1, Cox2, and Cox3 antibodies. (C) Nuclear-encoded subunits were probed using Sdh2, Rip1, Cox4, and Atp2. Porin was used as a loading control. Data are representative of at least three independent experiments.

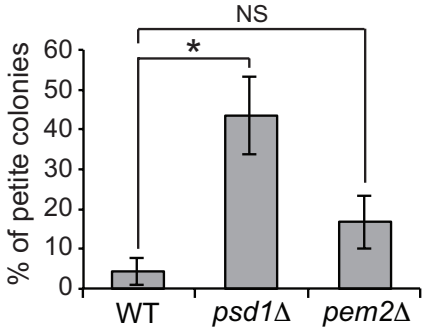

Figure 2.9 Depletion of mitochondrial PE in glucose grown *psd1Δ* cells results in enhanced petite formation.

Respiratory deficient petite cells from SC glucose grown WT, *psd1Δ*, and *pem2Δ* cells were quantified by counting colonies in fermentable and non-fermentable media. Data are expressed as mean ± S.D. (n=3), *p < 0.05.

PE Synthesized via Kennedy Pathway Completely Rescues Respiratory Defects of *psd1Δ* Cells by Restoring Mitochondrial PE Levels

In order to determine if PE synthesized in ER by the CDP-Etn branch of the Kennedy pathway could compensate for the loss of mitochondrial PE, we grew *psd1Δ* cells in the presence of Etn and measured cellular and mitochondrial phospholipids. Etn supplementation in *psd1Δ* cells completely restored cellular PE and significantly restored mitochondrial PE levels (Fig. 2.10A and B). Interestingly, supplementation of Etn not only rescued mitochondrial PE levels but also restored PA and CL levels in *psd1Δ* mitochondria (Fig. 2.10B), implying that a yet unidentified homeostatic mechanism regulates the precise proportion of individual phospholipids in mitochondrial membranes. Next, we asked whether the partial restoration of mitochondrial PE through exogenous Etn supplementation could restore the respiratory defects observed in *psd1Δ* cells. Indeed, Etn supplementation rescued the respiratory growth defect of *psd1Δ* cells in SC lactate medium (Fig. 2.10C and D). Consistent with the rescue of respiratory growth, Etn supplementation restored oxygen consumption (Fig. 2.10E) and cellular

ATP content (Fig. 2.10F) in *psd1Δ* cells to WT levels. In order to investigate the mechanism by which Etn rescued respiration, we measured MRC complex III and IV activities and found that their activities were restored to WT levels in Etn supplemented *psd1Δ* cells (Fig. 2.10G and H). Etn supplementation not only restored respiratory function in SC lactate, but also rescued petite formation and cellular ATP levels in SC glucose medium (Fig. 2.11). Taken together, these results show that PE synthesized in ER by the Kennedy pathway can replenish mitochondrial PE and restore MRC complex III and IV activities in *psd1Δ* cells.

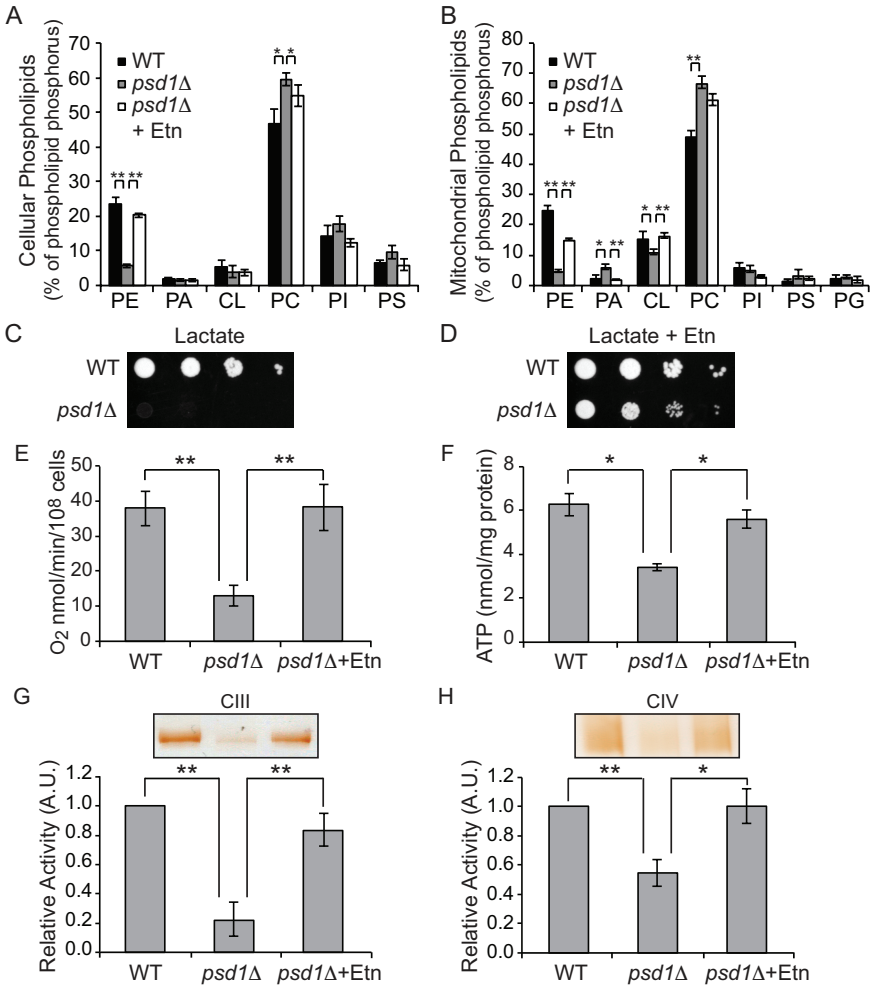

Figure 2.10 Ethanolamine supplementation rescues respiratory defects of *psd1Δ* cells by restoring mitochondrial PE levels.

(A) Cellular and (B) mitochondrial phospholipid composition of WT cells grown in SC lactate and *psd1Δ* cells grown in SC lactate with and without 2 mM Etn. Phospholipid levels are expressed as percentage of total phospholipid phosphorus in each phospholipid class. Data are expressed as mean ± SD (n = 3); **p < 0.005, *p < 0.05. Tenfold serial dilutions of WT and *psd1Δ* cells were spotted onto (C) SC lactate and (D) SC lactate + 2 mM Etn plates, and images were captured after 4 days of growth at 30°C. Data are representative of at least three independent trials. (E) Rate of oxygen consumption and (F) total cellular ATP levels of WT and *psd1Δ* cells grown in SC lactate ± 2 mM Etn to late logarithmic phase were quantified. Data are expressed as mean ± SD (n = 3); *p < 0.05, **p < 0.005 (G, H) Digitonin solubilized mitochondrial complexes from WT and *psd1Δ* cells grown in SC lactate ± 2 mM Etn were separated by CN-PAGE, followed by in-gel activity staining for (G) complex III and (H) complex IV. Densitometric quantifications of relative in-gel activities for complexes III and IV. Data were normalized to WT cells and are expressed as mean ± SD (n = 3); **p < 0.005, *p < 0.05. A.U., arbitrary units.

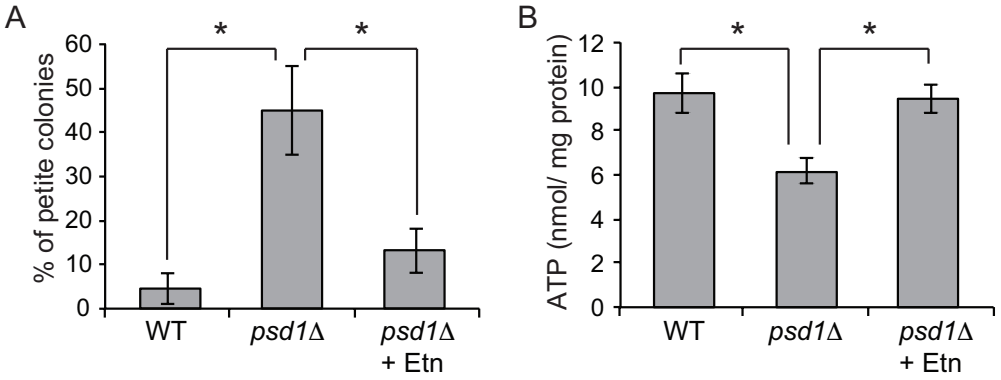

Figure 2.11 Ethanolamine supplementation reduces petite formation and restores cellular ATP levels in PE depleted cells.

(A) WT cells were grown in SC glucose and *psd1Δ* cells were grown in SC glucose ± 2 mM ethanolamine (Etn) for 16 hours. The percentage of petite colonies in these cultures was calculated by dividing the number of viable colonies in non-fermentable (YPlac) medium with the number of viable colonies in fermentable (YPD) medium. Data are expressed as mean ± S.D. (n=3) *$p < 0.05$. (B) Total cellular ATP levels of WT and *psd1Δ* cells cultured in SC glucose ± 2 mM Etn. Data are expressed as mean ± S.D. (n=3) *$p < 0.05$.

ERMES Facilitates Etn Dependent Rescue of Mitochondrial PE Deficiency

The complete rescue of mitochondrial bioenergetic phenotypes and respiratory growth of *psd1Δ* cells by Etn supplementation implies efficient transport of PE from ER to mitochondria (Fig. 2.12A). To understand the molecular basis of PE import to mitochondria, we focused on ERMES complex, a mitochondria-ER tethering structure proposed to be involved in trafficking phospholipids between ER and mitochondria (Kornmann et al., 2009). First, to rule out the possibility that Etn itself or one of its metabolite is responsible for the *psd1Δ* rescue, we deleted the Kennedy pathway enzyme Ect1 in *psd1Δ* cells and show that the rescue of *psd1Δ* cells by Etn is completely abrogated (Fig. 2.12B). This result clearly demonstrates that PE synthesized via the Kennedy pathway is essential for *psd1Δ* rescue. Next, we deleted two ERMES subunits, Mdm34 or Mdm12, both of which contain the synaptotagmin-like mitochondrial lipid

binding protein domain (SMP) (AhYoung et al., 2015), in *psd1Δ* cells and found that Etn rescue is reduced in the double mutants (Fig. 2.12C and D). To reveal the involvement of the ERMES complex in PE transport, we measured the phospholipid levels in mitochondria of *psd1Δmdm34Δ* cells with and without Etn supplementation. We did not observe any significant decrease in the steady levels of mitochondrial PE in the double mutant as compared to *psd1Δ* single mutant after Etn supplementation (Fig. 2.13). These results suggest that ERMES is not essential for the import of non-mitochondrial PE to mitochondria but may only indirectly facilitate Etn-mediated rescue of *psd1Δ* cells.

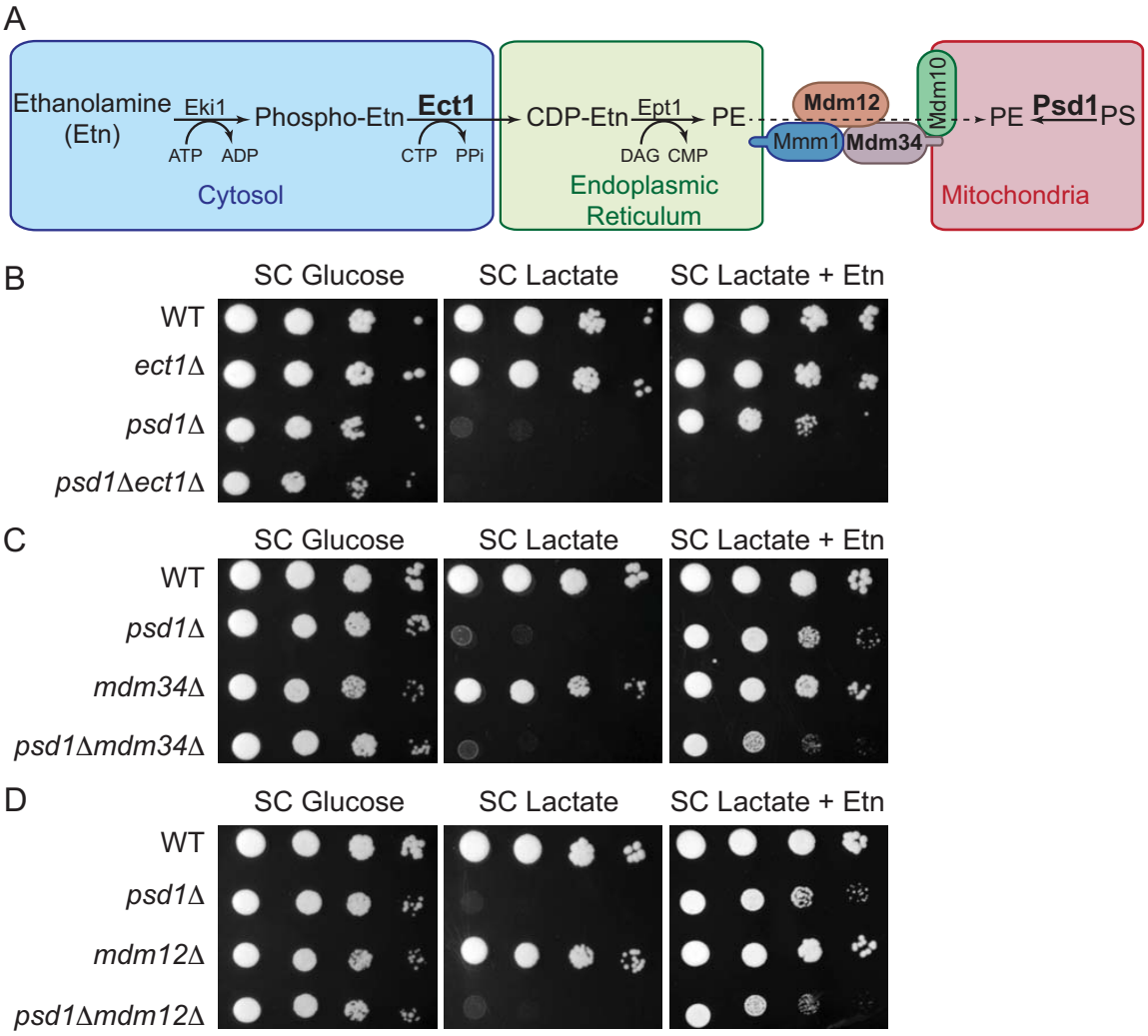

Figure 2.12 PE synthesized by the Kennedy pathway requires ERMES for complete rescue of mitochondrial PE deficiency.

(A) Schematic representation of the Kennedy pathway of PE biosynthesis and the ERMES complex. The Kennedy pathway enzyme Ect1, mitochondrial Psd1, and Mdm34 and Mdm12 of the ERMES complex are depicted in boldface to indicate that these genes are targeted to construct double-knockout strains. Tenfold serial dilutions of (B) WT, *ect1Δ*, *psd1Δ*, and *psd1Δect1Δ*, (C) WT, *psd1Δ*, *mdm34Δ*, and *psd1Δmdm34Δ*, and (D) WT, *psd1Δ*, *mdm12Δ*, and *psd1Δmdm12Δ* cells were spotted onto SC glucose and SC lactate ± Etn plates, and images were captured after 2 (SC glucose) or 5 d (SC lactate ± Etn) of growth at 30°C. Data are representative of at least three independent experiments.

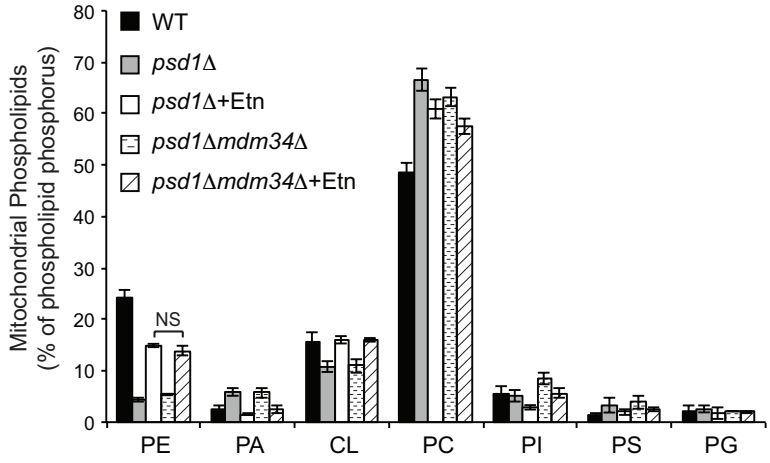

Figure 2.13 Mitochondrial phospholipid composition of indicated yeast mutants.
Mitochondrial phospholipids of WT cells grown in SC lactate and *psd1Δ* or *psd1Δmdm34Δ* cells grown in SC lactate with and without 2 mM ethanolamine (Etn). Phospholipid levels are expressed as the percentage of total phospholipid phosphorus in each phospholipid class. Data are expressed as mean ± S.D. (n=3). Mitochondrial phospholipid levels in WT and *psd1Δ* cells are from Figure 2.2.

Discussion

Perturbations in mitochondrial membrane phospholipid composition have been shown to cause MRC dysfunction (Lu and Claypool, 2015; Chicco and Sparagna, 2007). Therefore, delineating the specific roles of the individual phospholipids of mitochondrial membranes is critical in understanding MRC function. In this study, we used yeast mutants of PE and PC biosynthetic pathways to show a specific requirement of mitochondrial PE for MRC complex III and IV activities, whereas loss of PC was well tolerated. Furthermore, we show that PE synthesized in the ER via Kennedy pathway can be efficiently transported to the mitochondrial membranes, where it can completely substitute for the lack of mitochondrial PE biosynthesis. Our results suggest a specific requirement of non-bilayer promoting phospholipids, PE and CL, in MRC function and formation.

Analysis of the phospholipid profiles of *psd1Δ* and *pem2Δ* cells revealed a cellular homeostatic mechanism that maintained absolute phospholipid concentrations. For example, depletion of PE is always accompanied by an increase in the level of PC, and vice versa (Fig. 2.2A, B, and D). As a result, the mutants harboring PSD1 or PEM2 deletions had altered PE/PC ratios rather than a change in the absolute amount of one particular phospholipid (Fig. 2.2E-G). Therefore, it is important to interpret results in terms of alterations in relative levels of different classes of phospholipids rather than a single phospholipid. Currently, we do not know the molecular basis for homeostatic mechanisms that strictly maintain total cellular and mitochondrial phospholipid levels. We predict that such homeostatic mechanisms are likely mediated by feedback inhibition of phospholipid biosynthetic enzymes and cross-pathway regulations by phospholipid precursors, a prediction supported by previous studies (Carman and Han, 2011). Apart from the overall mitochondrial membrane phospholipid content, MRC assembly and activity has been linked to cristae shape (Cogliati et al., 2013). Therefore, we analyzed mitochondrial morphology of *psd1Δ* and *pem2Δ* mutants by transmission electron microscopy and found that the gross mitochondrial structure and overall cristae morphology remain unaffected in PE and PC deficient mitochondria (Fig. 2.3) with only a small reduction in the average mitochondrial cristae length in *psd1Δ* mutants (Fig. 2.3E).

Earlier studies focused on defining the role of PE in mitochondrial functions have been performed in different growth media, resulting in conflicting phenotypes (Birner et al., 2001; Chan and McQuibban, 2012). This is not surprising since it has been

long known that phospholipid composition is influenced by the growth conditions of yeast cells (Storey et al., 2001; Gohil et al., 2005). For example, the reduction in respiratory growth of *psd1Δ* cells is much more pronounced in synthetic lactate medium devoid of Etn (Birner et al., 2001) when compared to complex lactate media (Bottinger et al., 2012), which presumably contains enough Etn to drive PE synthesis by Kennedy pathway (Storey et al., 2001). Therefore, in the present study, all the experiments were performed in the synthetic defined medium to reproducibly control phospholipid levels. The *psd1Δ* cells cultured in synthetic medium showed a dramatic decrease in the mitochondrial PE/PC ratio (Fig. 2.2D), which reduced MRC function (Fig. 2.5). These bioenergetic deficits could be partly attributed to the reduced activities of the MRC complexes III and IV (Fig. 2.7C). Decreased ATP and respiration in *psd1Δ* cells could also be due to the reduced mitochondrial membrane potential and protein import, as has been previously described (Bottinger et al., 2012). Thus, our findings on the role of PE in mitochondrial bioenergetics are partly consistent with previous studies in yeast (Bottinger et al., 2012) and mammalian cell lines (Tasseva et al., 2013), but unlike these reports, we did not find any perturbations in MRC supercomplexes in PE-depleted mitochondria (Fig. 2.7A). This discrepancy could be due to use of different growth conditions. Indeed, we observed reduced levels of MRC supercomplexes in *psd1Δ* cells cultured in glucose-containing medium (Fig. 2.8A). Thus, our results obtained from isogenic yeast mutants grown under identical conditions clearly demonstrate that of the three most abundant mitochondrial phospholipids (PC, PE, and CL) only CL is essential for MRC supercomplex formation (Fig. 2.7A and B).

While previous studies have provided insights into the specific role of CL in MRC biogenesis (Wenz et al., 2009; Bazan et al., 2013), they did not address if the mitochondrial phospholipid requirement is specific for non-bilayer-forming phospholipids, or if any perturbation in phospholipid composition will result in MRC defects *in vivo*. We found that, unlike non-bilayer forming PE and CL, depletion in bilayer-forming PC did not alter mitochondrial bioenergetic parameters (Figs. 2.5-2.7). A five-fold depletion in mitochondrial PC had no effect on MRC function or formation, which is surprising, considering that PC constitutes almost half of all the mitochondrial membrane phospholipids. Three previous reports provide possible explanation to this observation. First, the loss of PC in yeast is accompanied by the remodeling of fatty acyl species of PE into more of a bilayer-forming phospholipid, thus maintaining the ratio of non-bilayer to bilayer-forming phospholipids (Boumann et al., 2006). Second, 90% of bacteria do not contain PC in the cellular membranes that harbor their oxidative phosphorylation machinery (Aktas et al., 2010). Third, elevation of non-bilayer phospholipids like PE and phosphatidylpropanolamine in PC lacking cells were able to support growth in non-fermentable medium, suggesting that bilayer-forming PC is not essential for respiratory growth of yeast *S. cerevisiae* (Choi et al., 2004). Collectively, these studies indicate that MRC activity or assembly is more resistant to perturbation in PC levels but is very sensitive to changes in non-bilayer phospholipids. Interestingly, we observed that depletion of PC with a concomitant increase in PE+PMME resulted in enhanced formation of the large supercomplex III_2IV_2 and free complex IV at the expense of the small supercomplex III_2IV (Fig. 2.7A), suggesting that formation of MRC

supercomplexes can be modulated by altering the bulk properties of membranes in addition to specific molecular interactions with CL. Additionally, PC-depleted cells showed an increased rate of oxygen consumption (Fig. 2.5C), a finding consistent with a recent study in mammalian cells lacking a mammalian homolog of yeast Pem2 (van der Veen et al., 2014). Thus, our findings in yeast cells are likely applicable to mammalian cells.

Next, we asked if PE synthesized in ER could be transported to mitochondria to compensate for the lack of mitochondrial PE biosynthesis. Previous reports paint a conflicting picture, one line of evidence shows that the reduced respiratory growth of *psd1Δ* cells is rescued by Etn supplementation (Birner et al., 2001; Riekhof and Voelker, 2006), whereas other studies show that PE synthesized by the Kennedy pathway does not meet the requirements for respiration in *psd1Δ* cells (Chan and McQuibban, 2012; Wang et al., 2014). Here, we show that exogenous Etn supplementation not only restores cellular PE levels but also significantly increases mitochondrial PE levels in *psd1Δ* cells and fully rescues all mitochondrial bioenergetic defects observed in *psd1Δ* cells (Fig. 2.10). These results imply that mitochondrial PE import pathway(s) exist and that non-mitochondrial PE can functionally compensate for the lack of mitochondrial PE biosynthesis. The requirement of ERMES complex for the efficient rescue suggested that the membrane contact sites between ER and mitochondria may facilitate PE import into mitochondria. However, steady state levels of mitochondrial PE did not reduce upon Etn supplementation in *psd1Δ* cells lacking the ERMES complex (Fig. 2.13), implying that ERMES is not essential for PE transport but may only play an indirect role in Etn-

mediated rescue (Fig. 2.12). In summary, as depicted in our model (Fig. 2.14), this work identified critical roles of non-bilayer phospholipids in MRC activity and assembly, respectively and showed that non-mitochondrial PE can be transported to mitochondria, where it can functionally substitute for PE deficiency.

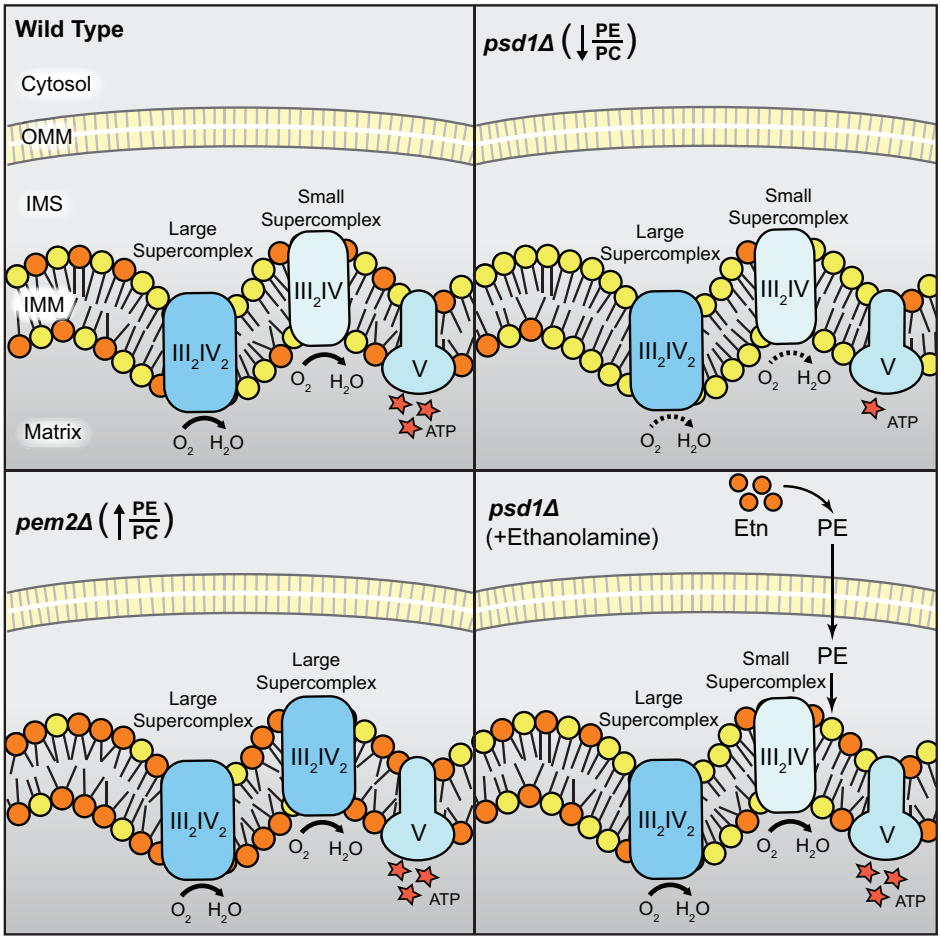

Figure 2.14 Model depicting the specific roles of mitochondrial PE and PC in MRC complex activity and assembly.

Reduced PE/PC ratio in mitochondrial PE–depleted *psd1Δ* cells leads to decreased MRC complex III and IV activities without affecting supercomplex formation. The increased PE/PC ratio in mitochondrial PC-depleted *pem2Δ* cells results in enhanced formation of the larger supercomplex (III_2IV_2) without altering the activities of complexes. PE synthesized in ER by exogenous supplementation of Etn is transported into mitochondria and completely restores MRC supercomplex activities in PE-deficient *psd1Δ* cells. IMM, inner mitochondrial membrane; IMS, intermembrane space; OMM, outer mitochondrial membrane.

Materials and Methods

Yeast Strains, Growth Medium Composition, and Culture Conditions

Saccharomyces cerevisiae strains used in this study are listed in Table 2.1. For growth in liquid media, strains were pre-cultured in YPLac medium (1% yeast extract, 2% peptone, and 2% lactate pH 5.5) and inoculated into SC media (0.2% dropout mix containing amino acid and other supplements as previously described (Amberg et al., 2005), 0.17% yeast nitrogen base without amino acids and ammonium sulfate, and 0.5% ammonium sulfate) containing either 2% glucose or 2% lactate (pH 5.5) and grown to late logarithmic phase. Solid media were prepared by the addition of 2% agar. Liquid SC glucose and SC lactate was inoculated with WT or the indicated strains to a starting A_{600} of 0.1 and growth was monitored for up to 30 h (SC glucose) or 60 h (SC lactate) at 30°C. For growth on solid media, ten-fold serial dilutions of overnight pre-cultures were spotted on SC glucose or SC lactate plates and incubated at 30°C for 2 days (SC glucose) and 4-5 days (SC lactate) respectively. For Etn supplementation experiments, 2 mM Etn was added to SC growth medium. Petite formation was determined by spreading glucose grown cells (200 cells/100 μL) onto YPD and YPlac plates. Petite formation was calculated based on the number of colonies that grew on YPD (total viable cells) compared to YPlac (respiratory competent) media. Single and double knockout yeast strains (Table 2.1) were constructed by one-step gene disruption using hygromycin cassette (Janke et al., 2004).

Table 2.1 Yeast strains used in this study

Yeast Strains	Genotype	Source
BY4741 WT	*MATa, his3Δ1, leu2Δ0, met15Δ0, ura3Δ0*	Greenberg, M.L.
BY4741 *psd1Δ*	*MATa, his3Δ1, leu2Δ0, met15Δ0, ura3Δ0, psd1Δ::kanMX4*	Open Biosystems
BY4741 *pem2Δ*	*MATa, his3Δ1, leu2Δ0, met15Δ0, ura3Δ0, pem2Δ::kanMX4*	Open Biosystems
BY4741 *crd1Δ*	*MATa, his3Δ1, leu2Δ0, met15Δ0, ura3Δ0, crd1Δ::kanMX4*	Open Biosystems
BY4741 *ect1Δ*	*MATa, his3Δ1, leu2Δ0, met15Δ0, ura3Δ0, ect1Δ::hphNT1*	This study
BY4741 *psd1Δ ect1Δ*	*MATa, his3Δ1, leu2Δ0, met15Δ0, ura3Δ0, psd1Δ::kanMX4, ect1Δ::hphNT1*	This study
BY4741 *mdm34Δ*	*MATa, his3Δ1, leu2Δ0, met15Δ0, ura3Δ0, mdm34Δ::kanMX4*	Open Biosystems
BY4741 *psd1Δ*	*MATa, his3Δ1, leu2Δ0, met15Δ0, ura3Δ0, psd1Δ::hphNT1*	This study
BY4741 *mdm12Δ*	*MATa, his3Δ1, leu2Δ0, met15Δ0, ura3Δ0, mdm12Δ::kanMX4*	Open Biosystems
BY4741 *mdm34Δ psd1Δ*	*MATa, his3Δ1, leu2Δ0, met15Δ0, ura3Δ0, mdm34Δ::kanMX4, psd1Δ::hphNT1*	This study
BY4741 *mdm12Δ psd1Δ*	*MATa, his3Δ1, leu2Δ0, met15Δ0, ura3Δ0, mdm12Δ::kanMX4, psd1Δ::hphNT1*	This study

Mitochondrial Isolation

Isolation of crude and pure mitochondria was performed as described previously (Meisinger et al., 2006). Mitochondria were isolated from yeast cells grown to late logarithmic phase and were subsequently used for western blot analysis as well as in-gel activity assays. For obtaining pure mitochondrial fractions, crude mitochondria were loaded onto a sucrose step gradient (60%, 32%, 23% and 15%) and centrifuged at 134,000 g for 1 h. The intact mitochondria recovered from the gradient interface (60% and 32%) were washed in isotonic buffer, pelleted at 10,000 g, and subsequently used for mitochondrial phospholipid quantification. Protein concentrations were determined by the BCA assay (Thermo Scientific).

Cellular and Mitochondrial Phospholipid Measurements

For the quantification of cellular and mitochondrial phospholipids, lipids were extracted from cells (1 g wet weight) or pure mitochondria (1.5 mg protein) using the Folch method (Folch et al., 1956), and individual phospholipids were separated by two-dimensional thin layer chromatography using the following solvent systems: chloroform/methanol/ammonium hydroxide (65:35:5) in first dimension followed by chloroform/acetic acid/methanol/water (75:25:5:2.2) in second dimension (Storey et al., 2001). Phospholipids were visualized with iodine vapor, scraped into glass tubes, and inorganic phosphate was quantified. The quantification of total cellular phospholipids was performed as previously described (Horvath et al., 2011). Briefly, 100 mg of SC glucose or SC lactate grown cells were digested with zymolyase, homogenized, and the cells debris were pelleted (3000 g, 5 min). Phospholipids were extracted from the cell free homogenate using the Folch method (Folch et al., 1956) and the total phospholipid phosphate was quantified using the Bartlett method (Bartlett, 1959). The mitochondrial phospholipid phosphate was extracted from 1.5 mg of pure mitochondria and was quantified using the Bartlett method (Bartlett, 1959).

Electron Microscopy

Yeast cells cultured in SC lactate medium were harvested and fixed in 3% glutaraldehyde contained in 0.1 M sodium cacodylate, pH 7.4, 5 mM $CaCl_2$, 5 mM $MgCl_2$, and 2.5% (w/v) sucrose for 1 h at room temperature with gentle agitation, spheroplasted, embedded in 2% ultra low temperature agarose (prepared in water), cooled, and subsequently cut into small pieces (~1 mm^3). The cells were then post-fixed

in 1% OsO_4 and 1% potassium ferrocyanide contained in 0.1 M sodium cacodylate for 1 h at room temperature. The blocks were washed thoroughly three times with double distilled H_2O, transferred to 1% thiocarbohydrazide at room temperature for 3 min, washed in double distilled H_2O twice, and transferred to 1% OsO_4 and 1% potassium ferrocyanide in 0.1 M sodium cacodylate, for an additional 3 min at room temperature. The cells were washed three times with double distilled H_2O and stained in Kellenberger's uranyl acetate at room temperature overnight. Cells were then dehydrated through a graded series of cold ethanol followed by room temperature 100% ethanol exchanges, washed twice in propylene oxide, left overnight in propylene oxide/Epon with gentle agitation and subsequently embedded in Epon resin. Sections were cut on a Leica Ultracut UCT ultramicrotome, and observed on a Philips EM420 transmission electron microscope at 100 kV. Images were recorded with a Soft Imaging System Megaview III digital camera, and figures were assembled in Adobe Photoshop with only linear adjustments in contrast and brightness.

Measurement of Oxygen Consumption and ATP Levels

For measurements of respiration rates, cells were grown to late-log phase in SC glucose or SC lactate media, resuspended in fresh media at 10^8 cells/ml (SC glucose) or $2x10^7$ cells/ml (SC lactate), and the rate of oxygen consumption was measured at 30°C using Oxytherm (Hansatech). Cyanide-sensitive respiration was calculated after the addition of 1 mM KCN, and the cyanide-insensitive respiration was subtracted from the total respiration. For cellular ATP quantification, cells were seeded at 250,000 cells/well in a 96-well plate, and ATP was measured using the BacTiter-Glo Microbial Cell

Viability Assay (Promega) kit according to the manufacturer's instructions. All data were normalized to the protein concentration, determined by the BCA assay (Thermo Scientific).

Sodium Dodecylsulfate (SDS)- Blue Native (BN)- Polyacrylamide Gel Electrophoresis (PAGE) and Immunoblotting

SDS-PAGE was performed on mitochondrial samples solubilized in lysis buffer (150 mM NaCl, 1 mM EDTA, 50 mM Tris–HCl, pH 7.4, 1% NP-40, 0.5% sodium deoxycholate and 0.1% SDS) supplemented with protease inhibitor cocktail (Roche Diagnostic). Protein extracts were separated on NuPAGE 4-12% Bis-Tris gels (Life-Technologies), transferred on PVDF membranes using a Trans–Blot transfer cell (Bio-Rad). Membranes were blocked in 5% fatty acid-free BSA dissolved in Tris–buffered saline with 0.1% Tween 20 and probed with antibodies as indicated. Blue native polyacrylamide gel electrophoresis (BN-PAGE) was performed to separate native MRC protein complexes as previously described (Wittig et al., 2006). Briefly, yeast mitochondria were solubilized in buffer containing 1% digitonin (Life-Technologies), and incubated for 15 min at 4°C. Following a clarifying spin at 20,000 × g (30 min, 4°C), 50x G-250 sample additive was added to the supernatant and 20 µg of protein was loaded on a 3-12% gradient native PAGE Bis–Tris gel (Life-Technologies). Western blot was performed using a Mini-PROTEAN Tetra cell (Bio-rad). Membrane was blocked in 5% nonfat milk in Tris–buffered saline with 0.1% Tween 20 and probed with antibodies as indicated. Primary antibodies for yeast proteins used were: Cox1, 1:5,000 (Abcam 110 270); Cox2, 1:50,000 (Abcam 110 271); Cox3, 1:5,000 (Abcam 110 259);

Cox4, 1:5,000 (Abcam 110 272): Sdh2, 1:5,000 (from Dr. Dennis Winge); Rip1, 1:100,000 (from Dr. Vincenzo Zara); Atp2, 1:40,000 (from Dr. Sharon Ackerman); Porin, 1:50,000 (Abcam 110 326); Dpm1, 1:250 (Abcam 113 686); Pho8, 1:250 (Abcam 113 688); Pgk1, 1:5,000 (Abcam 113 687). Secondary antibodies (1:5,000) were incubated for 1 h at room temperature, and membranes were developed using Western Lightning Plus-ECL (PerkinElmer).

In-gel Activity Measurements

In-gel activities for mitochondrial respiratory chain complexes were performed as described previously (Wittig et al., 2007). Clear Native Polyacrylamide Gel Electrophoresis (CN-PAGE) was used to avoid interference of Coomassie blue with activity measurements. Briefly, mitochondria solubilized in 1% digitonin were resolved on a 4-16% gradient native PAGE BisTris gel (Life-Technologies) using the following additions to the cathode buffer: for complex II, 0.01% n-Dodecyl β-D-maltoside (DDM) and 0.05% sodium deoxycholate (DOC) were added, for complex III there was no addition, for complex IV, 0.05% DDM and 0.05% DOC were added, and for complex V, 0.01% DDM and 0.05% DOC were added. Gels were loaded with 30 μg of protein for complex II, 90 μg of protein for complex III and IV, and 20 μg of protein for complex V, and incubated in activity staining solutions for complex II, III, IV, or V as reported previously (Wittig et al., 2007). Band intensity quantification was done using the gel analysis method in ImageJ. Equal loading was determined by Coomassie blue stain, and total protein and band intensity quantification was done using the gel analysis method in ImageJ.

CHAPTER III

ETHANOLAMINE ALLEVIATES OXIDATIVE STRESS AND MITOCHONDRIAL SUPERCOMPLEX ASSEMBLY DEFECTS IN CARDIOLIPIN DEFICIENT CELLS

Disclaimer

I did all the experiments described in this chapter except for the ones reported in Fig. 3.2, 3.3, 3.5, 3.6, 3.8, 3.14, and 3.15, which were performed by Dr. Writoban Basu Ball, John K. Neff, and Gabriel L. Apfel.

Summary

Barth syndrome (BTHS) is a severely debilitating genetic disorder characterized by perturbations in mitochondrial phospholipid composition derived from a primary defect in cardiolipin (CL) biosynthesis. CL, like phosphatidylethanolamine (PE), is a non-bilayer forming phospholipid that is synthesized in the mitochondria. Due to their similar biophysical properties, PE and CL have been proposed to have overlapping functions, raising an intriguing possibility that elevating mitochondrial PE levels may compensate for CL deficiency in BTHS mitochondria. To test this hypothesis, we used an ethanolamine (Etn) supplementation strategy to elevate mitochondrial PE, and demonstrated that Etn supplementation rescues the respiratory growth of CL deficient cells. Surprisingly, Etn-mediated rescue was independent of PE biosynthesis and was solely dependent on soluble phospholipid precursors Etn and propanolamine, but not choline. Etn rescued respiratory growth by restoring respiratory chain supercomplex assembly and reducing oxidative stress in CL deficient *taz1Δ* cells, a yeast model of BTHS. Although Etn partially rescued the respiratory growth defect of *crd1Δ* cells, which are completely devoid of CL, it failed to rescue supercomplex formation, suggesting that supercomplex formation *in vivo* requires a critical amount of CL. Etn-mediated rescue was specific to CL deficiency because Etn supplementation did not rescue respiratory defects caused by the loss of mitochondrial supercomplex assembly factors. Taken together, our work highlights a new role of Etn in attenuating mitochondrial dysfunction caused by CL deficiency.

Introduction

Barth syndrome (BTHS) is a severely debilitating X-linked genetic disorder characterized by cardiomyopathy, skeletal muscle myopathy, neutropenia, growth-delay, and exercise intolerance (Barth et al., 1983). BTHS is caused by loss-of-function mutations in the evolutionarily conserved tafazzin (*TAZ*) gene (Bione et al., 1996). *TAZ* encodes a mitochondrial transacylase that remodels cardiolipin (CL), a signature phospholipid of mitochondrial membranes (Xu et al., 2003; Xu et al., 2006). Studies from BTHS patient cells - as well as a number of model systems, including the yeast *Saccharomyces cerevisiae* - have shown that mitochondrial dysfunction caused by perturbation of mitochondrial membrane phospholipid composition is the primary cause of BTHS pathology (Vreken et al., 2000; Schlame et al., 2003; Gu et al., 2004). Specifically, a decrease in remodeled CL species and an increase in monolysocardiolipin (MLCL) levels have been identified as the main factors that lead to altered mitochondrial structure and function (Ye et al., 2014; Baile et al., 2014).

Apart from alterations in CL, perturbations in levels of other abundant mitochondrial phospholipids, including phosphatidylethanolamine (PE), have been observed in BTHS model organisms. For example, phospholipid analysis of yeast *taz1Δ* cells showed a significant increase in PE (Gu et al., 2004). Similarly, phospholipid analyses of cardiac tissue from children with BTHS showed a small increase in total PE, but almost a six-fold increase in C18:0-C18:2 species (Schlame et al., 2003; Valianpour et al., 2005). The downstream consequences of this altered mitochondrial phospholipid composition include the destabilization of the mitochondrial respiratory chain (MRC)

supercomplexes and increased oxidative stress (Brandner et al., 2005; McKenzie et al., 2006; Jiang et al., 2000; Chen et al., 2008).

PE and CL are both cone-shaped phospholipids with a tendency to form non-bilayer structures in membranes (Holthuis and Menon, 2014). The non-bilayer forming phospholipids are proposed to facilitate membrane fusion and influence the binding and activity of membrane proteins (van den Brink-van der Laan et al., 2004). Unlike the bilayer-forming phospholipids phosphatidylcholine (PC) and phosphatidylserine (PS), mitochondrial PE and CL are synthesized *in situ* from their precursors PS and phosphatidic acid (PA), respectively, which are imported from the endoplasmic reticulum (Fig. 3.1). In addition to the mitochondrial pathway that involves the decarboxylation of PS by Psd1, PE can be synthesized either by a non-mitochondrial ethanolamine-Kennedy pathway or by a lyso-PE requiring pathway (Fig. 3.1). Compared to other subcellular organelles, the mitochondrial inner membrane is highly enriched with PE and CL, which constitute up to half of the total phospholipids (Zinser et al., 1991). This suggests that these non-bilayer phospholipids have an important role in the structural organization of membranes harboring the MRC complexes. Indeed, previous studies using yeast *crd1Δ* cells that are deficient in CL biosynthesis have identified a specific role of CL in the MRC supercomplex formation (Zhang et al., 2002; Pfeiffer et al., 2003). Loss of CL is also accompanied by compromised mitochondrial bioenergetics (Jiang et al., 2000; Koshkin et al., 2000; Koshkin et al., 2002). More recently, it was shown that the loss of PE reduces MRC function in both yeast and mammalian cells due

to diminished MRC complex III and IV activities (Bottinger et al., 2012; Tasseva et al., 2013; Baker et al., 2016).

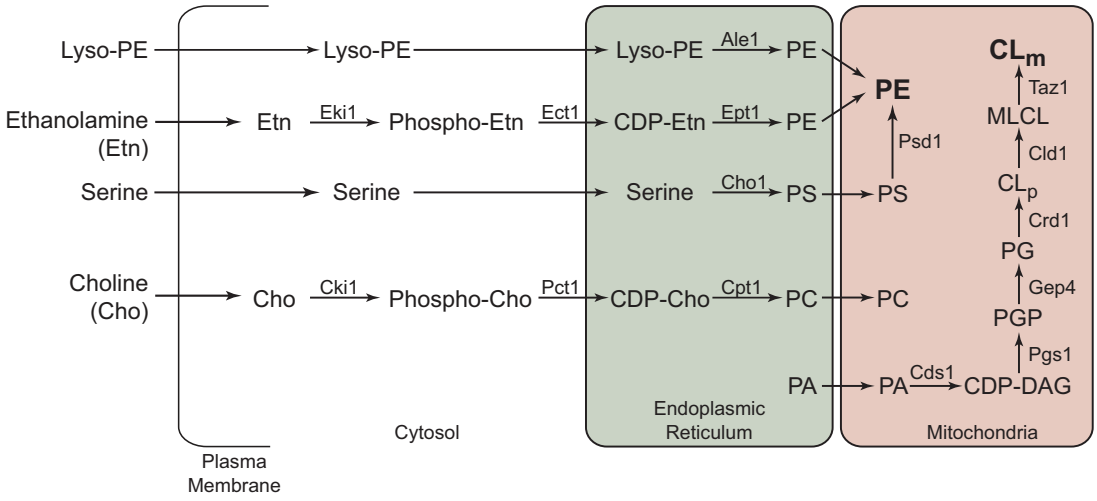

Figure 3.1 Biochemical pathways for PE, PC, and CL biosynthesis in the yeast *Saccharomyces cerevisiae*.

CL biosynthesis occurs exclusively in the mitochondria, where Crd1 synthesizes nascent CL_p from PG. The resulting CL_p is deacylated by the phospholipase Cld1 to produce monolysocardiolipin (MLCL), which is then reacylated by the transacylase Taz1 to form mature cardiolipin (CL_m). Mutations in the human homolog of TAZ1 result in Barth Syndrome. CL biosynthesis is dependent on the import of PA from endoplasmic reticulum (ER), which is converted to CDP-DAG by Cds1. Pgs1 catalyzes conversion of CDP-DAG to PGP, which is then dephosphorylated to PG by Gep4. PE biosynthesis in yeast occurs by three major pathways: (1) Psd1-catalyzed decarboxylation of PS in the mitochondria, (2) incorporation of Etn via the cytosolic/ER Kennedy pathway enzymes Eki1, Ect1, and Ept1, respectively, and (3) the acylation of lyso-PE by Ale1. The Kennedy pathway enzymes Cki1, Pct1, and Cpt1 can utilize choline to biosynthesize PC, a bilayerforming phospholipid that must be imported into mitochondria. CL_p, precursor cardiolipin; CL_m, mature cardiolipin; MLCL, monolysocardiolipin; PG, phosphatidylglycerol; PGP, phosphatidylglycerol phosphate; CDP, cytidine diphosphate; DAG, diacylglycerol; PA, phosphatidic acid; PS, phosphatidylserine; PE, phosphatidylethanolamine; PC, phosphatidylcholine.

Owing to their similar shape, site of biosynthesis, and propensity to form non-bilayer structures, PE and CL have been proposed to have overlapping functions (Gohil et al., 2005, Gohil and Greenberg 2009). For example, the simultaneous loss of mitochondrial PE and CL biosynthetic enzymes leads to synthetic lethality (Gohil et al.,

2005; Osman et al., 2009). Furthermore, both PE and CL are required for mitochondrial fusion (Joshi et al., 2012), protein import (Becker et al., 2013) and MRC activities (Jiang et al., 2000; Bottinger et al., 2012). In an *Escherichia coli* strain lacking PE, there is a three to five fold elevation of CL (Rietveld et al., 1993). Similarly, the disruption of CL biosynthesis in yeast results in increased mitochondrial PE (Zhong et al., 2004; Tuller et al., 1998), suggesting a compensatory mechanism in which the loss of one non-bilayer forming phospholipid is compensated by an increase in the levels of another. Together, these findings led us to hypothesize that MRC defects due to disruptions in CL biosynthesis may be rescued by increasing mitochondrial PE levels.

We recently showed that ethanolamine (Etn) supplementation increases mitochondrial PE levels in yeast (Baker et al., 2016), providing us with means to test our hypothesis. In the present study, we used an Etn-supplementation strategy in combination with yeast models of CL deficiency to demonstrate that Etn can rescue the respiratory growth of CL-depleted strains by restoring MRC supercomplex biogenesis and decreasing oxidative stress, both of which are key phenotypes associated with BTHS. Surprisingly, Etn-mediated rescue of CL-dependent respiratory phenotypes was found to be independent of PE biosynthesis, suggesting a novel role of Etn in rescuing the mitochondrial defects specific to CL deficient cells.

Results

Ethanolamine Supplementation Rescues the Respiratory Growth of CL Deficient Cells

Previous reports have shown that CL deficiency in yeast cells is accompanied by an increase in PE levels (Gu et; al., 2004; Zhong et. al., 2004; Tuller et al., 1998), suggesting a compensatory response to make up for the lack of CL. Therefore, we asked if further elevation of mitochondrial PE levels in CL deficient *taz1Δ* or *crd1Δ* cells could compensate for the loss of CL and rescue the respiratory growth defect observed in synthetic growth medium with ethanol as a carbon source (Ye et. al, 2014). To elevate mitochondrial PE levels, we utilized our recently described Etn supplementation strategy (Baker et. al, 2016) and found that 2 mM Etn rescued the respiratory growth defect of *taz1Δ* and *crd1Δ* cells in both solid and liquid growth media (Fig. 3.2A and B). Etn supplementation fully rescued the respiratory growth defect of CL-depleted *taz1Δ* cells and partially rescued the growth of CL-lacking *crd1Δ* cells (Fig. 3.2A and B). In order to rule out strain-specific effects, we also performed Etn supplementation experiments in a different mating-type strain and demonstrated similar respiratory growth rescue of CL-deficient cells (Fig 3.3).

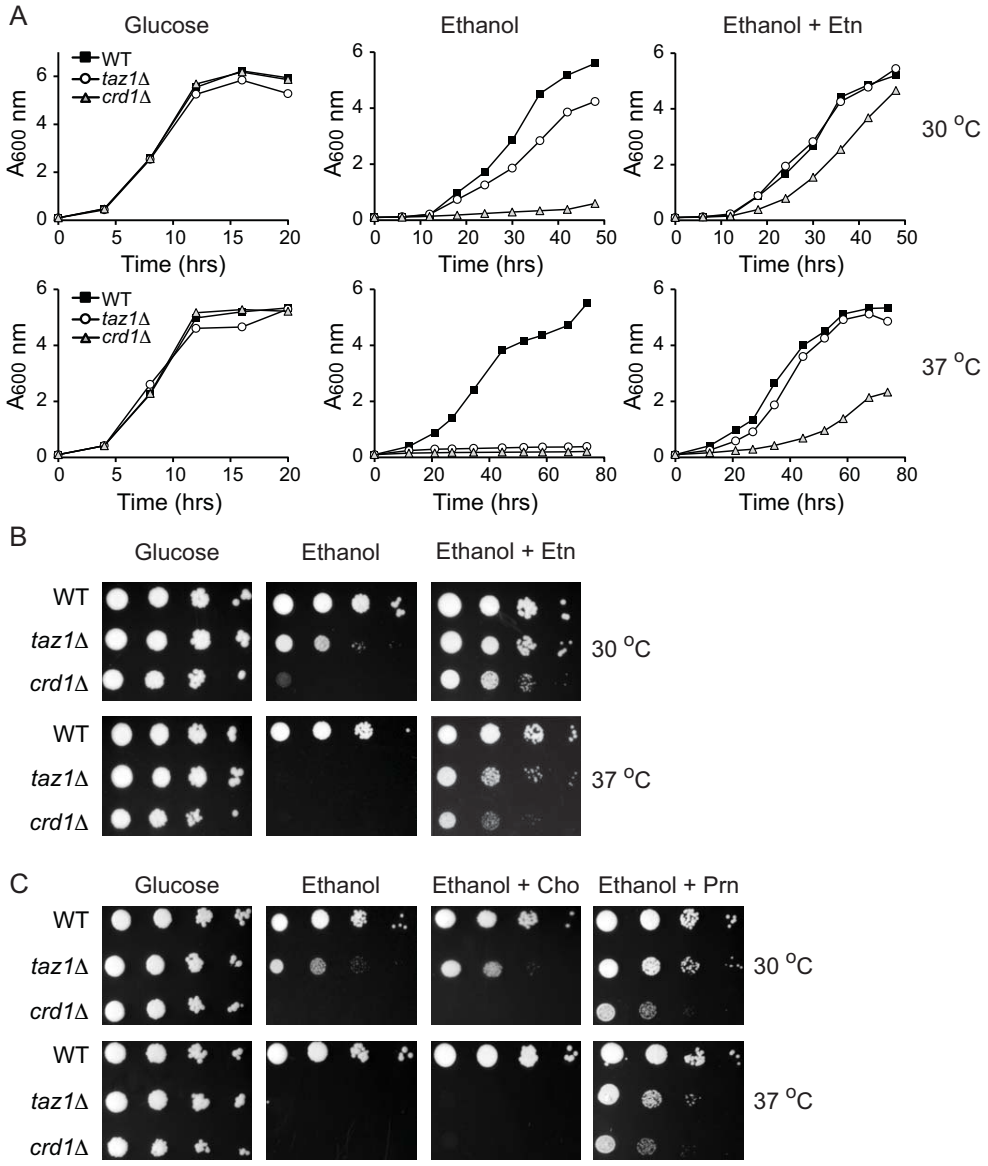

Figure 3.2 Ethanolamine supplementation rescues reduced respiratory growth of CL deficient yeast cells.

(A) The growth of wildtype (WT), *taz1Δ* and *crd1Δ* cells in SC glucose, SC ethanol, and SC ethanol + 2 mM ethanolamine (Etn) media at 30°C (upper panel) and 37°C (lower panel) was monitored by measuring absorbance at 600 nm. Data are representative of at least three independent measurements. (B) Ten-fold serial dilutions of WT, *taz1Δ* and *crd1Δ* cells were seeded on to SC glucose, SC ethanol and SC ethanol + 2 mM Etn and (C) SC ethanol + 2 mM choline (Cho) or 2 mM propanolamine (Prn) and images were captured after 2 days of growth on SC glucose, 5 days of growth on SC ethanol ± Etn, Cho or Prn at 30°C, and 7 days of growth on SC ethanol ± Etn, Cho or Prn at 37°C. Data are representative of at least three independent experiments.

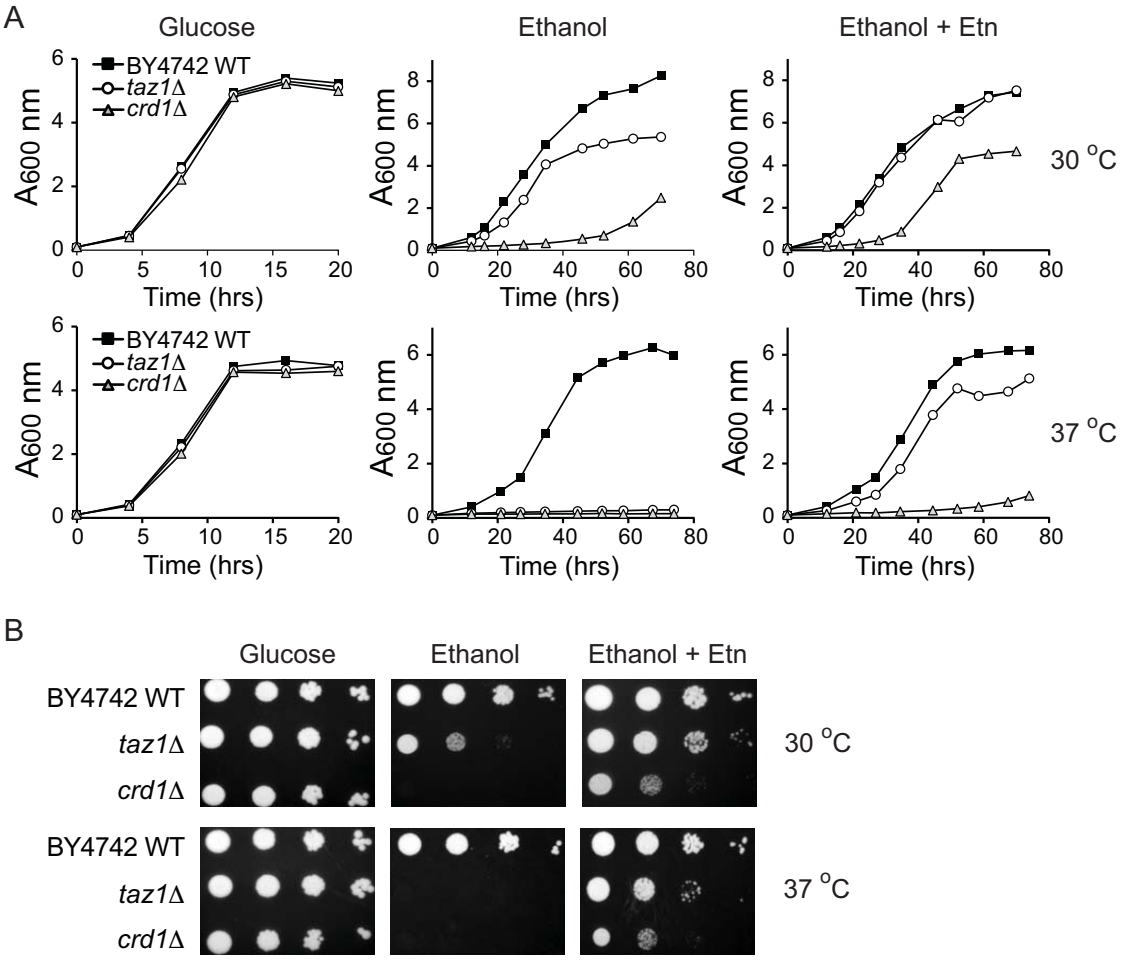

Figure 3.3 Ethanolamine supplementation rescues respiratory growth of CL-deficient cells in the BY4742 background.

(A) The growth of BY4742 WT, *taz1Δ* and *crd1Δ* cells in SC glucose, SC ethanol, and SC ethanol + 2 mM ethanolamine (Etn) at 30°C (upper panel) and 37°C (lower panel) was monitored by measuring absorbance at 600 nm. Data are representative of at least three independent measurements. (B) Ten-fold serial dilutions of WT, *taz1Δ* and *crd1Δ* cells were seeded on to the indicated media and images were captured after 2 days of growth on SC glucose, 5 days on SC ethanol ± 2 mM Etn at 30°C, and 7 days on SC ethanol ± 2 mM Etn at 37°C. Data are representative of at least three independent experiments.

To determine the specificity of Etn-mediated rescue, we supplemented respiratory media with other soluble phospholipid precursors utilized by the Kennedy pathway, including choline (Cho) and propanolamine (Prn). Cho is a substrate for the

biosynthesis of phosphatidylcholine, a major bilayer forming phospholipid of yeast cells, whereas Prn is a substrate for the non-natural, non-bilayer forming phospholipid phosphatidylpropanolamine (PP) (Storey et. al., 2001). We found that Prn supplementation rescued respiratory growth of *taz1Δ* and *crd1Δ* cells in a manner comparable to Etn, while Cho supplementation could not restore the respiratory growth of *taz1Δ* and *crd1Δ* cells (Fig. 3.2C). These results suggest a specific role of non-bilayer forming phospholipids or their precursors in compensating for the loss of CL.

Ethanolamine Supplementation Increases Mitochondrial PE in CL Deficient Yeast Cells

To confirm that Etn supplementation results in increased mitochondrial PE in *taz1Δ* and *crd1Δ* cells, we analyzed the mitochondrial phospholipid composition of cells grown with and without Etn. Consistent with the previous reports (Tuller et al., 1998, Gu et. al., 2004, Zhong et. al., 2004), mitochondrial phospholipid analysis of CL deficient cells revealed that, when compared to WT cells, PE was already elevated by 26% and 50% in *taz1Δ* and *crd1Δ* cells, respectively (Fig. 3.4A). The addition of Etn to the media resulted in a further 25% increase of mitochondrial PE levels in *taz1Δ* cells with a concomitant decrease in PC levels and a small but significant increase in MLCL levels (Fig. 3.4A). In *crd1Δ* cells, neither PE nor PC was significantly altered upon Etn supplementation, although there was a trend towards increased PE/PC ratio (Fig. 3.4A). Like Etn, Prn supplementation resulted in increased mitochondrial non-bilayer to bilayer phospholipid ratio in *taz1Δ* cells, with phoshphatidylpropanolamine (PP) forming almost 12% of total mitochondrial membrane phospholipids with a concomitant reduction in PC

(Fig. 3.4B). These results demonstrate that exogenous supplementation of phospholipid precursors Etn and Prn leads to increased levels of PE and PP in mitochondria.

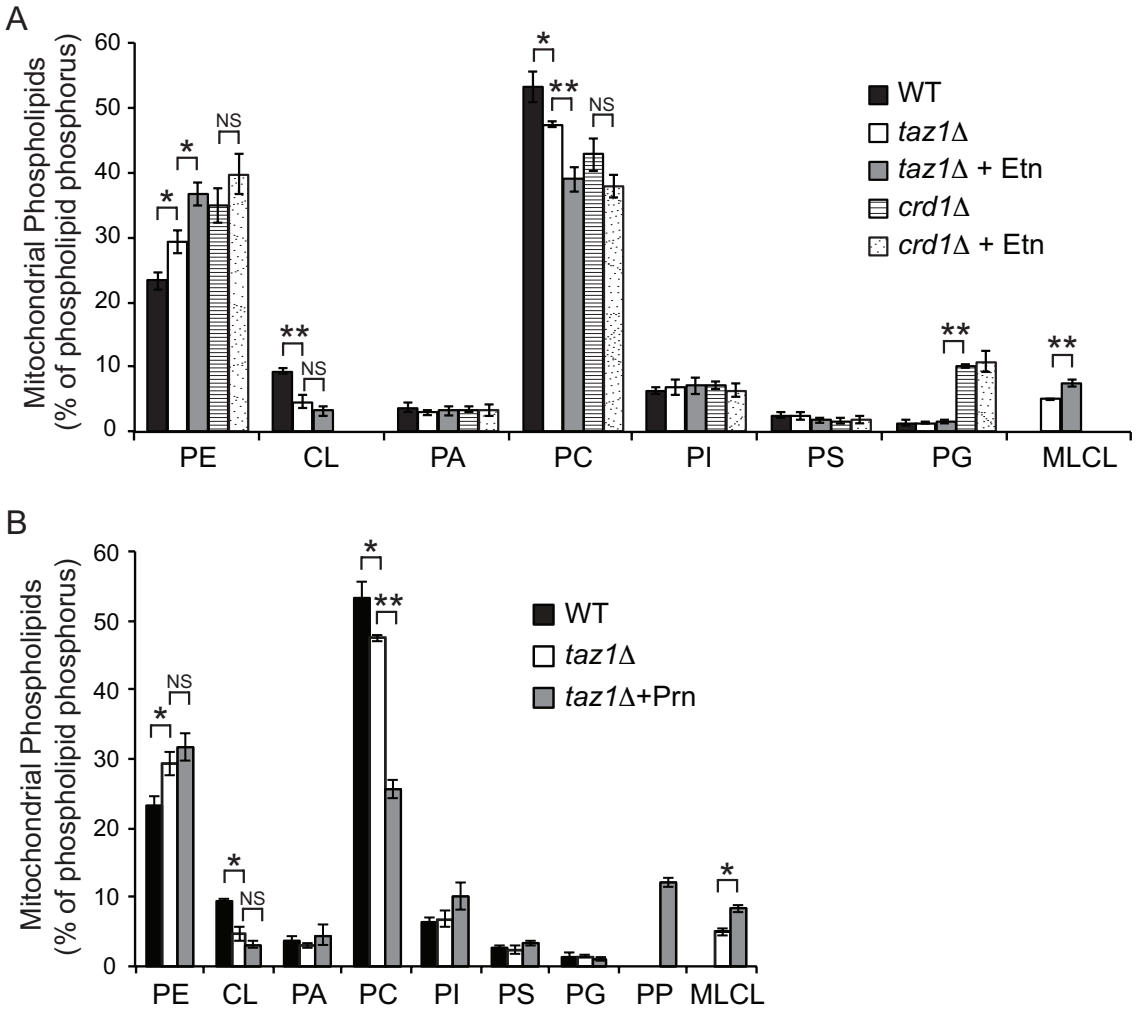

Figure 3.4 Ethanolamine and propanolamine supplementation elevates mitochondrial PE and PP levels in CL deficient cells.

(A) The mitochondrial phospholipid composition of WT cells grown in SC ethanol and *taz1Δ* and *crd1Δ* cells grown in SC ethanol with and without ethanolamine (Etn). Data are expressed as mean ± S.D. (n=3), **P < 0.005, *P < 0.05, NS = Not significant. (B) The mitochondrial phospholipid composition of WT cells grown in SC ethanol and *taz1Δ* cells grown in SC ethanol with and without 2 mM propanolamine (Prn). Data are expressed as mean ± S.D. (n=3), **P < 0.005, *P < 0.05, NS = Not significant. PE, phosphatidylethanolamine; CL, cardiolipin; PA, phosphatidic acid; PC, phosphatidylcholine; PI, phosphatidylinositol; PS, phosphatidylserine; PG, phosphatidylglycerol; PP, phosphatidylpropanolamine; MLCL, monolysocardiolipin.

Ethanolamine-Mediated Rescue of Respiratory Growth in CL Deficient Cells is Independent of PE Biosynthesis

While significant elevation of PE in *taz1Δ* cells can explain the rescue of respiratory growth, the lack of a further increase in PE upon Etn supplementation in *crd1Δ* cells suggests that PE may not be responsible for the observed rescue. To test the role of PE in rescuing CL deficiency, we used lyso-PE supplementation, which activates an alternate pathway for mitochondrial PE elevation (Riekhof and Voelker, 2006) (Fig. 3.1) and found that it did not rescue the respiratory growth of *taz1Δ* and *crd1Δ* cells (Fig. 3.5). Notably, lyso-PE and Etn supplementation fully rescued the reduced respiratory growth of mitochondrial PE depleted *psd1Δ* cells, indicating that these PE precursors get incorporated into mitochondrial PE (Fig. 3.6).

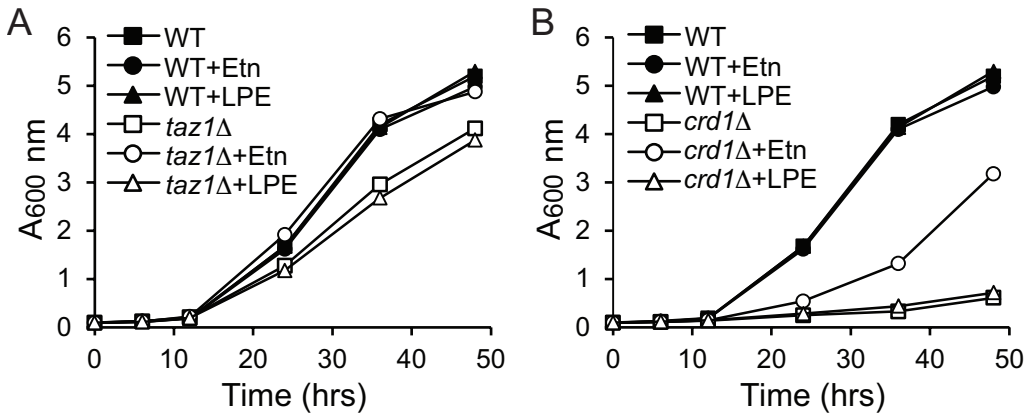

Figure 3.5 Lyso-PE supplementation does not rescue the respiratory growth of CL deficient cells.

(A) The growth of WT, *taz1Δ*, and (B) *crd1Δ* cells cultured in SC ethanol, SC ethanol + 2 mM Etn, and SC ethanol + 0.5 mM LPE media at 30°C was monitored by measuring absorbance at 600 nm. Data are representative of at least two independent measurements.

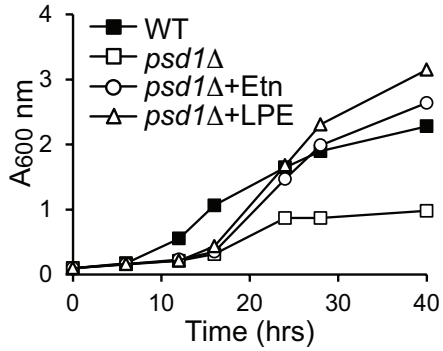

Figure 3.6 Lyso-PE supplementation rescues the respiratory growth of PE-deficient *psd1Δ* cells.

The growth of WT cells grown in SC lactate and *psd1Δ* cells grown in SC lactate, SC lactate + 2 mM ethanolamine (Etn), and SC lactate + 0.5 mM lyso-PE (LPE) media at 30°C was monitored by measuring absorbance at 600 nm. Data are representative of at least two independent measurements.

To completely rule out the requirement of PE biosynthesis from Etn supplementation, we deleted the gene encoding the rate-limiting enzyme of the Kennedy pathway, ethanolamine-phosphate cytidylyltransferase (Ect1), in *taz1Δ* and *crd1Δ* backgrounds. We analyzed the growth of *taz1Δect1Δ* and *crd1Δect1Δ* cells in respiratory media with and without Etn and observed that Etn supplementation rescued growth of the double mutants despite the absence of Ect1 (Fig. 3.7A and B). To confirm that the disruption of *ECT1* abolished the increased PE levels observed with Etn supplementation, we measured the cellular PE levels in WT and individual single and double mutants with and without Etn supplementation. As expected in the *ect1Δ* genetic background, cellular PE did not increase with Etn supplementation (Fig. 3.7C). Together, these results suggest that Etn-mediated rescue of *taz1Δ* and *crd1Δ* cells is independent of PE biosynthesis and mediated by either Etn itself or its downstream metabolites.

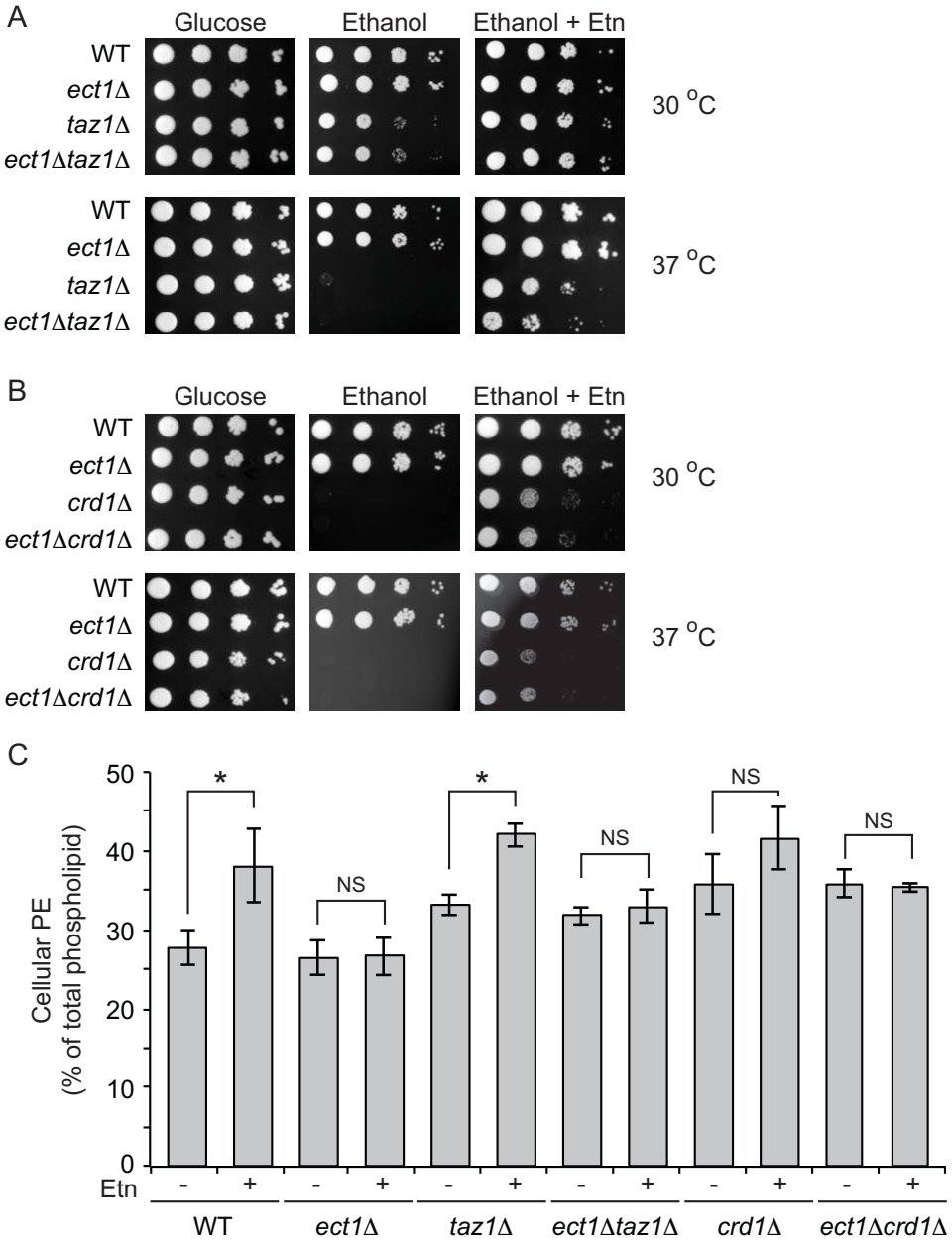

Figure 3.7 Ethanolamine-mediated rescue of respiratory growth of CL deficient cells is independent of PE biosynthesis.

(A) Ten-fold serial dilutions of WT, *ect1Δ*, *taz1Δ*, and *taz1Δect1Δ* cells and (B) WT, *ect1Δ*, *crd1Δ*, and *crd1Δect1Δ* cells were seeded on to the indicated media and images were captured after 2 days of growth on SC glucose, 5 days on SC ethanol ± 2 mM Etn at 30°C, and 7 days on SC ethanol ± 2 mM Etn at 37°C. Data are representative of at least three independent experiments. (C) Total cellular PE levels of the indicated strains grown in SC ethanol ± 2 mM Etn. Data are expressed as mean ± S.D. (n=3), *P<0.05, NS = Not significant.

The Kennedy pathway is not Required for the Ethanolamine-Mediated Rescue of the Respiratory Growth of *taz1Δ* and *crd1Δ* Cells

To examine the requirement of the Kennedy pathway in Etn-mediated rescue of *taz1Δ* and *crd1Δ* cells, we deleted ethanolamine kinase (Eki1) and choline kinase (Cki1), the enzymes that catalyze the first step in Etn and Cho conversion to PE and PC, respectively (Fig. 3.1). Both Eki1 and Cki1 have been shown to utilize Etn as a substrate, converting it into phosphoethanolamine (PEtn) (Kim et al., 1999). Therefore, we constructed the triple mutant *taz1Δeki1Δcki1Δ* and analyzed its growth on respiratory media in the absence and presence of Etn. We found that Etn supplementation was able to rescue the reduced respiratory growth of *taz1Δeki1Δcki1Δ* cells in a manner similar to *taz1Δ* cells (Fig. 3.8A). This result suggests that Etn itself, not PEtn or the downstream metabolites of the Kennedy pathway, mediates the respiratory growth rescue observed in CL deficient cells.

To determine if the import of Etn is necessary to rescue the observed growth defects, we performed co-supplementation assays with Cho because it negatively regulates the Etn importer (Fernández-Murray et al., 2013). Therefore, we supplemented the Etn-containing media with varying amounts of Cho and observed that the co-supplementation almost completely inhibited Etn rescue in a dose-dependent manner (Fig. 3.8B). Taken together, these results suggest a specific role of Etn in alleviating the respiratory growth defect in *taz1Δ* and *crd1Δ* cells.

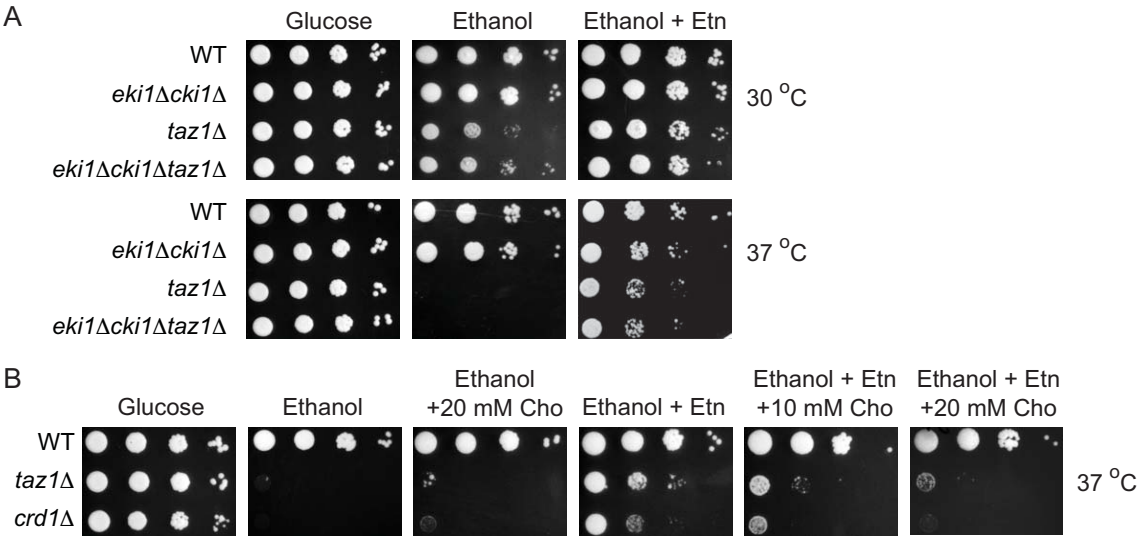

Figure 3.8 The Kennedy pathway metabolites are not required for the ethanolamine-mediated rescue of respiratory growth of *taz1Δ* and *crd1Δ* cells.

(A) Ten-fold serial dilutions of WT, *eki1Δcki1Δ*, *taz1Δ*, and *eki1Δcki1Δtaz1Δ* cells were seeded on to the indicated media and images were captured after 2 days of growth on SC glucose, 5 days on SC ethanol ± 2 mM Etn at 30°C, and 7 days on SC ethanol ± 2 mM Etn at 37°C. Data are representative of at least three independent experiments. (B) Ten-fold serial dilutions of WT, *taz1Δ*, and *crd1Δ* cells were spotted on to SC glucose, SC ethanol, SC ethanol + 20 mM choline (Cho), SC ethanol + 2 mM Etn, and SC ethanol + 2 mM Etn in combination with the indicated amount of Cho and images were captured after 2 days of growth on SC glucose, and 7 days on SC ethanol ± Etn, Cho or both at 37°C. Data are representative of at least three independent experiments.

Ethanolamine Supplementation Restores the Formation of Respiratory Supercomplexes in *taz1Δ* Cells

CL deficiency disrupts MRC supercomplex formation (Zhang et al., 2002; Pfeiffer et al., 2003; Brandner et al., 2005). To determine if Etn-mediated rescue of respiratory growth is due to the restoration of supercomplexes, we examined supercomplex formation in *taz1Δ* cells. Etn supplementation in *taz1Δ* cells partially restored the formation of the large supercomplex (III_2IV_2) and reduced the amounts of free complex III dimer (III_2) (Fig. 3.9A and B) and complex IV monomer (Fig. 3.9C and D). Etn supplementation did not result in alteration in the total amount of complex III

(Fig. 3.10A), but it did increase the total amount of complex IV (Fig. 3.10B). Consistent with the respiratory growth rescue, Prn supplementation also resulted in the restoration of MRC supercomplex formation in *taz1Δ* cells (Fig. 3.11). To determine if the Etn-mediated restoration of supercomplex levels in *taz1Δ* cells was due to increased mitochondrial PE levels, we examined supercomplex formation in *taz1Δect1Δ* cells, which cannot synthesize PE via the Kennedy pathway. In a manner identical to *taz1Δ* cells, Etn was able to promote the formation of the large supercomplex in *taz1Δect1Δ* cells (Fig. 3.9E and F). These results clearly indicate that Etn promotes respiratory supercomplex formation in CL depleted *taz1Δ* cells independent of increased PE biosynthesis.

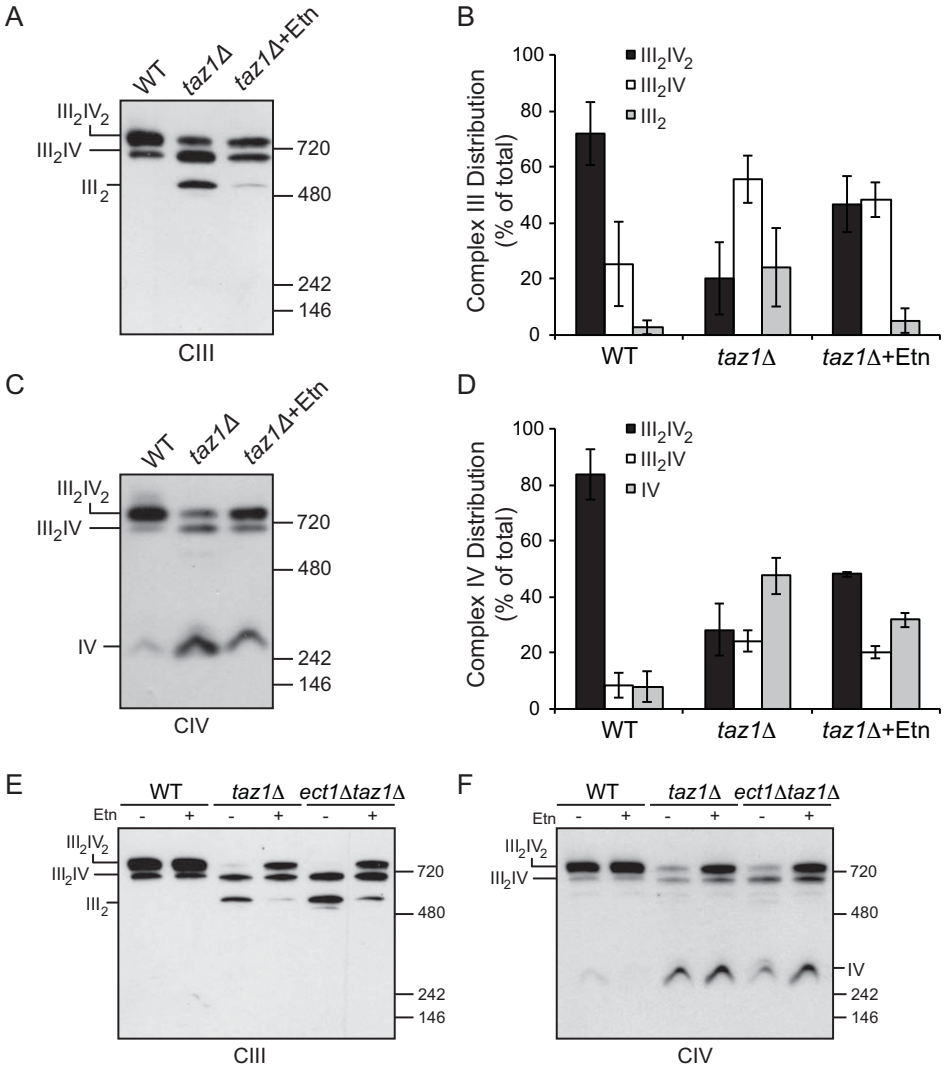

Figure 3.9 Ethanolamine supplementation restores supercomplex formation in *taz1Δ* and *taz1Δect1Δ* cells.

(A) Mitochondria from WT cells grown in SC ethanol and *taz1Δ* cells grown in SC ethanol ± 2 mM Etn were solubilized by 1% digitonin and subjected to BN-PAGE/western blot analysis. Complexes containing MRC complex III were detected by anti-Rip1 antibody. (B) The relative abundance of MRC complex III containing complexes from (A) were quantified by densitometric analysis. Data are expressed as mean ± S.D. (n=3) (C) Samples from (A) were probed with anti-Cox2 antibody to detect MRC complex IV containing supercomplexes and free complex IV. (D) Relative abundance of MRC complex IV containing complexes from (C) were quantified by densitometric analysis. Data are expressed as mean ± S.D. (n=3) (E) Mitochondria from WT, *taz1Δ*, and *taz1Δect1Δ* cells grown in SC ethanol ± 2 mM Etn were solubilized by 1% digitonin and subjected to BN-PAGE/western blot analysis, and MRC complexes III and (F) IV were detected by probing with anti-Rip1 and anti-Cox2 antibodies, respectively. (III_2IV_2, large supercomplex; III_2IV, small supercomplex; III_2, complex III dimer and IV, free complex IV)

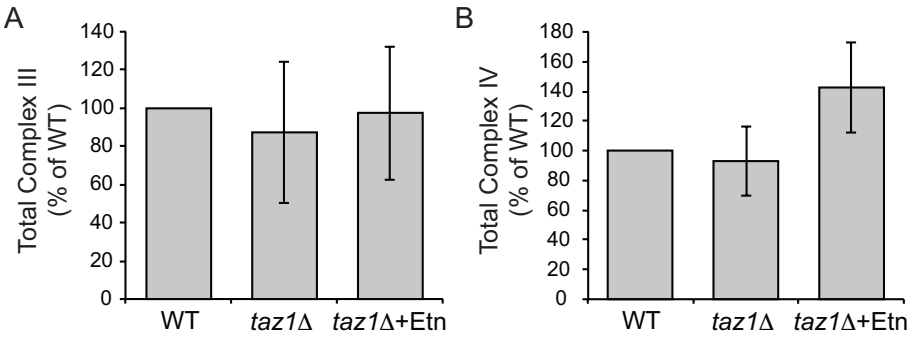

Figure 3.10 Ethanolamine supplementation elevates MRC complex IV levels in CL-deficient *taz1Δ* cells.

(A) MRC complex III levels from BN-PAGE/western blots shown in Figure 3.9A and (B) MRC complex IV levels from BN-PAGE/western blots shown in Figure 3.9C were quantified by densitometric analysis. Data are expressed as mean ± S.D. (n=3)

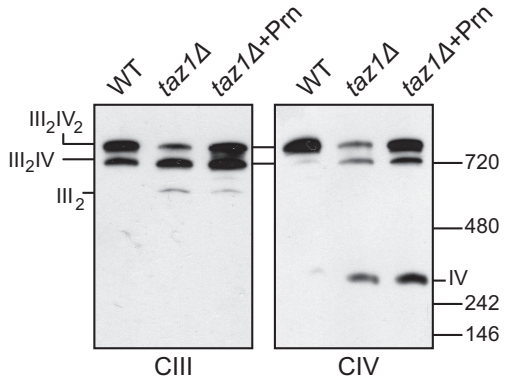

Figure 3.11 Propanolamine supplementation partially restores supercomplex formation in CL-deficient *taz1Δ* cells.

Mitochondria from WT cells grown in SC ethanol and *taz1Δ* cells grown in SC ethanol with and without 2 mM propanolamine (Prn) were solubilized by 1% digitonin and subjected to BN-PAGE/western blot analysis. Anti-Rip1 and anti-Cox2 antibodies detected mitochondrial respiratory chain supercomplexes containing complex III and complex IV, respectively. Data are representative of at least three independent experiments.

Ethanolamine-Mediated Rescue of Mitochondrial Function is Specific to CL Deficiency

Previous reports have shown that a complete lack of CL in *crd1Δ* cells results in a more pronounced decrease in supercomplex formation, and that CL is specifically and absolutely required for supercomplex reconstitution *in vitro* (Bazan et al., 2013).

Consistent with these reports, we found that supercomplex formation in *crd1Δ* cells was not restored with Etn supplementation (Fig. 3.12A-D). Interestingly, Etn supplementation increased the levels of the complex IV monomer as well as total complex IV levels in *crd1Δ* cells (Fig. 3.12C, D, and F), without altering the levels of complex III (Fig. 3.12E). In order to determine if the increased levels of complex IV upon Etn supplementation resulted in increased complex IV activity, we performed in-gel activity measurements and observed the restoration of complex IV activity in *crd1Δ* mitochondria (Fig. 3.12G and H). These results indicate that Etn-mediated rescue of respiratory growth in *crd1Δ* cells could be due to restoration of complex IV activity and not supercomplex formation per se.

Figure 3.12 Ethanolamine supplementation restores MRC complex IV activity in *crd1Δ* cells.

(A) Mitochondria from WT cells grown in SC ethanol and *crd1Δ* cells grown in SC ethanol ± 2 mM Etn were solubilized by 1% digitonin and subjected to BN–PAGE/western analysis. MRC complex III containing complexes were detected by anti-Rip1 antibody. (B) Relative abundance of MRC complex III containing complexes from (A) were quantified by densitometric analysis. Data are expressed as mean ± S.D. (n=3). (C) Samples from (A) were probed with anti-Cox2 antibody to detect MRC complex IV containing supercomplexes and free complex IV. (D) Relative abundance of MRC complex IV containing complexes from (C) were quantified by densitometric analysis. Data are expressed as mean ± S.D. (n=3). (E) Total levels of MRC complex III and (F) complex IV from samples (A) and (C) respectively. (G) Digitonin-solubilized MRC complexes from WT and *crd1Δ* cells were separated by Clear Native (CN-PAGE), followed by in-gel activity staining for complex IV. (H) In-gel activity of complex IV was quantified by densitometric analysis, and relative activity was plotted. Data were normalized to WT cells and expressed as mean ± SD (n = 3); *$p < 0.05$.

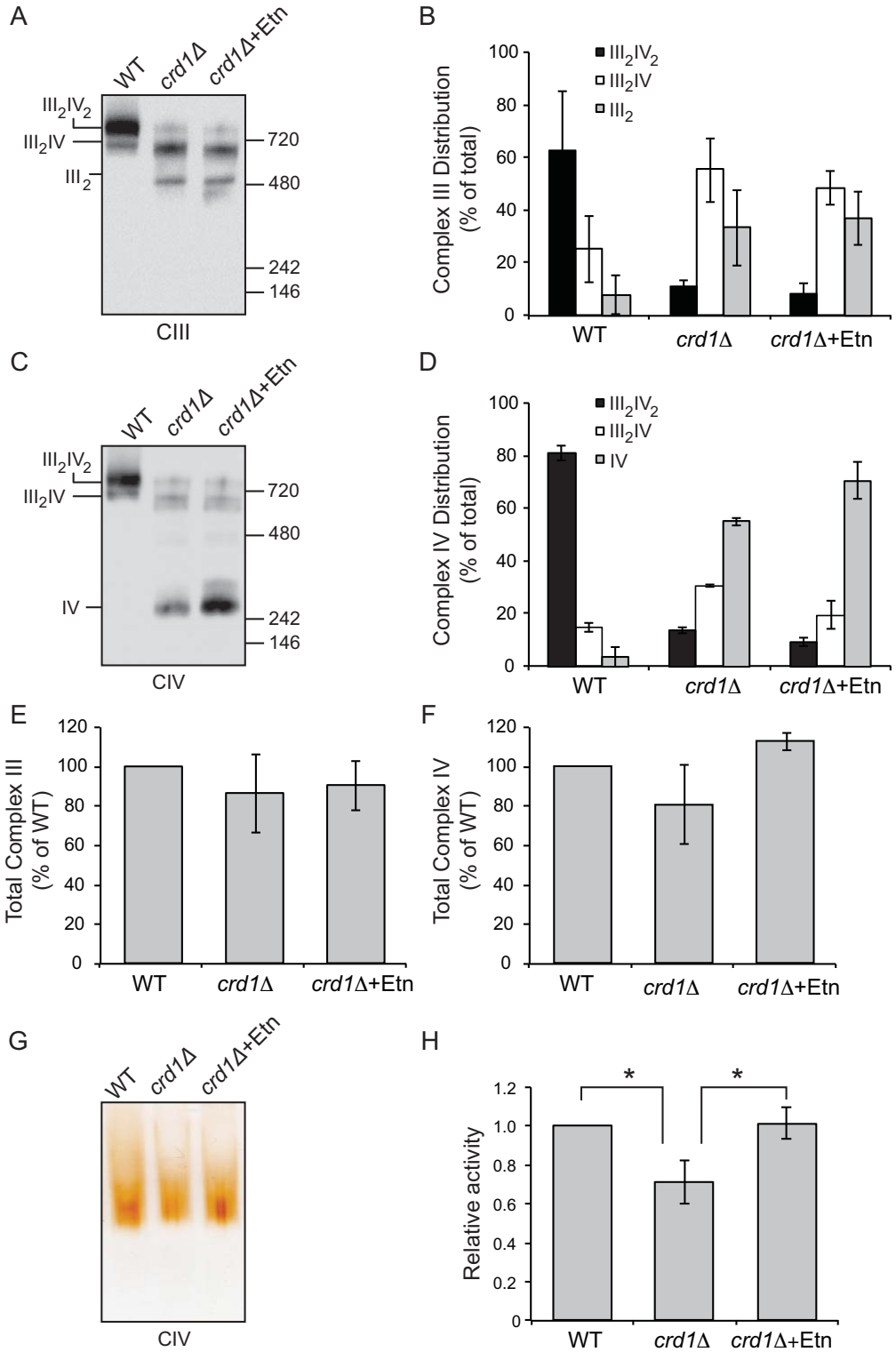
A
WT
crd1Δ
crd1Δ+Etn
III2IV2
III2IV
III2
720
480
242
146
CIII
B
Complex III Distribution (% of total)
III2IV2
III2IV
III2
100
80
60
40
20
0
WT
crd1Δ
crd1Δ+Etn
C
WT
crd1Δ
crd1Δ+Etn
III2IV2
III2IV
IV
720
480
242
146
CIV
D
Complex IV Distribution (% of total)
III2IV2
III2IV
IV
100
80
60
40
20
0
WT
crd1Δ
crd1Δ+Etn
E
Total Complex III (% of WT)
120
100
80
60
40
20
0
WT
crd1Δ
crd1Δ+Etn
F
Total Complex IV (% of WT)
120
100
80
60
40
20
0
WT
crd1Δ
crd1Δ+Etn
G
WT
crd1Δ
crd1Δ+Etn
CIV
H
Relative activity
1.2
1.0
0.8
0.6
0.4
0.2
0
*
*
WT
crd1Δ
crd1Δ+Etn

Recently, two respiratory supercomplex assembly factors, Rcf1 and Rcf2, were shown to associate with MRC complex III and IV, thereby stabilizing MRC supercomplex formation (Strogolova et al., 2012; Chen et al., 2012). In order to determine if Etn-mediated rescue of mitochondrial defects is specific to CL related deficiencies, we monitored the growth of *rcf1Δ* and *rcf2Δ* cells in non-fermentable media with and without Etn. Consistent with the previous report (Chen et al., 2012), *rcf1Δ* cells exhibited more pronounced growth defect compared to *rcf2Δ* cells in respiratory media (Fig. 3.13). However, Etn-supplementation failed to rescue the reduced respiratory growth of either *rcf1Δ* or *rcf2Δ* cells (Fig. 3.13). Finally, in order to determine if Etn supplementation could rescue the lack of a functional respiratory chain, we monitored the growth of *sdh2Δ, bcs1Δ, shy1Δ,* and *atp12Δ* cells, which are mutants defective in MRC complexes II-V respectively. We found that Etn supplementation did not rescue respiratory growth of these MRC mutants (Fig. 3.14). Together, these results suggest that Etn-mediated rescue of mitochondrial defects is specific to CL deficiency and not the lack of MRC assembly factors.

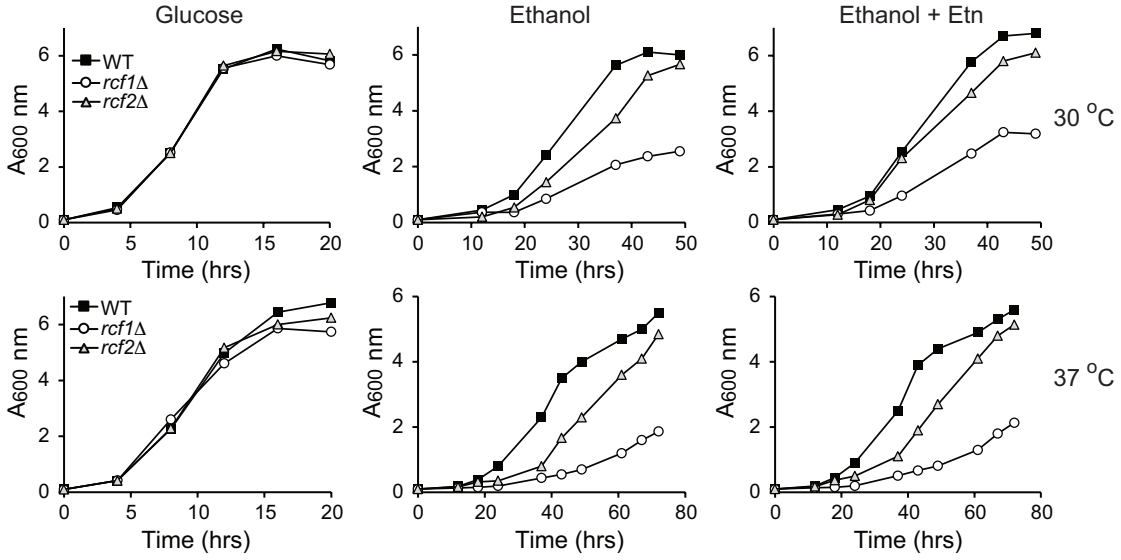

Figure 3.13 Ethanolamine supplementation does not rescue the respiratory growth defect of *rcf1Δ* and *rcf2Δ* cells.

The growth of WT, *rcf1Δ* and *rcf2Δ* cells in SC glucose, SC ethanol, and SC ethanol + 2 mM ethanolamine (Etn) media was monitored at 30°C (upper panel) and 37°C (lower panel) by measuring absorbance at 600 nm. Data are representative of at least two independent measurements.

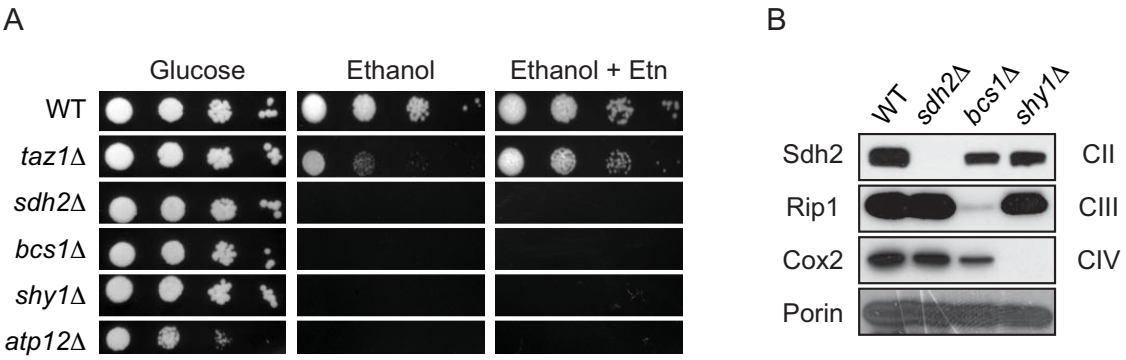

Figure 3.14 Ethanolamine supplementation does not rescue the respiratory growth of mitochondrial respiratory chain mutants.

(A) Ten-fold serial dilutions of WT, *taz1Δ*, *sdh2Δ*, *bcs1Δ*, *shy1Δ*, and *atp12Δ* cells were seeded on to plates containing the indicated media and images were captured after 2 days of growth on SC glucose and 5 days of growth on SC ethanol ± 2 mM Etn at 30°C. Data are representative of at least three independent experiments. (B) Mitochondria from YP galactose grown WT, *sdh2Δ*, *bcs1Δ* and *shy1Δ* cells were subjected to western bot analysis. Mitochondrial respiratory chain complexes II, III, and IV (CII, CIII, and CIV) were probed using anti-Sdh2, anti-Rip1, and anti-Cox2 antibodies, respectively. Porin was used as a loading control.

Ethanolamine Supplementation Reduces Protein Carbonylation in CL Deficient Cells

One of the hallmarks of CL depletion and BTHS pathology across multiple model systems, including the yeast BTHS model *taz1Δ*, is increased oxidative stress (Chen et al., 2008; Hsu et al., 2015; Wang et al., 2014). To determine if Etn supplementation could alleviate oxidative stress in CL deficient cells, we measured cellular protein carbonylation, a sensitive indicator of oxidative stress (Chen et al., 2008). Consistent with a previous report (Chen et al., 2008), we also observed that *taz1Δ* and *crd1Δ* cells had increased cellular protein carbonylation. Etn supplementation reduced protein carbonylation in both *taz1Δ* and *crd1Δ* cells (Fig. 3.15A). In order to determine if Etn-mediated reduction of protein carbonylation was independent of PE biosynthesis, we measured protein carbonylation in the double mutants *taz1Δ*ect*1Δ* and *crd1Δ*ect*1Δ* and found that Etn was still able to reduce carbonylation (Fig. 3.15B). Together, these results demonstrate that Etn supplementation reduces oxidative stress in *taz1Δ* and *crd1Δ* cells.

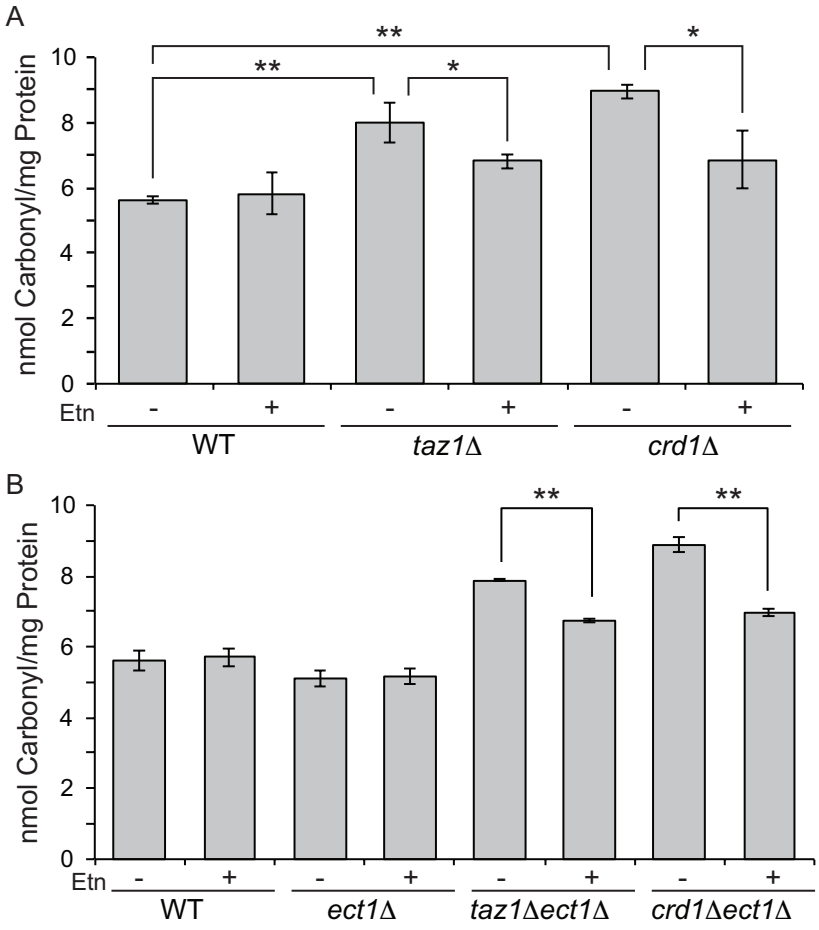

Figure 3.15 Ethanolamine supplementation reduces protein carbonylation in CL deficient cells.

(A) WT, *taz1Δ*, and *crd1Δ* or (B) WT, *ect1Δ*, *taz1Δect1Δ*, and *crd1Δect1Δ* cells were grown in SC ethanol ± 2 mM Etn to early stationary phase, protein was extracted and protein carbonylation was measured as described in Materials and Methods. Data are expressed as mean ± S.D. (n=3), **P < 0.005 and *P < 0.05.

Discussion

We report a novel role for the phosphatidylethanolamine precursor Etn in ameliorating mitochondrial dysfunction caused by perturbations in mitochondrial membrane phospholipid composition due to CL deficiency. We serendipitously discovered this new role of Etn while testing the hypothesis that elevating mitochondrial

PE by exogenous Etn supplementation could rescue mitochondrial defects of CL deficient BTHS yeast model. Here, we show that Etn ameliorates mitochondrial dysfunction in CL deficient cells without increasing PE levels. Specifically, Etn exerted its protective effect by restoring MRC supercomplex formation and reducing oxidative stress in CL depleted cells. Notably, Etn supplementation failed to alleviate the respiratory defects caused by the loss of MRC supercomplex assembly factors and thus, was specific to CL deficiency.

While the phospholipid precursors including choline and inositol are known to influence cellular physiology by regulating the expression of phospholipid biosynthetic genes (Henry et al., 2012), very little is known about the role of Etn outside of its incorporation into PE. Previous work has shown that Etn and phosphoethanolamine can directly modulate mitochondrial function (Modica-Napolitano and Renshaw, 2004). In fact, pharmacological elevation of phosphoethanolamine by meclizine, an anti-nausea drug, has been shown to protect the kidney from the ischemia-reperfusion injury by altering mitochondrial bioenergetics (Kishi et al., 2015). Therefore, we asked whether Etn mediated its effect by incorporation into phosphoethanolamine. We addressed this question by constructing the triple knockout strain, *taz1Δeki1Δcki1Δ*, which cannot phosphorylate ethanolamine. Our results show that Etn supplementation was still able to rescue the respiratory deficient growth of the triple knockout cells, indicating that phosphethanolamine is unlikely to contribute to the observed rescue (Fig. 3.8).

In order to understand the biochemical basis by which Etn restored the respiratory growth of CL depleted cells, we examined the formation and function of

MRC supercomplexes. Previous reports have shown that CL deficiency results in diminished MRC supercomplexes, leading to respiratory defects in both the yeast and mammalian models of BTHS (Brandner et al., 2005; McKenzie et al., 2006). Remarkably, exogenous supplementation of the soluble phospholipid precursor Etn was able to rescue MRC supercomplex levels in the CL-depleted mitochondrial membranes of *taz1Δ* cells (Fig. 3.9). Interestingly, there was no restoration of supercomplexes in *crd1Δ* cells (Fig. 3.12A-D), which are completely devoid of CL (Fig. 3.4). The lack of supercomplex formation in CL deficient *crd1Δ* cells grown in the presence of Etn suggests that a critical amount of CL is absolutely essential for supercomplex formation and may explain why Etn only partially rescued the respiratory growth of *crd1Δ* cells (Fig. 3.2). These findings are consistent with the *in vitro* supercomplex reconstitution experiments showing a specific requirement of CL for supercomplex assembly (Bazan et al., 2013; Mileykovskaya and Dowhan, 2014).

One of the proposed roles of MRC supercomplex formation is to reduce the generation of reactive oxygen species by efficient substrate channeling (Acin-Perez and Enriquez, 2014; Genova and Lenaz, 2014). Consistent with this idea, increased oxidative stress has been observed in different models of BTHS, possibly due to reduced MRC supercomplex levels (Chen et al., 2008; Hsu et al., 2015; Wang et al., 2014). Our results show that Etn supplementation reduced protein carbonylation in *taz1Δ* and *crd1Δ* cells (Fig. 3.15). Interestingly, reduction in oxidative stress in *crd1Δ* cells was not accompanied by the restoration of supercomplex formation (Fig. 3.12). This finding not only raises questions about the physiological role of supercomplex formation, but also

about the cause(s) of increased oxidative stress in CL deficient cells. It is possible that the decreased MRC complex IV activity observed in *crd1Δ* cells leads to increased oxidative stress, which could explain why Etn-mediated restoration of complex IV activity concurrently reduced oxidative stress (Figs. 3.12G, H and 3.15). However, the cause-effect relationship between supercomplex biogenesis and oxidative stress has been difficult to determine because the two phenomena influence one another (Genova and Lenaz, 2014).

The most important question raised by our study is how does Etn reduce oxidative stress and elevate MRC supercomplex levels in CL deficient *taz1Δ* cells. A number of physiological parameters have been shown to influence supercomplex formation. For example, the protein to phospholipid ratio of membranes governs the extent of supercomplex formation (Genova and Lenaz, 2014). In a recent study, increased complex IV biogenesis was shown to stabilize supercomplexes (Genova et al., 2008). Similarly, we also observe an increase in complex IV levels upon Etn supplementation (Fig. 3.10), which provides a potential mechanism for increased supercomplex formation. The abundance of supercomplex formation is correlated with the unsaturation and homogeneity of CL species (Genova et al. 2008). Additionally, lipid peroxidation has also been suggested to regulate supercomplex formation (Genova and Lenaz, 2014). Finally, membrane shape has also been proposed to influence supercomplex formation (Cogliati et al., 2013). Etn may directly or indirectly affect any of these parameters to promote supercomplex formation. Lipidomic and microscopic

analysis of Etn supplemented cells could provide clues to the novel functions of Etn, experiments that are currently underway in our laboratory.

While the precise mechanism by which Etn promotes supercomplex formation and reduces oxidative stress remains elusive at this time, a number of important conclusions can be drawn from this study. First, Etn mediates its effect on mitochondria - either directly or by incorporation into a yet unidentified metabolite that is not PE (Fig. 3.7). Second, the protective effect of Etn is specific to CL deficiency because Etn-supplementation fails to rescue mitochondrial dysfunction in cells lacking MRC assembly factors (Figs. 3.13 and 3.14). Third, Etn is able to overcome the accumulation of MLCL (Fig. 3.4), which has recently been shown to be the main cause of mitochondrial dysfunction in yeast models of BTHS (Ye et al., 2014; Bale et al., 2014).

Henry and colleagues (Henry et al., 2012) predicted novel roles of lipid precursors in cellular physiology and suggested the suitability of the yeast *Saccharomyces cerevisiae* model system to uncover such processes. Our work, demonstrating a novel role of the soluble lipid precursor Etn in ameliorating mitochondrial dysfunction caused by CL deficiency in yeast model of BTHS, provides strong support for their prediction.

Materials and Methods

Yeast Strains, Growth Medium Composition, and Culture Conditions

Saccharomyces cerevisiae strains used in this study are listed in Table 3.1. These strains were confirmed by polymerase chain reaction as well as by replica plating on

dropout plates. Single and double knockout yeast strains were constructed by one-step gene disruption using hygromycin or clonNat (nourseothricin) resistance cassettes amplified from pFA6a-hphNT1 or pFA6a-natNT2 plasmids, respectively (Janke et al., 2004). The primers used for one-step gene disruption are listed in Table 3.2. For growth in liquid media, strains were pre-cultured in YPD medium [1% yeast extract, 2% peptone, and 2% dextrose] and inoculated into SC media [0.2% dropout mix containing amino acid and other supplements as previously described (Amberg et al., 2005), 0.17% yeast nitrogen base without amino acids and ammonium sulfate, and 0.5% ammonium sulfate] containing either 2% glucose, 2% lactate (pH 5.5) or 2% ethanol and grown to late logarithmic phase. Solid media were prepared by the addition of 2% agar to the media described above. Yeast strains were inoculated into liquid SC glucose, SC lactate and SC ethanol at a starting at an optical density 0.1 at 600 nm and growth was monitored for up to 20 hrs (SC glucose), 40 hrs (SC lactate) or 80 hrs (SC ethanol) at 30°C and 37°C. For growth on solid media, ten-fold serial dilutions of overnight pre-cultures were seeded on SC glucose or SC ethanol plates and incubated at 30°C or 37°C for 2 days (SC glucose) and 5 or 7 days (SC ethanol), respectively. For Etn supplementation experiments, 2 mM Etn was added to SC growth medium. For media containing lyso-PtdEtn, 1% (v/v) Tergitol Nonidet P-40 was included, and lyso-PtdEtn was added to the final concentration of 0.5 mM from a sterile 25 mM stock solution in 10% (v/v) Tergitol Nonidet P-40 (Riekhof and Voelker, 2006).

Table 3.1 *Saccharomyces cerevisiae* strains used in this study

Yeast Stains	Genotype	Source
BY4742 WT	*MATα, his3Δ1, leu2Δ0, lys2Δ0, ura3Δ0*	Greenberg, M.L.
BY4742 *taz1Δ*	*MATα, his3Δ1, leu2Δ0, lys2Δ0, ura3Δ0, taz1Δ::hphNT1*	This study
VGY1	*MATα, his3Δ1, leu2Δ0, lys2Δ0, ura3Δ0, crd1Δ::URA3*	Greenberg, M.L.
BY4741 WT	*MATa, his3Δ1, leu2Δ0, met15Δ0, ura3Δ0*	Greenberg, M.L.
BY4741 *taz1Δ*	*MATa, his3Δ1, leu2Δ0, met15Δ0, ura3Δ0, taz1Δ::kanMX4*	Open Biosystems
BY4741 *crd1Δ*	*MATa, his3Δ1, leu2Δ0, met15Δ0, ura3Δ0, crd1Δ::kanMX4*	Open Biosystems
BY4741 *psd1Δ*	*MATa, his3Δ1, leu2Δ0, met15Δ0, ura3Δ0, psd1Δ::kanMX4*	Open Biosystems
BY4741 *ect1Δ*	*MATa, his3Δ1, leu2Δ0, met15Δ0, ura3Δ0, ect1Δ::hphNT1*	This study
BY4741 *taz1Δect1Δ*	*MATa, his3Δ1, leu2Δ0, met15Δ0, ura3Δ0, taz1Δ::kanMX4, ect1Δ::hphNT1*	This study
BY4741 *crd1Δect1Δ*	*MATa, his3Δ1, leu2Δ0, met15Δ0, ura3Δ0, crd1Δ::kanMX4, ect1Δ::hphNT1*	This study
BY4741 *eki1Δcki1Δ*	*MATa, his3Δ1, leu2Δ0, met15Δ0, ura3Δ0, eki1Δ::natNT2, cki1Δ::hphNT1*	This study
BY4741 *eki1Δcki1Δtaz1Δ*	*MATa, his3Δ1, leu2Δ0, met15Δ0, ura3Δ0, taz1Δ::kanMX4, eki1Δ::natNT2, cki1Δ::hphNT1*	This study
BY4741 *sdh2Δ*	*MATa, his3Δ1, leu2Δ0, met15Δ0, ura3Δ0, sdh2Δ::kanMX4*	Open Biosystems
BY4741 *bcs1Δ*	*MATa, his3Δ1, leu2Δ0, met15Δ0, ura3Δ0, bcs1Δ::kanMX4*	Open Biosystems
BY4741 *shy1Δ*	*MATa, his3Δ1, leu2Δ0, met15Δ0, ura3Δ0, shy1Δ::kanMX4*	Open Biosystems
BY4741 *atp12Δ*	*MATa, his3Δ1, leu2Δ0, met15Δ0, ura3Δ0, atp12Δ::kanMX4*	Open Biosystems
BY4741 *rcf1Δ*	*MATa, his3Δ1, leu2Δ0, met15Δ0, ura3Δ0, rcf1Δ::kanMX4*	Open Biosystems
BY4741 *rcf2Δ*	*MATa, his3Δ1, leu2Δ0, met15Δ0, ura3Δ0, rcf2Δ::kanMX4*	Open Biosystems

Table 3.2 Primers used in this study

The bold face letters represent sequences that are complementary to the flanking sequences of the hygromycin and clonNat (nourseothricin) resistance cassettes of pFA6a-hphNT1 or pFA6a-natNT2 plasmids, respectively.

Name	Sequence (5' to 3')
TAZ1 S1	CATTTTCAAAAAAAAAAAAAGTAAAGTTTTCCCTATCAAATG**CGTAC GCTGCAGGTCGAC**
TAZ1 S2	TGAAATTTAAGCAATTAAATTCGTGTAAATACTAGCATGTA**ATCGATG AATTCGAGCTCG**
ECT1 S1	AATGCTTTACAGGATCGGGACTTGAAATATACTGACTGGATG**CGTAC GCTGCAGGTCGAC**
ECT1 S2	CCATTTAATTTACGTTCGAAGAAGTTTTCAACATTTGTTTA**ATCGATG AATTCGAGCTCG**
EKI1 S1	TAGCAGAAATTAACAGATACAGATCTGCAATTTGGCATAATG**CGTAC GCTGCAGGTCGAC**
EKI1 S2	ATCGCAGTGAATAGAAAAATACTTGATTGTGTATACAGCTT**ATCGATG AATTCGAGCTCG**
CKI1 S1	TACACACACATAGATACGCACGTAAAATTAGAGCAAAAGATG**CGTAC GCTGCAGGTCGAC**
CKI1 S2	TTATTTCCTTGGCCTTTGTTGAAGGAATTCGTATACGTATT**ATCGATGA ATTCGAGCTCG**

Mitochondrial Isolation

Isolation of crude and pure mitochondria was performed as described previously (Meisinger et al., 2006). Mitochondria were isolated from yeast cells grown to late logarithmic phase and were subsequently used for SDS-PAGE western blot analysis as well as in-gel activity assays. For obtaining gradient purified mitochondrial fractions, crude mitochondria were loaded onto a sucrose step gradient (60%, 32%, 23% and 15%) and centrifuged at 134,000 g for 1 h. The intact mitochondria recovered from the gradient interface (60% and 32%) were washed in isotonic buffer, pelleted at 10,000 g, and subsequently used for BN-PAGE/western blot analysis and mitochondrial phospholipid quantification. Protein concentrations were determined by the BCA assay (Thermo Scientific).

Cellular and Mitochondrial Phospholipid Measurements

For the quantification of mitochondrial phospholipids, lipids were extracted from gradient purified mitochondria (1.5 mg protein) using the Folch method (Folch et al., 1956), and individual phospholipids were separated by two-dimensional thin layer chromatography using the following solvent systems: chloroform/methanol/ammonium hydroxide (65:35:5) in first dimension followed by chloroform/acetic acid/methanol/water (75:25:5:2.2) in second dimension (Storey et al., 2001). Phospholipids were visualized with iodine vapor, scraped into glass tubes, and inorganic phosphate was quantified (Bartlett, 1959). For the quantification of cellular PE, phospholipids were extracted from yeast cells (0.5 g wet weight) using the Folch method (Folch et al., 1956), inorganic phosphate was quantified, 30 nmol of phospholipids were loaded onto HPTLC silica gel 60 plates (EMD Millipore 1.11764.0001) and individual phospholipids were separated by one-dimensional thin layer chromatography using chloroform/methanol/ammonium hydroxide (50:50:3) (Connerth et al., 2012). Phospholipids were visualized with copper sulfate charring and bands were quantified using ImageJ (Connerth et al., 2012).

Sodium Dodecylsulfate and Blue Native PAGE and Immunoblotting

Sodium dodecylsulfate polyacrylamide gel electrophoresis (SDS-PAGE) was performed on mitochondrial samples solubilized in lysis buffer (150 mM NaCl, 1 mM EDTA, 50 mM Tris–HCl, pH 7.4, 1% NP-40, 0.5% sodium deoxycholate and 0.1% SDS) supplemented with protease inhibitor cocktail (Roche Diagnostic). Protein extracts were separated on NuPAGE 4-12% Bis-Tris gels (Life-Technologies), transferred to

PVDF membranes using a Trans–Blot transfer cell (Bio-Rad). Membranes were blocked in 5% fatty acid-free BSA dissolved in Tris–buffered saline with 0.1% Tween 20 and probed with the indicated antibodies. Blue native polyacrylamide gel electrophoresis (BN-PAGE) was performed to separate native MRC complexes as previously described (Wittig et al., 2006). Briefly, yeast gradient purified mitochondria were solubilized in buffer containing 1% digitonin (Life-Technologies), and incubated for 15 min at 4°C. Following a clarifying spin at 20,000 × g (30 min, 4°C), 50x G-250 sample additive was added to the supernatant and 20 µg of protein was loaded on a 3-12% gradient native PAGE Bis–Tris gel (Life-Technologies). Western blot was performed using a Mini-PROTEAN Tetra cell (Bio-rad). The membrane was blocked in 5% nonfat milk in Tris–buffered saline with 0.1% Tween 20 and probed with antibodies as indicated. Primary antibodies used for yeast proteins were: Cox2, 1:50,000 (Abcam 110 271); Sdh2, 1:5,000 (from Dr. Dennis Winge); Rip1, 1:100,000 (from Dr. Vincenzo Zara); Porin, 1:100,000 (Abcam 110 326). Anti-mouse (NA93IV) and anti-rabbit (32460) secondary antibodies (1:5,000) were incubated for 1 h at room temperature, and membranes were developed using Western Lightning Plus-ECL (PerkinElmer). Quantification was performed using the gel analysis method in ImageJ.

In-Gel Activity Measurements

In-gel activities for mitochondrial respiratory chain complexes were performed as described previously (Wittig et al., 2007). Clear Native Polyacrylamide Gel Electrophoresis (CN-PAGE) was used to avoid interference of Coomassie blue with activity measurements. Briefly, mitochondria solubilized in 1% digitonin were resolved

on a 4-16% gradient native PAGE Bis– Tris gel (Life-Technologies) with the addition of 0.05% *n*-dodecyl β-D-maltoside and 0.05% sodium deoxycholate in the cathode buffer. Gels were loaded with 90 μg of protein and incubated in MRC complex IV activity staining solutions as reported previously (Wittig et al., 2007). Equal loading was determined by Coomassie blue stain, and total protein and band intensity quantification was determined using the gel analysis method in ImageJ.

Quantification of Protein Carbonyl Content

The protein carbonyl content was measured by determining the amount of 2,4-dinitrophenylhydrazone (DNP) formed upon reaction with 2,4-dinitrophenyl hydrazine (DNPH), as described previously (Reznick and Packer, 1994; Dirmeier et al., 2004; Chen et al., 2008). Yeast cells were grown at 30°C to the early stationary phase in SC ethanol, harvested and cell extracts were used for subsequent protein carbonylation measurements. Nucleic acids were removed from the cell extracts with 1.0% streptomycin sulfate, and the resulting protein samples were incubated with 10 mM DNPH in 2 M HCl at room temperature for 60 min in the dark. Proteins were precipitated by addition of trichloroacetic acid to a final concentration of 10%, and the pellets were washed with ethanol/ethyl acetate (1:1) to remove the free DNPH. The final protein pellets were dissolved in 6 M guanidine hydrochloride solution containing 20 mM potassium phosphate, pH 2.4. The carbonyl content was calculated from the absorbance maximum of DNP measured at 370 nm.

CHAPTER IV

MECLIZINE INHIBITS MITOCHONDRIAL RESPIRATION THROUGH DIRECT TARGETING OF CYTOSOLIC PHOSPHOETHANOLAMINE METABOLISM*

Disclaimer

The work described in this chapter comprises reprints of a publication to which I contributed as a third author. The summary is a reprint of the publication abstract and the rest of the sections are as published. Figure contribution in this publication: Fig. 4.1D, Fig. 4.4E, Fig. 4.6, and Fig. 4.7.

---

* This research was originally published in Journal of Biological Chemistry. Gohil V.M., Zhu L., Baker C.D., Cracan V., Yaseen A., Jain M., Clish C.B., Brookes P.S., Bakovic M., Mootha V.K. Meclizine Inhibits Mitochondrial Respiration Through Direct Targeting of Cytosolic Phosphoethanolamine Metabolism. *J. Biol. Chem*. 2013; 49:35387-35395 © the American Society for Biochemistry and Molecular Biology.

Summary

We recently identified meclizine, an over-the-counter drug, as an inhibitor of mitochondrial respiration. Curiously, meclizine blunted respiration in intact cells, but not in isolated mitochondria, suggesting an unorthodox mechanism. Using a metabolic profiling approach, we now show that treatment with meclizine leads to a sharp elevation of cellular phosphoethanolamine, an intermediate in the ethanolamine branch of the Kennedy pathway of phosphatidylethanolamine biosynthesis. Metabolic labeling and in vitro enzyme assays confirm direct inhibition of the cytosolic enzyme CTP:phosphoethanolamine cytidylyltransferase (Pcyt2). Inhibition of Pcyt2 by meclizine leads to rapid accumulation of its substrate phosphoethanolamine, which is itself an inhibitor of mitochondrial respiration. Our work identifies the first pharmacologic inhibitor of the Kennedy pathway, demonstrates that its biosynthetic intermediate is an endogenous inhibitor of respiration, and provides key mechanistic insights that may facilitate repurposing meclizine for disorders of energy metabolism.

Introduction

Although mitochondrial respiration is crucial for cellular energetics and redox balance, during certain pathological conditions respiration can actually contribute to pathogenesis (Vafai and Mootha, 2012). Attenuation of mitochondrial respiration has been proposed as therapeutic strategy in a number of human disorders, including ischemia-reperfusion injury, neurodegeneration, autoimmune disease, and cancer (Armstrong, 2007). Many naturally occurring as well synthetic compounds targeting the mitochondrial respiratory chain are available, but their clinical utility is limited by their narrow therapeutic index (Dykens and Will, 2007); thus, there is an unmet need for discovering new classes of drugs that can safely modulate mitochondrial respiration.

We recently identified meclizine, an over-the-counter anti-nausea drug, in a 'nutrient-sensitized' chemical screen aimed at identifying compounds that attenuate mitochondrial respiration (Gohil et al., 2010). *In vivo* follow-up studies demonstrated that meclizine could be protective against heart attack (Gohil et al., 2010), stroke (Gohil et al., 2010), and neurodegeneration (Gohil et al., 2011) in animal models. Meclizine is a first-generation piperazine class of H_1-antihistamine that has been in use for decades for prophylaxis against nausea and vertigo (Cohen and DeJong, 1972). Like many H_1-antihistamines, meclizine has anti-cholinergic activity, (Kubo et al., 1987) and it has also been shown to target constitutive androstane receptors (Huang et al., 2004).

Meclizine's inhibition of respiration had not been reported before, and unlike classical respiratory inhibitors (e.g., antimycin, rotenone), meclizine did not inhibit respiration in isolated mitochondria, but rather, only in intact cells (Gohil et al., 2010).

We previously reported that this effect was independent of its anti-histaminergic and anti-cholinergic activity (Gohil et al., 2010), but the precise mechanism remained unknown. Curiously, the kinetics of meclizine-mediated inhibition of respiration were on the time-scale of minutes (Gohil et al., 2010), far too fast for a transcriptional mechanism, but slower than direct inhibitors of the respiratory chain, suggesting that the inhibition arose from a potentially novel mechanism, perhaps through intracellular accumulation of a meclizine-derived active metabolite, or by perturbing metabolism.

To gain insights into the mechanism of meclizine action, we performed global metabolic profiling of meclizine treated cells to detect alterations in intracellular metabolites of intermediary metabolism. Metabolic profiling revealed a sharp increase in intracellular levels of phosphoethanolamine (PEtn), an intermediate in the CDP-ethanolamine (Etn) Kennedy pathway of phosphatidylethanolamine (PE) biosynthesis. Follow up biochemical experiments confirmed the direct inhibition of phosphoethanolamine cytidylyltransferase (PCYT2), a rate-limiting enzyme of CDP-Etn Kennedy pathway. The inhibition of PCYT2 results in the buildup of its substrate, PEtn, which itself directly inhibits mitochondrial respiration. Our work thus identifies a novel molecular target of meclizine and links the CDP-Etn Kennedy pathway to mitochondrial respiration.

Materials and Methods

Metabolite Profiling

Metabolite profiling was performed on MCH58 fibroblasts following treatment with 50 μM meclizine or vehicle control for five hours, using methods similar to those previously described (Shaham et al., 2010). Briefly, low passage MCH58 cells were cultured on 6-cm tissue culture dishes in 4 mL of culture media to 90% confluency and a final yield of $1x10^6$ cells. For assessment of intracellular metabolites, media was aspirated from the above tissue culture dishes and cells were gently washed with 4 mL of phosphate buffered saline (PBS), to ensure complete removal of residual media metabolites. After removal of PBS cellular metabolism was quenched with immediate addition of 1 mL of pre-cooled (-80^{o}C) methanol extraction solution (80% methanol, 20% H_2O). Cells were scraped in extraction solution, vortexed, centrifuged and the resulting supernatant was collected and stored at -80^{o}C. At the time of measurement, 100 μl of supernatant was diluted 1:1 with methanol extraction solution. The resulting solution was evaporated under nitrogen and the samples were reconstituted in 60 μl of high-performance liquid chromatography (HPLC)-grade water and metabolites assessed. Six biological replicates were assessed for each group. Analyses of endogenous metabolites were performed using a liquid chromatography tandem mass spectrometry (LC-MS) system composed of a 4000 QTRAP triple quadrupole mass spectrometer (AB SCIEX) coupled to three Agilent 1100 binary HPLC pumps (Agilent Technologies) and an HTS PAL autosampler (LEAP Technologies) equipped with three injection ports and a column selector valve. Three multiplexed chromatographic methods were configured

for the analyses of each sample: LC method 1 used a Luna Phenyl-Hexyl column (Phenomenex) with a linear gradient of water/acetonitrile/acetic acid (initial proportions 100/0/0.001, final proportions 10/90/0.001); LC method 2 used a Luna NH_2 column (Phenomenex) with a linear gradient using acetonitrile/water containing 0.25% ammonium hydroxide and 10 mM ammonium acetate (acetonitrile/water proportions were 80/20 at the beginning of the gradient and 20/80 at its conclusion); LC method 3 used a Synergi Polar-RP column (Phenomenex), gradient elution with 5% acetonitrile/5 mM ammonium acetate (mobile phase A) and 95% acetonitrile/5 mM ammonium acetate (mobile phase B). MS data were acquired using multiple reaction monitoring (MRM) in both the positive (LC method 1) and negative (LC methods 2 and 3) ion modes. During the development of this method, authentic reference compounds were used to determine LC retention times and to tune MRM transitions. Metabolite quantification was performed by integrating peak areas for specific MRM transitions using MultiQuant software (version 1.1; AB SCIEX), and all integrated peaks were manually reviewed for quality. Extraction and quantification procedures were optimized prior to assessment of samples in this study to ensure measured intracellular and media metabolites were within the linear range of detection. Confirmation of the PEtn peak was performed using an exogenous PEtn standard (Sigma P0503). The relative quantification of PEtn in MCH58 skin fibroblasts or mouse striatal cells ($STHdh^{Q7/7}$) was also confirmed using hydrophilic interaction liquid chromatography (HILIC) (Roberts et al., 2012).

Determination of the Intracellular Concentration of PEtn and Phosphocholine (PCho)

Intracellular concentration of PEtn and PCho in meclizine treated MCH58 fibroblasts and *PCYT2* knockdown cells was determined as follows: MCH58 fibroblast cells were seeded into a 6-well plate (0.2 x 10^6 cells/well). After 20h of growth, three wells were treated with 50 μM meclizine and the three remaining wells were treated with DMSO for approximately 5h. Cells were scraped, collected in methanol extraction solution (80% methanol, 20% H_2O), and PEtn and PCho levels were quantified by LC-MS using commercially available standards. Cell number and mean cellular diameter of MCH58 cells were determined using a Beckman Coulter Z-series cell counter in a parallel plate, which was subsequently used to calculate the intracellular concentration of PEtn and PCho.

Radiolabeling of Kennedy Pathway Intermediates

Radiolabeling of CDP-Etn Kennedy pathway intermediates was performed as described previously (Zhu et al., 2008). Briefly, MCH58 fibroblasts were cultured in the presence of 50 μM meclizine for 5h to 60% confluency at which point ^{14}C-Etn (0.5 μCi/dish) was added and cells were further incubated for 24h. Lipids were extracted using the method of Bligh and Dyer (Bligh and Dyer, 1959). The total radioactivity from the water/methanol phase and that of the lipid phase were measured separately. ^{14}C-PE was separated from the lipid phase using TLC in a solvent consisting of methanol/chloroform/ammonia (65/35/5). Etn, PEtn, and CDP-Etn were separated from the water/methanol phase using TLC in a solution of methanol/0.5% NaCl/ammonia

(50/50/5). The separated ^{14}C labeled compounds were measured by scintillation counting.

PCYT2 Enzyme Assay

Pcyt2 activity was assayed as described previously with minor modifications (Tie and Bakovic, 2007). Briefly, a 50 µl mixture of 20 mM Tris-HCl buffer, pH 7.8, 10 mM $MgCl_2$, 5 mM DTT, 650 µM CTP, 650 µM unlabeled PEtn, and 65 µM ^{14}C-PEtn was incubated with 0.4 µg of purified Pcyt2 at 37°C for 15min. Reactions were terminated by boiling for 2min. Meclizine was added at the indicated concentration in the reaction mixture. Reaction mixtures were then loaded onto silica gel G plates with CDP-Etn and PEtn standards and separated in a solvent system of methanol/0.5% NaCl/ammonia (50/50/5). Plates were then sprayed with 1% ninhydrin, and the CDP-Etn product was quantified by liquid scintillation counting.

Construction of PCYT2 Knockdown Cell Lines

The shRNA constructs targeting Pcyt2 were purchased from Open Biosystems and the empty vector pLKO.1 was obtained from The Broad Institute (Cambridge, MA). Five independent shRNAs were used to construct MCH58 knockdown cell lines. We chose the two best knockdowns cell lines to perform radiolabeling and bioenergetics assays. The shRNA sequences for the two best knockdowns are (kd1: 5'CCCATCATGAATCTGCATGAA3', kd2: 5'TCACGGCAAGACAGAAATTAT3'). The lentiviral particles were produced in HEK293T cells as described previously (Moffat et al., 2006). Infection of MCH58 fibroblasts with lentiviral particles, selection

in puromycin (2 μg/ml) and their expansion to make stable knockdowns was performed essentially as described before (Gohil et al., 2010). The *PCYT2* mRNA levels in knockdowns were quantified by qRT-PCR using TaqMan assay (Applied Biosystems).

Bioenergetic Assays

Oxygen consumption rate (OCR, a measure of mitochondrial respiration) and extracellular acidification rate (ECAR, a measure of glycolysis) measurements in intact cells were carried out as previously described (Gohil et al., 2010; Gohil et al., 2010) with minor modifications. Briefly, MCH58 fibroblasts (control and *PCYT2* knockdowns) were seeded in XF24-well cell culture microplates (Seahorse Bioscience) at 30,000 cells/well in 25 mM glucose containing DMEM media and incubated at 37°C/ 5% CO_2 for ~ 20h. Prior to the measurements, the growth medium was replaced with ~925 μL of assay medium (Seahorse Bioscience). The cells were incubated at 37°C for 60min in the assay medium prior to OCR/ECAR measurements. The measurements were performed simultaneously every 7min after a 2min mix and 2min wait period. Three baseline OCR/ECAR measurements were recorded prior to the addition of 50 μM meclizine dihydrochloride (MP Biomedical 155341). To test the effect of PEtn *in vitro*, mitochondria were isolated from C57BL/6 mouse kidneys as previously described (Gohil et al., 2010). Simultaneous monitoring of oxygen consumption, membrane potential, NADH and FAD^+ fluorescence were performed using a custom made spectrophotometer. Reaction mixture contained in 0.5 ml of buffer A (137 mM KCl, 10 mM HEPES pH 7.4, 2.5 mM $MgCl_2$, 0.1% BSA) mitochondria (0.35 mg/ml) and tetramethylrhodamine methyl ester (TMRM) (0.5 μM). During the experiment

glutamate/malate (4.6 mM), ADP (180 μM) and PEtn (0, 3.2 mM, 8 mM) were added. The following excitations wavelengths were used for NADH, FAD^+ and TMRM: 365 nm, 470 nm and 530 nm. Data was acquired by integrating emission signals at 430-480 nm, 520-560 nm and 580-600 nm for NADH, FAD^+ and TMRM, respectively. For traces showing oxygen consumption of purified mitochondria in the presence of PCho, 0.5 ml of buffer A contained kidney mitochondria (0.2 mg/ml), glutamate/malate (4.6 mM), ADP (200 μM) and PCho (0-8 mM). Since PCho was commercially available only as a Ca^{2+} salt, a 160 mM stock was prepared in 500 mM EGTA/H_2O solution.

Determination of IC50 for PEtn Inhibition of Mitochondrial Oxygen Consumption

MitoXpress oxygen sensitive probe (Luxcel Biosciences, Ireland) was used to monitor glutamate/malate-driven respiration of mouse kidney mitochondria in 96-well plate format (Will et al., 2006). Each well contained glutamate/malate (11.5 mM), 20 μl of MitoExpress probe (dry probe was dissolved in 1 ml of water), mitochondria (0.5 mg/ml), PEtn (0-50 mM) in 200 μl total volume of buffer A. Two injections of ADP (487 μM final) were made using the injector of EnVision 2104 plate reader (Perkin-Elmer, MA). Time-resolved fluorescence (TR-F) was measured with the following settings: delay and gate times 70 μs and 30 μs respectively. Data analysis was performed using SigmaPlot 12.3. Briefly, slopes of basal respiration (state 2) and ADP-activated respiration (state 3) were taken, and the data was normalized against maximum respiration with no PEtn.

PE Determination

MCH58 fibroblasts were treated with 50 μM meclizine or DMSO for 5h. Mitochondria were isolated from approximately 1.5 g of cells (wet weight) using the Mitochondria Isolation Kit for Cultured Cells (Abcam MS852). Total phospholipids were extracted from whole cells or isolated mitochondria (1.5 mg of mitochondrial protein) as described previously (Folch et al., 1956). Briefly, phospholipids were extracted in 3 mL of chloroform/methanol (2:1) by shaking for 1hr, followed by addition of 600 μL of 0.9% NaCl solution and vortexing for an additional 15min. The aqueous and organic layers were separated via centrifugation (300 xg, 5min) followed by an additional wash with 500 μL of H_2O. The bottom layer (organic phase) was evaporated to dryness under N_2 gas. The resulting lipid film was resuspended in 90 μL of 2:1 chloroform/methanol and separated on silica gel 60 TLC plates (EMD Millipore 1.05721.0001) using a solvent system consisting of chloroform/acetic acid/methanol/water (75/25/5/2.2). The TLC plates were then dried and exposed to iodine vapor to visualize phospholipid spots. The identity of each spot was verified using phospholipids standards (Sigma PH9-1KT). Individual spots were scrapped and phospholipid phosphorus was quantified using the Bartlett method (Bartlett, 1959).

Testing the Combined Effect of Meclizine and Etn on MCH58 Fibroblast ATP Levels

MCH58 fibroblasts were seeded at 10,000 cells/well in a 96-well plate in DMEM high glucose medium and allowed to grow overnight. After ~ 20h, growth medium was replaced with 10 mM galactose medium containing different concentrations of meclizine

(0, 12.5, 25, 50 μM) and Etn (0, 0.2, 1 and 5 mM). The ATP levels in the cells were measured by CellTiter-Glo reagent (Promega) 24h after the treatment.

Results

Meclizine Treatment Results in the Elevation of PEtn across Multiple Mammalian Cell Types

To decipher the mechanism by which meclizine blunts respiration we used a metabolomics approach, since previous reports have shown that the technology can reveal targets of desired and undesired actions of drugs (Webhofer et al., 2011, Watkins and German, 2002). We performed mass spectrometry-based metabolic profiling of human immortalized skin fibroblasts (MCH58) cells treated with 50 μM meclizine for 5h. Our choice of MCH58 immortalized human skin fibroblasts was guided by our previous study characterizing the effect of meclizine on mitochondrial energy metabolism (Gohil et al., 2010). Of the 124 metabolites that were measured reproducibly across 6 biological replicates, the most striking change corresponded to PEtn signal, which increased nearly 35-fold ($P\text{-}_{adj}<0.005$), well outside the background distribution (Fig. 4.1A). We further confirmed the identity and up regulation of PEtn levels using HILIC-mass spectrometry in human fibroblasts and mouse striatal cells (Fig. 4.1B). These data are consistent with our previous observation showing that meclizine attenuates respiration across multiple cell types (Gohil et al., 2010). Using PEtn standards, we quantified the absolute levels of PEtn in fibroblasts and showed that within 5h of meclizine treatment the intracellular concentration of PEtn increases from approximately 1.5 mM to 4 mM (Fig. 4.1C and D).

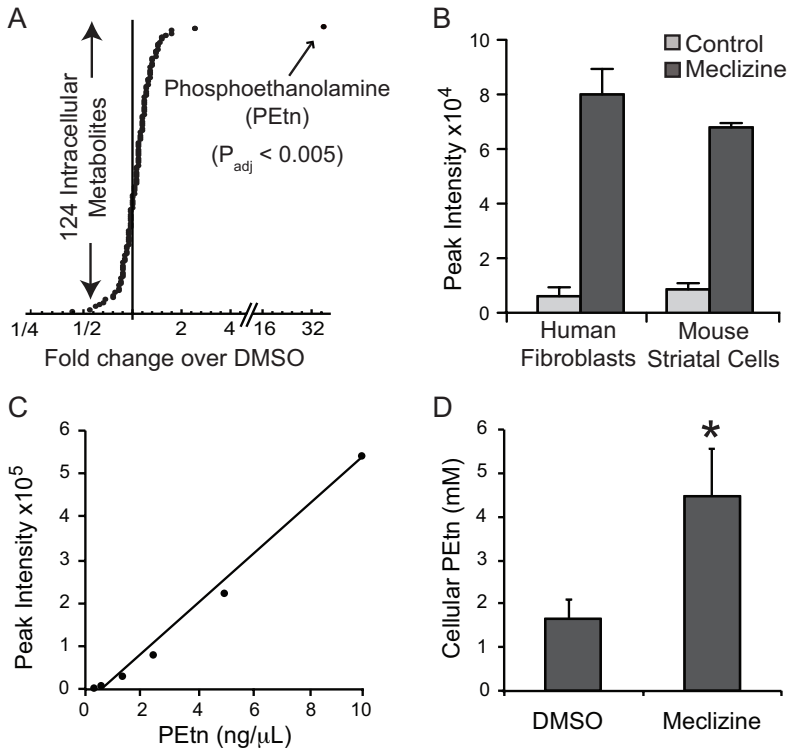

Figure 4.1 Phosphoethanolamine is elevated in meclizine treated cells.

(A) Mass-spectrometry based quantification of 124 intracellular metabolites from MCH58 human fibroblasts treated with 50 μM meclizine for 5h. Each data point represents an average of 6 values for DMSO and meclizine treated samples. (B) Hydrophilic interaction liquid chromatography (HILIC)/mass-spectrometry based relative quantification of PEtn from human fibroblasts (MCH58) or mouse striatal cells (STHdhQ7/7) treated with DMSO or 50 μM meclizine for 5h. Data are expressed as mean ± S.D (n=6 for fibroblasts; n=3 for striatal cells). (C) The calibration curve used for the quantitative analysis of PEtn in meclizine treated samples was obtained by LC-MS using PEtn standards. (D) The cellular concentration of PEtn in MCH58 fibroblasts treated with meclizine (50 μM) or DMSO was determined by counting cell number, calculating total cellular volume using Beckman Coulter Z-series cell counter and measuring absolute PEtn levels by mass-spectrometry. Data are expressed as mean ± S.D. (n=3).

The Pattern of CDP-Etn Kennedy Pathway Intermediates in Meclizine-treated Cells Is Consistent with PCYT2 Inhibition

PEtn is an intermediate in the CDP-Etn Kennedy pathway of PE biosynthesis (Vance, 2008; Pavlovic and Bakovic, 2013). The mammalian CDP-Etn Kennedy pathway consists of three enzymatic steps: Etn is first phosphorylated by Etn kinase (EK) to PEtn, which is converted to cytidine diphospho-Etn (CDP-Etn) by

CTP:phosphoethanolamine cytidylyltransferase (PCYT2 also referred to as ECT), finally Etn phosphotransferase (CEPT1) catalyzes the CDP-Etn conversion to PE (Fig. 4.2A). To understand why PEtn levels rise with meclizine, vehicle and meclizine treated cells, were incubated with ^{14}C-Etn for 24h, and the incorporation of the radiolabel was measured in the intermediates of the CDP-Etn Kennedy pathway. With meclizine treatment, ^{14}C-PEtn levels were increased while radiolabel incorporation into downstream metabolites, CDP-Etn and PE, were decreased (Fig. 4.2B). These results raise the hypothesis that meclizine directly blocks PCYT2 enzymatic activity, which catalyzes the conversion of PEtn to CDP-Etn.

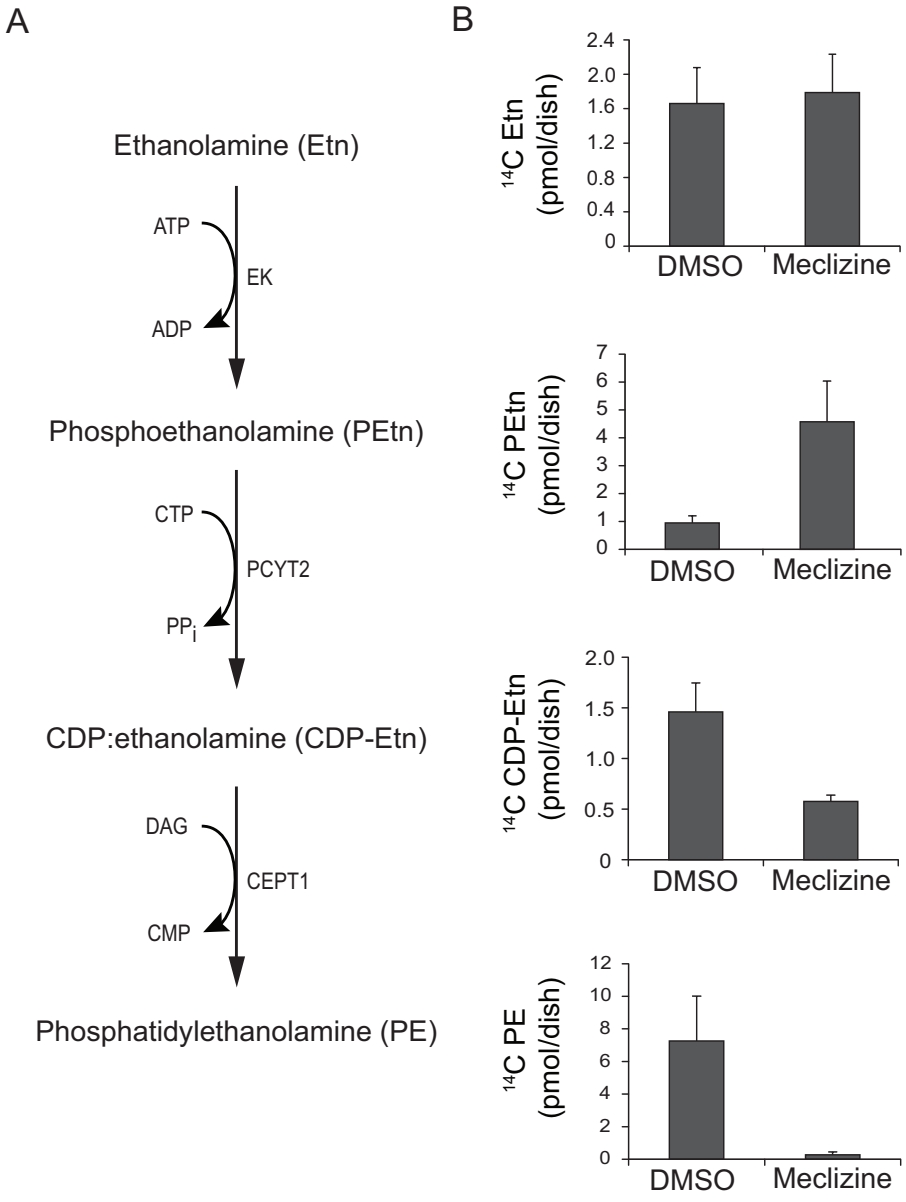

Figure 4.2 Metabolic labeling of Kennedy pathway intermediates.

(A) Enzymatic reactions depicting synthesis of Kennedy pathway intermediates. (B) Quantification of radiolabeled Kennedy pathway intermediates in meclizine treated MCH58 fibroblasts. MCH58 fibroblasts were cultured in the presence of 50 μM meclizine or DMSO for 5h at which point ^{14}C-Etn (0.5 μCi/dish) was added and cells were further incubated for 24h. The ^{14}C labeled compounds were separated as described under "Experimental Procedures" and measured by scintillation counting. Data are expressed as mean ± S.D. (n=5).

Meclizine Is a Non-competitive Inhibitor of PCYT2

To confirm whether meclizine directly inhibits Pcyt2, we performed an *in vitro* enzyme assay with purified recombinant mouse Pcyt2 (Tie and Bakovic, 2007) in the presence of varying concentrations of meclizine. Meclizine inhibited Pcyt2 enzyme activity in a dose dependent manner (Fig. 4.3A), and the Lineweaver-Burke plot of the Pcyt2 enzyme kinetics suggests a non-competitive inhibition with an approximate K_i of 31 μM (Fig. 4.3B).

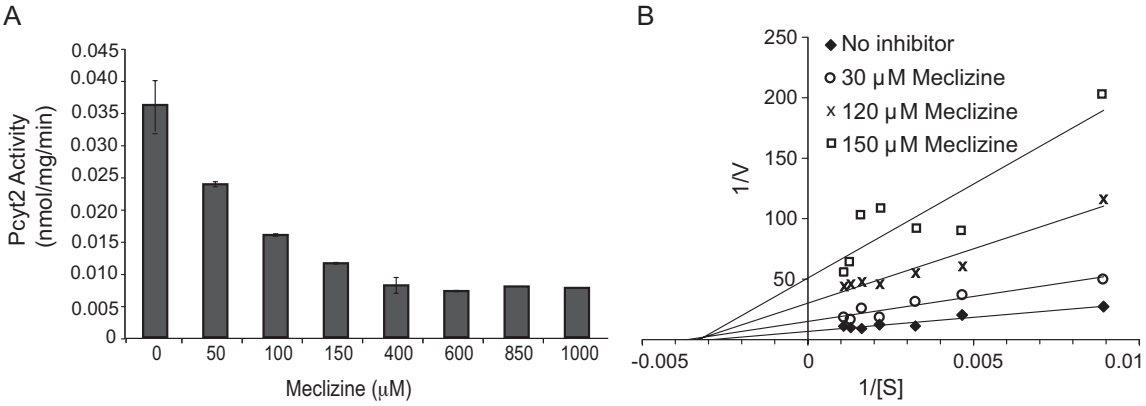

Figure 4.3 Meclizine inhibits recombinant purified Pcyt2.
(A) In vitro activity of Pcyt2 (0.4 μg) measured using 650 μM CTP, 650 μM PEtn and 65 μM ^{14}C-labeled PEtn (55 μCi/μmol) in the presence of varying meclizine concentrations. (B) Inhibition kinetics of Pcyt2 with PEtn at a fixed concentration of 650 μM and 65 μM ^{14}C-labeled PEtn (55 μCi/μmol) in the presence of varying concentrations of CTP (100-1000 μM) and meclizine (0-150 μM). All experiments were performed twice in duplicates. Data are expressed as mean ± S.D.

PCYT2 Knockdown Cells Partially Mimic the Meclizine Effect

We next sought to phenocopy the effects of meclizine using RNAi against *PCYT2*. We stably silenced *PCYT2* in MCH58 human skin fibroblasts using five hairpins and focused on two hairpins that achieved 77% and 90% knockdown at the RNA level (Fig. 4.4A). We treated control and knockdown cells with ^{14}C-Etn and quantified CDP-

Etn Kennedy pathway intermediates. As expected, we observed an increase in ^{14}C-PEtn levels and a decrease in downstream PCYT2 products ^{14}C-CDP-Etn and ^{14}C-PE, though the magnitude of changes was not as striking as with meclizine (Fig. 4.4B). The best knockdown of *PCYT2* showed a slight reduction in basal oxygen consumption, and a corresponding increase in glycolysis (Fig. 4.4C); though, the magnitude of effect was small when compared to meclizine treated fibroblasts (Fig. 4.4D). This difference between chemical inhibition of Pcyt2 by meclizine and genetic depletion of *PCYT2* by shRNA was consistent with our observation that a stable *PCYT2* knockdown is incomplete and does not result in the sustained accumulation of PEtn (Fig. 4.4E).

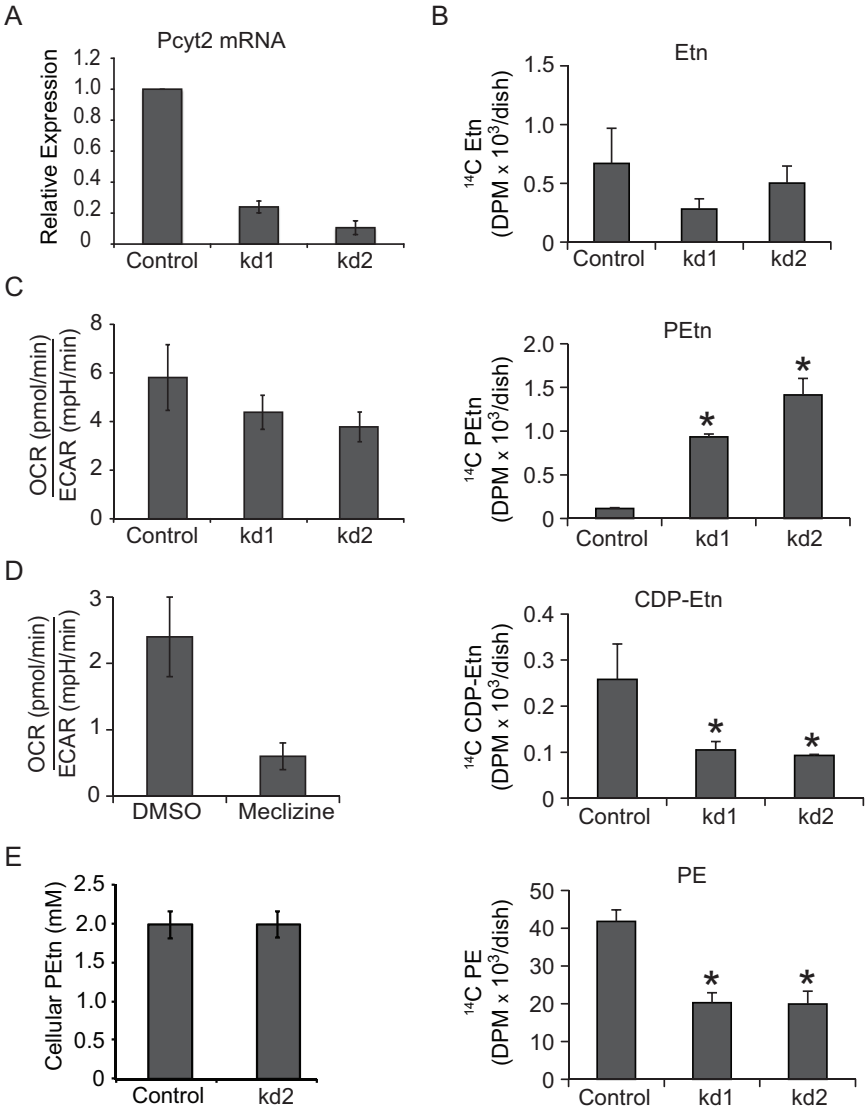

Figure 4.4 Characterization of PCYT2 knockdown cells.

(A) PCYT2 mRNA quantified by performing qRT-PCR on RNA extracted from MCH58 fibroblasts infected with an empty vector (Control) or 2 independent shRNAs (kd1 and kd2) targeting *PCYT2*. (B) Quantification of the Kennedy pathway intermediates in control and *PCYT2* knockdown fibroblasts. Experiments were done two times independently in triplicates, $P<0.05$ as determined by t-Test. (C) Ratio of OCR, a measure of mitochondrial respiration, to ECAR, a measure of glycolysis, in control and PCYT2 knockdown fibroblasts. Data are expressed as mean ± S.D. ($n \geq 5$). (D) OCR to ECAR ratio in vehicle (DMSO) or meclizine (50 μM) treated fibroblasts. Data are expressed as mean ± S.D. ($n \geq 4$). (E) The cellular concentration PEtn in control and PCYT2 knockdown fibroblasts was determined by counting cell number, calculating total cellular volume using Beckman Coulter Z-series cell counter and measuring absolute PEtn levels by mass spectrometry. Data are expressed as mean ± S.D. (n=3).

PEtn Inhibits Respiration in Suspensions of Isolated Mitochondria

It is notable that a previous study showed that Etn and PEtn can directly inhibit respiration in isolated suspensions of mitochondria (Modica-Napolitano and Renshaw, 2004), raising the hypothesis that meclizine is blunting respiration *in vivo* via an elevation of PEtn. We found that PEtn does not impact basal (state 2) mitochondrial respiration, but indeed, has a strong inhibitory effect on ADP-stimulated (state 3) respiration (Fig. 4.5A), with an IC_{50} of 3.13 ± 0.54 mM. PEtn inhibited ADP-driven respiration either with glutamate/malate (Fig. 4.5A and B) or with succinate/rotenone respiration (data now shown), suggesting that the inhibitory effect is not specific to respiratory complex I or complex II or to a specific fuel substrate. In assays for mitochondrial physiology we find that the addition of PEtn leads to decreased NADH and increased FAD^+ intrinsic fluorescence together with reduction of membrane potential (Fig. 4.5B). Notably, similar concentrations of phosphocholine (PCho), an intermediate in the CDP-Choline branch of the Kennedy pathway of phosphatidylcholine biosynthesis, did not inhibit respiration in suspensions of isolated mitochondria indicating that the inhibitory effect of PEtn on mitochondrial respiration was specific (Fig. 4.5C). Moreover, we also measured PCho levels in order to determine if meclizine mediated elevation of PEtn is due to the specific inhibition of PCYT2. We observed a decrease in the cellular concentration of PCho from 6.14 ± 0.43 mM to 2.79 ± 0.37 mM with meclizine treatment, making PCho an unlikely contributor to meclizine's effect on mitochondrial respiration *in vivo.*

Figure 4.5 Effects of phosphoethanolamine on mitochondrial bioenergetics.

(A) The effect of increasing PEtn concentrations on glutamate/malate-driven ADP-activated respiration (●) and basal respiration (○) in isolated mouse kidney mitochondria. Rates of oxygen consumption are normalized to ADP stimulated respiration in the absence of PEtn. Data are representative of three independent trials. Error bars represent deviation from a linear fit when corresponding slopes were analyzed. (B) Simultaneous measurements of oxygen consumption, membrane potential, NADH and FAD^+ fluorescence. Purified mouse kidney mitochondria (0.35 mg/ml) and TMRM (0.5 μM) were incubated in buffer A (137 mM KCl, 10 mM HEPES pH 7.4, 2.5 mM MgCl2, 0.1% BSA). Glutamate/malate (G/M) (4.6 mM), ADP (180 μM) and PEtn (0, 3.2, and 8 mM) were added at the time points indicated by arrows. Traces are representative of at least three independent experiments. (C) For traces showing oxygen consumption in the presence of PCho the assay mixture contained mouse kidney mitochondria (0.2 mg/ml) in buffer A. The respiratory substrates glutamate/malate (G/M) (4.6 mM), ADP (200 μM) and phosphocholine (PCho) (0, 3 mM and 8 mM) were added at the time points indicated by arrows. Traces are representative of three independent experiments.

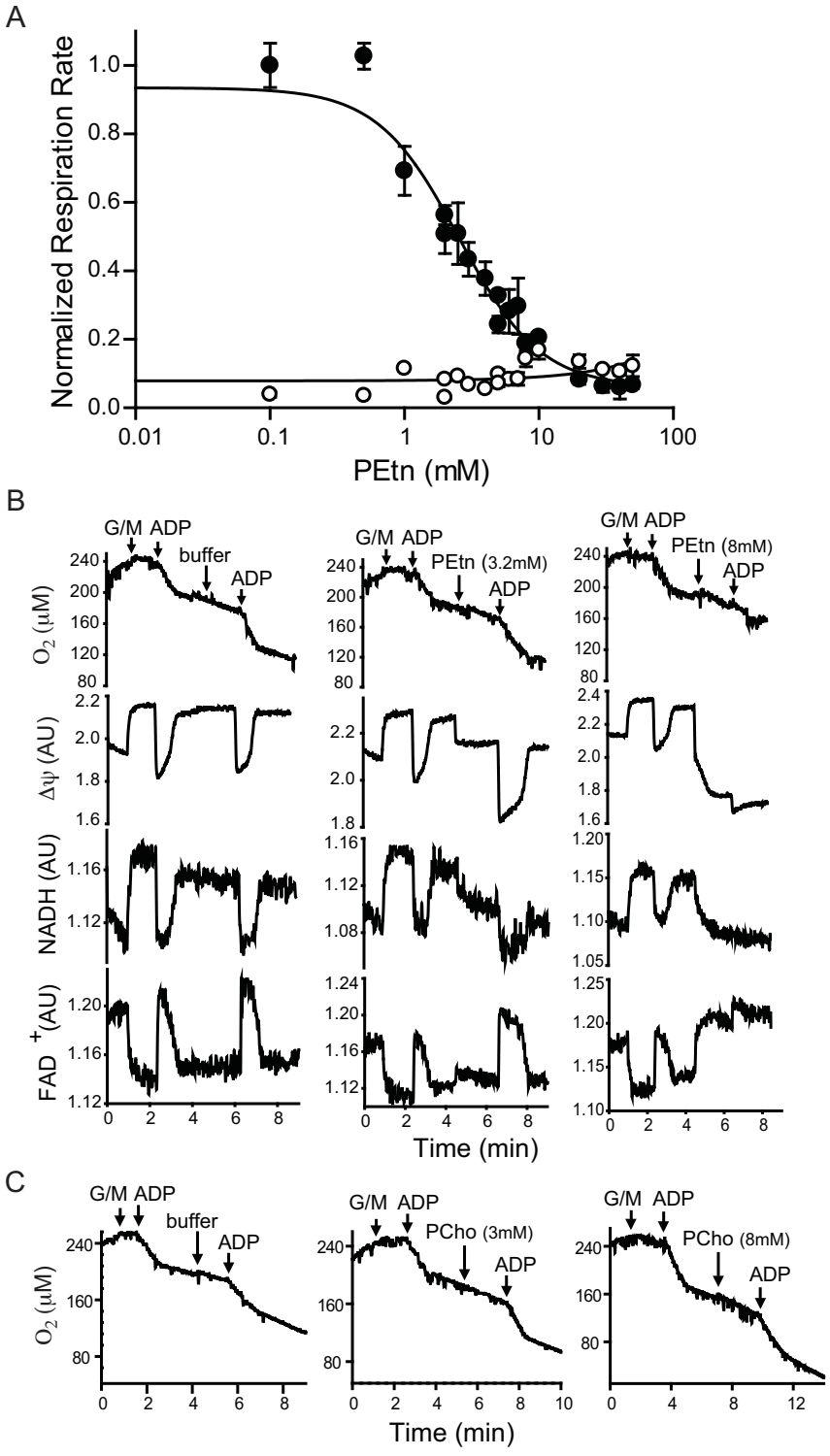
A
Normalized Respiration Rate
1.0
0.8
0.6
0.4
0.2
0.0
0.01
0.1
1
10
100
PEtn (mM)
B
G/M ADP
buffer
ADP
PEtn (3.2mM)
PEtn (8mM)
O2 (μM)
Δψ (AU)
NADH (AU)
FAD+ (AU)
Time (min)
C
PCho (3mM)
PCho (8mM)

Meclizine Treatment Does Not Alter Steady State Levels of Mitochondrial PE

Recently, it has been shown that a modest reduction in PE in mammalian mitochondria impairs oxidative phosphorylation, reducing respiration (Tasseva et al., 2013). Therefore, we asked if short-term (5 h) inhibition of the Kennedy pathway of PE synthesis by meclizine causes a decrease in cellular and mitochondrial PE levels and contributes to reduced respiration. As shown in Fig. 4.6A and B, we did not observe a significant decrease in the cellular or mitochondrial PE levels of human fibroblasts treated with meclizine, ruling out a reduction in PE as a cause for decreased respiration *in vivo.*

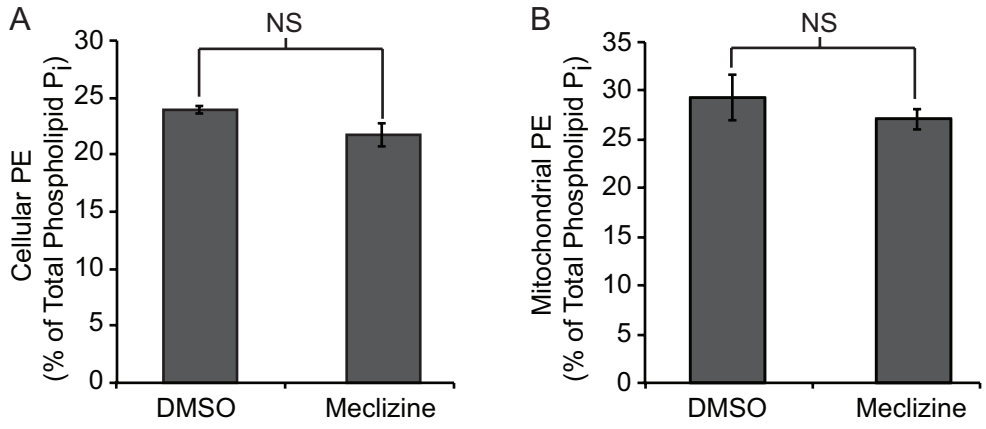

Figure 4.6 Total cellular and mitochondrial phosphatidylethanolamine levels in meclizine treated fibroblasts.

MCH58 fibroblasts were grown in the presence of Meclizine (50 μM) or DMSO for 5 h, followed by (A) cellular and (B) mitochondrial phospholipid extraction as described under "Experimental Procedures." Phospholipids were separated using one-dimensional TLC and phosphorous was quantified using the Bartlett method. Data are expressed as the percentage of PE relative to total phospholipids and represent the average of three independent experiments (NS: not significant).

Inhibition of Respiratory Growth by Meclizine Is Accentuated through Addition of Ethanolamine

We originally identified meclizine as an agent that inhibits the growth of human skin fibroblasts grown in galactose versus glucose. It has long been known that when human cells are grown in galactose, they are highly reliant on mitochondrial respiration. In the current study, we have shown that in the presence of meclizine, the phospholipid biosynthetic intermediate PEtn accumulates and directly inhibits mitochondrial respiration. Our model predicts that exogenous Etn should have an additive or synergistic effect with meclizine in inhibiting respiratory growth. Consistent with our model, we found that a combination of meclizine treatment with Etn supplementation synergistically reduced cellular ATP levels (Fig. 4.7).

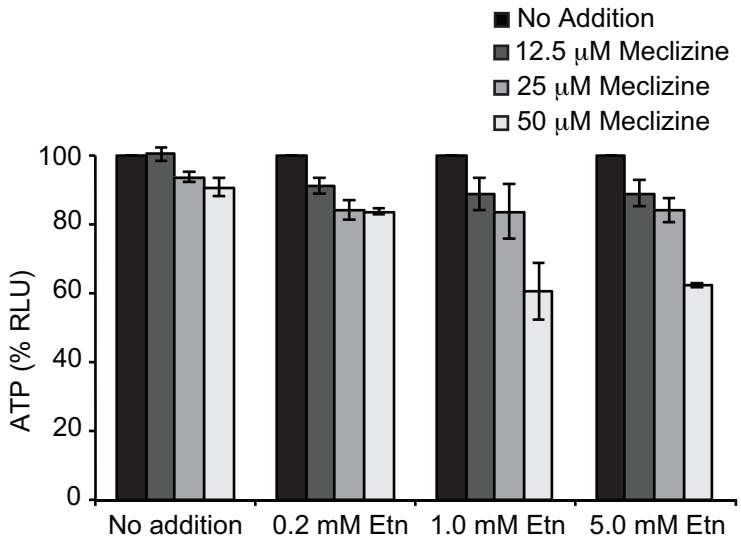

Figure 4.7 Meclizine mediated respiratory growth inhibition of human skin fibroblasts is enhanced by exogenous addition of ethanolamine.

MCH58 cells cultured in 10 mM galactose medium were exposed to different concentrations of meclizine and Etn for 24 h followed by the measurement of cellular ATP levels. Data was normalized to 100% for no treatment controls and errors bars represent standard deviation from mean (n=3).

Discussion

The current study provides the molecular basis for inhibition of respiration by meclizine, an over-the-counter anti-nausea and anti-vertigo drug. Using a combination of mass spectrometry, metabolic labeling and *in vitro* biochemical assays we found that CTP:phosphoethanolamine cytidylyltransferase (PCYT2) is a direct target of meclizine. Our study highlights the use of metabolic profiling in deciphering mechanisms of drug action, with important biological and clinical implications.

To our knowledge, this study is the first to pharmacologically link the Kennedy pathway of PE biosynthesis to mitochondrial energy metabolism and is consistent with a previous report showing that mice heterozygous for the *Pcyt2* gene have reduced energy production from fatty acid oxidation (Fullerton et al., 2009). PE is an essential phospholipid present in eukaryotic membranes and is highly enriched in mitochondrial membranes. It has overlapping functions with cardiolipin (Gohil et al., 2005), a mitochondria-specific phospholipid that is essential for optimal respiration (Jiang et al., 2000). PE is synthesized by multiple biochemical pathways (Vance, 2008; Pavlovic and Bakovic, 2013), including the phosphatidylserine decarboxylase catalyzed mitochondrial pathway and the cytosolic/ER CDP-Etn Kennedy pathway. The mitochondrial pathway contributes the bulk of mitochondrial PE that is retained in this organelle and contributes to mitochondrial function (Steenbergen et al., 2005; Bleijerveld et al., 2007). Recently, it has been shown that a decrease in mitochondrial PE by deletion of phosphatidylserine decarboxylase in the yeast *S. cerevisiae* results in reduced respiration (Bottinger et al., 2012). Similar reduction in mitochondrial respiration has been observed in mammalian

cells where mitochondrial phosphatidylserine decarboxylase is depleted (Tasseva et al., 2013). However, the non-mitochondrial CDP-Etn Kennedy pathway of PE synthesis has never been linked to respiratory defect either in yeast or mammalian cells.

How does direct inhibition of PCYT2 lead to attenuation of mitochondrial respiration? Two possibilities exist: (1) the accumulation of upstream metabolites (PEtn) could interfere with mitochondrial respiration or (2) depletion of downstream metabolites (PE) could alter mitochondrial membrane structure thereby inhibiting respiration. We favor the first hypothesis, which is supported by our observation that the intracellular concentration of PEtn in meclizine treated fibroblasts increases to a level sufficient to inhibit mitochondrial respiration (Figs. 4.1D and 4.5A and B). Notably, our *in vitro* data on PEtn inhibition of mitochondrial respiration is consistent with a previous study that showed both Etn and PEtn inhibit respiration in isolated mitochondria (Modica-Napolitano and Renshaw, 2004). The second mechanism seems less likely since the bulk of mitochondrial PE is synthesized *in situ* by the action of phosphatidylserine decarboxylase. Moreover, we did not observe any decrease in cellular mitochondrial PE of the meclizine treated fibroblasts discounting the second possibility (Fig. 4.6). The synthetic interaction between meclizine and Etn in MCH58 cells further buttress the first model, since addition of Etn to meclizine treated cells exacerbated, rather than alleviated, the cell viability as measured by ATP levels (Fig. 4.7).

According to our model, meclizine itself has no effect on mitochondria, but rather blocks PCYT2, leading to the accumulation of PEtn, which is itself an endogenous

inhibitor of respiration. Although multiple lines of evidence support our model, questions still remain. First the genetic depletion of *PCYT2* by RNAi did not completely phenocopy meclizine's effect on mitochondrial respiration, though this could be due to incomplete knockdown and the lack of sustained accumulation of PEtn (Fig. 4.4E). The inability of genetic silencing to fully phenocopy drug treatment is not uncommon (Weiss et al., 2007), and in principle could be due to the presence of residual enzyme activity of PCYT2. Second, overexpression of *PCYT2* did not confer resistance to meclizine's effect on respiration (data not shown), which could be due to tight regulation of its intracellular levels. Given that meclizine is known to target multiple cellular proteins (Cohen and DeJong, 1972; Huang et al., 2004; Kubo et al., 1987), we cannot exclude additional mechanisms that may underlie its impact on respiration.

Regardless, we have clearly shown that meclizine inhibits PCYT2 and causes an increase in cytosolic PEtn to a level sufficient to inhibit mitochondrial respiration. To our knowledge, such a mechanism of respiratory inhibition has never been described before. The mechanism of PEtn-mediated inhibition of respiration appears to be distinct from canonical inhibitors of respiration, including inhibitors of electron transport (rotenone, antimycin), uncouplers (CCCP, dinitrophenol) and ATP synthesis (oligomycin). PEtn addition to mitochondria resulted in reduced oxygen consumption, diminished membrane potential and a decrease in NADH levels (Fig. 4.5), whereas treatment with rotenone or antimycin would have increased NADH levels, CCCP would have increased oxygen consumption, and oligomycin would have increased membrane potential. The inhibition does not appear to be substrate specific, as we observed

inhibition of respiration using complex I or complex II linked substrates. The precise mechanism by which accumulation of cytosolic PEtn inhibits respiration is currently not known, but our bioenergetics measurements suggest a mechanism whereby PEtn may interfere with the generation of reducing equivalents that feed into the respiratory chain.

Importantly, our work identifies for the first time an inhibitor of the CDP-Etn Kennedy pathway with therapeutic potential. This pathway has been implicated in a range of human disorders including cancer (Ferreira et al., 2012), ischemia-reperfusion injury of brain and heart (Kelly et al., 2010), as well as infectious disorders including African sleeping sickness and malaria (Gibellini et al., 2009, Maheshwari et al., 2013). Our own previous work has shown that meclizine, through blunting of respiration, is cytoprotective against ischemic injury to the brain and the heart (Gohil et al., 2010) as well as polyQ toxicity observed in Huntington's disease (Gohil et al., 2011). Currently, effective therapies are not available for these disorders, making meclizine an attractive drug for repurposing. An intriguing question is to what extent the anti-vertigo and anti-nausea effects of meclizine may be occurring through targeting of PCYT2. A recent pharmacokinetics study on human subjects given an oral dose of 25 mg result in a peak plasma concentration of 80 ng/ml (~0.2 μM) (Wang et al., 2012), which is almost 70 fold below the minimum concentration required for inhibition of respiration in cell lines we have tested (Gohil et al., 2010), thus currently approved doses are unlikely to be active on mitochondrial respiration. We anticipate that identification of PCYT2 as a direct molecular target of meclizine may help to guide its clinical development for new uses. It is notable that PEtn, which accumulates following inhibition, can be detected

noninvasively using phosphorus ^{31}P-NMR, providing a facile marker of pharmacodynamics.

CHAPTER V

SUMMARY AND CONCLUSIONS

Summary

My work is focused on understanding how mitochondrial membrane phospholipid composition impacts mitochondrial function by influencing the biogenesis of the mitochondrial respiratory chain (MRC). I examined the role of the most abundant mitochondrial phospholipids, phosphatidylcholine (PC), phosphatidylethanolamine (PE), and cardiolipin (CL) in MRC function and formation. I showed a specific requirement of mitochondrial PE for MRC complex III and IV activities. Additionally, I found that CL is specifically required for MRC supercomplex formation *in vivo*. While the non-bilayer forming phospholipids PE and CL have specific roles in MRC function and formation, PC is redundant for mitochondrial bioenergetics. Furthermore, I assessed the ability of PE synthesized outside of the mitochondria, from exogenous ethanolamine (Etn), to compensate for the depletion of mitochondrial PE. I showed that PE synthesized outside of the mitochondria is imported into the mitochondria where it functionally substitutes for the lack of mitochondrial PE synthesis. This finding suggest the existence of a mitochondrial PE import pathway, which can be utilized to manipulate MRC function by altering mitochondrial PE levels. PE and CL are both cone-shaped, non-bilayer forming phospholipids that have been proposed to have overlapping functions (Gohil et al., 2005; Osman et al., 2009). I tested this proposition by elevating mitochondrial PE with exogenous Etn supplementation in a CL deficient yeast model. Indeed, I found that Etn supplementation rescued the respiratory growth of CL deficient cells, but surprisingly,

Etn-mediated rescue was independent of PE biosynthesis and solely dependent on supplementation with the soluble phospholipid precursors - Etn and propanolamine. In order to determine the biochemical basis for Etn-mediated growth rescue of CL deficient cells, I examined MRC function and formation in CL mutants grown in the presence of exogenous Etn. I found that Etn supplementation restores mitochondrial respiratory chain supercomplex assembly and reduces oxidative stress in CL deficient *taz1Δ* cells – a yeast model of Barth syndrome. Interestingly, Etn supplementation fails to rescue supercomplex formation in *crd1Δ* cells that are completely devoid of CL, suggesting that supercomplex formation requires a critical amount of CL. I determined that Etn supplementation rescued MRC complex IV activity and ameliorated oxidative stress in *crd1Δ* cells, suggesting that these phenotypes are independent of supercomplex formation. These findings describe a novel role of Etn in mitochondrial physiology and support a link between Kennedy pathway metabolites and mitochondrial function. In line with this observation, we found that blocking the Etn-Kennedy pathway of PE biosynthesis by meclizine, a clinically used anti-nausea drug, attenuates MRC function. I worked in collaboration with Dr. Vamsi Mootha's team at the Massachusetts General Hospital, Boston to determine that meclizine-mediated attenuation of mitochondrial respiration was not due to depleted mitochondrial PE levels, but most likely due to the cellular accumulation of phosphoethanolamine, a PE intermediate. Taken together, my work highlights the specific roles of non-bilayer forming phospholipids in MRC function and formation and suggests new roles of the Kennedy pathway PE precursors Etn and PEtn in modulating mitochondrial function.

Future Directions

One major outcome of my work was the finding that non-mitochondrial PE can be imported into the mitochondria, where it can functionally substitute for the lack of mitochondrial PE biosynthesis. The mechanism by which non-mitochondrial PE is imported into the mitochondria is yet to be determined and represents an important goal for future studies. Based on the recent discoveries in cell biology about the existence of membrane contact sites between mitochondria, ER, and vacuoles, I predict that the contact site protein complexes will likely play a role in the mitochondrial PE import. This can be examined using a candidate-based approach that involves genetically deleting components of membrane contact sites between the mitochondria and other organelles in *psd1*Δ cells and attempting a rescue of the double mutant by Etn supplementation. A lack of rescue of the double mutant in respiratory growth medium will suggest a potential role of the candidate gene in mitochondrial PE import.

Intra-organelle phospholipid transport processes are still poorly understood and one of the major unanswered questions in mitochondrial membrane biogenesis is how the PE substrate PS is transported from the ER to the mitochondria. A genome-scale Etn-sensitized screen involving the combination of a DNA barcoded yeast deletion mutant library and next generation sequencing could be used to identify the PS transporter protein(s). The screen will be based on the idea that cells lacking in the PS transporter will phenocopy *psd1*Δ cells, in that they will be respiratory deficient and their respiratory deficiency will be overcome by stimulating non-mitochondrial PE biosynthesis by Etn supplementation. To identify deletion strains that contain defects in

mitochondrial respiration, the deletion pool will be grown in either MRC-dependent conditions (SC lactate) or MRC-independent conditions (SC glucose). Deletion strains that show a severe growth defect in SC lactate media and are rescued by Etn supplementation will be considered candidate genes for putative involvement in mitochondrial PS import.

Another important question that emerged from my studies regards the novel role of Etn in attenuating MRC function in CL deficient yeast cells. Future studies focused on identifying the mechanism by which Etn mediates the rescue of CL depleted cells would require a multi-prong approach involving genetics, genomics, and metabolomics. In my initial attempts to unravel the mechanism of Etn-mediated rescue of CL deficiency, I utilized a candidate-based genetic approach where I deleted candidate genes in a *taz1*Δ background in an attempt to disrupt Etn-mediated rescue (Figs. A-1 and A-2B). The candidate genes were selected based on their putative role in the incorporation of Etn into cellular metabolites, including N-acylethanolamines and polyamines. Future studies will be driven by mass spectrometry based non-targeted metabolic profiling, an unbiased approach to identify relative changes in metabolites of Etn treated versus untreated cells. Heavy isotope labeled Etn could also be utilized in an attempt to follow Etn into the cell or its incorporation into other metabolites that are mediating the rescue. In addition, a synthetic genetic array of *crd1*Δ cells crossed with all of the viable yeast deletion strains could be utilized to screen for the loss of Etn-mediated rescue. Identification of genes that participate in Etn-mediated rescue will provide clues for the underlying mechanism of the observed rescue.

REFERENCES

Aaltonen MJ, Friedman JR, Osman C, Salin B, di Rago JP, Nunnari J, Langer T, Tatsuta T (2016). MICOS and phospholipid transfer by Ups2-Mdm35 organize membrane lipid synthesis in mitochondria. J Cell Biol 213, 525-534.

Acin-Perez R, Fernandez-Silva P, Peleato ML, Perez-Martos A, Enriquez JA (2008). Respiratory active mitochondrial supercomplexes. Mol Cell 32, 529-539.

Acin-Perez R, Enriquez JA (2014). The function of the respiratory supercomplexes: the plasticity model. Biochim Biophys Acta 1837, 444-450.

AhYoung AP, Jiang J, Zhang J, Khoi Dang X, Loo JA, Zhou ZH, Egea PF (2015). Conserved SMP domains of the ERMES complex bind phospholipids and mediate tether assembly. Proc Natl Acad Sci USA 112, 3179-3188.

Aktas M, Wessel M, Hacker S, Klusener S, Gleichenhagen J, Narberhaus F (2010). Phosphatidylcholine biosynthesis and its significance in bacteria interacting with eukaryotic cells. Eur J Cell Biol 89, 888-894.

Althoff T, Mills DJ, Popot JL, Kuhlbrandt W (2011). Arrangement of electron transport chain components in bovine mitochondrial supercomplex $I_1III_2IV_1$. EMBO J 30, 4652-4664.

Amberg DC, Burke DJ, Strathern JN (2005). Methods in Yeast Genetics. A Cold Spring Harbor Laboratory Course Manual. Cold Spring Harbor Laboratory Press, 201-202.

Armstrong JS (2007). Mitochondrial medicine: pharmacological targeting of mitochondria in disease. Br J Pharmacol 151, 1154-1165

Attard GS, Templer RH, Smith WS, Hunt AN, Jackowski S (2000). Modulation of CTP:phosphocholine cytidylyltransferase by membrane curvature elastic stress. Proc Natl Acad Sci USA 97, 9032-9036.

Baile MG, Sathappa M, Lu YW, Pryce E, Whited K, McCaffery JM, Han X, Alder NN, Claypool SM (2014). Unremodeled and remodeled cardiolipin are functionally indistinguishable in yeast. J Biol Chem 289, 1768-1778.

Baker CD, Basu Ball W, Pryce EN, Gohil VM (2016). Specific requirements of nonbilayer phospholipids in mitochondrial respiratory chain function and formation. Mol Biol Cell 27, 2161-2171.

Baracca A, Chiaradonna F, Sgarbi G, Solaini G, Alberghina L, Lenaz G (2010). Mitochondrial Complex I decrease is responsible for bioenergetic dysfunction in K-

ras transformed cells. Biochim Biophys Acta 1797, 314-323.

Barth PG, Scholte HR, Berden JA, Van der Klei-Van Moorsel JM, Luyt-Houwen IE, Van't Veer-Korthof ET, Van der Harten JJ, Sobotka-Plojhar MA (1983). An X-linked mitochondrial disease affecting cardiac muscle, skeletal muscle and neutrophil leucocytes. J Neurol Sci 62, 327-355.

Bartlett GR (1959). Phosphorus assay in column chromatography. J Biol Chem 234, 466–468.

Bazan S, Mileykovskaya E, Mallampalli VK, Heacock P, Sparagna GC, Dowhan W (2013). Cardiolipin-dependent reconstitution of respiratory supercomplexes from purified *Saccharomyces cerevisiae* complexes III and IV. J Biol Chem 288, 401-411.

Becker T, Horvath SE, Bottinger L, Gebert N, Daum G, Pfanner N (2013). Role of phosphatidylethanolamine in the biogenesis of mitochondrial outer membrane proteins. J Biol Chem 288, 16451-16459.

Beyer K, Klingenberg M (1985). ADP/ATP carrier protein from beef heart mitochondria has high amounts of tightly bound cardiolipin, as revealed by ^{31}P nuclear magnetic resonance. Biochemistry 24, 3821-3826.

Bione S, D'Adamo P, Maestrini E, Gedeon AK, Bolhuis PA, Toniolo D (1996). A novel X-linked gene, G4.5 is responsible for Barth syndrome. Nat Genet 12, 385-389.

Birner R, Bürgermeister M, Schneiter R, Daum G (2001). Roles of phosphatidylethanolamine and of its several biosynthetic pathways in *Saccharomyces cerevisiae*. Mol Biol Cell 12, 997-1007.

Blanchet L, Smeitink JA, van Emst-de Vries SE, Vogels C, Pellegrini M, Jonckheere AI, Rodenburg RJ, Buydens LM, Beyrath J, Willems PH, Koopman WJ (2015). Quantifying small molecule phenotypic effects using mitochondrial morpho-functional fingerprinting and machine learning. Sci Rep 5, 8035-8039.

Blaza JN, Serreli R, Jones AJ, Mohammed K, Hirst J (2014). Kinetic evidence against partitioning of the ubiquinone pool and the catalytic relevance of respiratory-chain supercomplexes. Proc Natl Acad Sci USA 111, 15735-15740.

Bleijerveld OB, Brouwers JF, Vaandrager AB, Helms JB, Houweling M (2007). The CDP-ethanolamine pathway and phosphatidylserine decarboxylation generate different phosphatidylethanolamine molecular species. J Biol Chem 282, 28362-28372.

Bligh EG, Dyer WJ (1959). A rapid method of total lipid extraction and purification. Can J Biochem Physiol 37, 911-917

Bogdanov M, Dowhan W (1995). Phosphatidylethanolamine is required for *in vivo* function of the membrane-associated lactose permease of *Escherichia coli*. J Biol Chem 270, 732-739.

Bogdanov M, Dowhan W (1998). Phospholipid-assisted protein folding: phosphatidylethanolamine is required at a late step of the conformational maturation of the polytopic membrane protein lactose permease. EMBO J 17, 5255-5264.

Bogdanov M, Dowhan W (1999). Lipid-assisted protein folding. J Biol Chem 274, 36827-36830.

Botelho AV, Gibson NJ, Thurmond RL, Wang Y, Brown MF (2002). Conformational energetics of rhodopsin modulated by nonlamellar-forming lipids. Biochemistry 41, 6354-6368.

Bottinger L, Horvath SE, Kleinschroth T, Hunte C, Daum G, Pfanner N, Becker T (2012). Phosphatidylethanolamine and cardiolipin differentially affect the stability of mitochondrial respiratory chain supercomplexes. J Mol Biol 423, 677-686.

Boumann HA, Damen MJ, Versluis C, Heck AJ, de Kruijff B, de Kroon AI (2003). The two biosynthetic routes leading to phosphatidylcholine in yeast produce different sets of molecular species. Evidence for lipid remodeling. Biochemistry 42, 3054-3059.

Boumann HA1, Gubbens J, Koorengevel MC, Oh CS, Martin CE, Heck AJ, Patton-Vogt J, Henry SA, de Kruijff B, de Kroon AI (2006). Depletion of phosphatidylcholine in yeast induces shortening and increased saturation of the lipid acyl chains: evidence for regulation of intrinsic membrane curvature in a eukaryote. Mol Bio Cell 17, 1006-1017

Brandner K, Mick DU, Frazier AE, Taylor RD, Meisinger C, Rehling P (2005). Taz1, an outer mitochondrial membrane protein, affects stability and assembly of inner membrane protein complexes: implications for Barth Syndrome. Mol Biol Cell 16, 5202-5214.

Bürgermeister M[a], Birner-Grunberger R, Nebauer R, Daum G (2004). Contribution of different pathways to the supply of phosphatidylethanolamine and phosphatidylcholine to mitochondrial membranes of the yeast *Saccharomyces cerevisiae*. Biochim Biophys Acta 1686, 161-168.

Bürgermeister M[b], Birner-Grünberger R, Heyn M, Daum G (2004). Contribution of different biosynthetic pathways to species selectivity of aminoglycerophospholipids assembled into mitochondrial membranes of the yeast *Saccharomyces cerevisiae*. Biochim Biophys Acta 1686, 148-160.

Carman GM, Han GS (2011). Regulation of phospholipid synthesis in the yeast *Saccharomyces cerevisiae*. Annu Rev Biochem 80, 859-883.

Chan EY, McQuibban GA (2012). Phosphatidylserine decarboxylase 1 (Psd1) promotes mitochondrial fusion by regulating the biophysical properties of the mitochondrial membrane and alternative topogenesis of mitochondrial genome maintenance protein 1 (Mgm1). J Biol Chem 287, 40131-40139.

Chen S, He Q, Greenberg ML (2008). Loss of tafazzin in yeast leads to increased oxidative stress during respiratory growth. Mol Microbiol 68, 1061-1072.

Chen YC, Taylor EB, Dephoure N, Heo JM, Tonhato A, Papandreou I, Nath N, Denko NC, Gygi SP Rutter J (2012). Identification of a protein mediating respiratory supercomplex stability. Cell Metab 15, 348-360.

Chicco AJ, Sparagna GC (2007). Role of cardiolipin alterations in mitochondrial dysfunction and disease. Am J Physiol Cell Physiol 292, 33-44.

Choi JY, Martin WE, Murphy RC, Voelker DR (2004). Phosphatidylcholine and N-methylated phospholipids are nonessential in *Saccharomyces cerevisiae*. J Biol Chem 279, 42321-42330.

Claypool SM (2009). Cardiolipin, a critical determinant of mitochondrial carrier protein assembly and function. Biochim Biophys Acta 1788, 2059-2068.

Cogliati S, Frezza C, Soriano ME, Varanita T, Quintana-Cabrera R, Corrado M, Cipolat S, Costa V, Casarin A, Gomes LC et al. (2013). Mitochondrial cristae shape determines respiratory chain supercomplexes assembly and respiratory efficiency. Cell 155, 160-171.

Cohen B, DeJong JM (1972). Meclizine and placebo in treating vertigo of vestibular origin. Relative efficacy in a double-blind study. Arch Neurol 27, 129-135.

Connerth M, Tatsuta T, Haag M, Klecker T, Westermann B, Langer T (2012). Intramitochondrial transport of phosphatidic acid in yeast by a lipid transfer protein. Science 338, 815-818.

Daum G (1985). Lipids of mitochondria. Biochim Biophys Acta 822, 1-42.

de Kroon AI, Rijken PJ, De Smet CH (2013). Checks and balances in membrane phospholipid class and acyl chain homeostasis, the yeast perspective. Prog Lipid Res 52, 374-394.

Dirmeier R, O'Brien K, Engle M, Dodd A, Spears E, Poyton RO (2004). Measurement of oxidative stress in cells exposed to hypoxia and other changes in oxygen concentration. Methods Enzymol 381, 589-603.

Distelmaier F, Valsecchi F, Liemburg-Apers DC, Lebiedzinska M, Rodenburg RJ, Heil S, Keijer J, Fransen J, Imamura H, Danhauser K et al. (2015). Mitochondrial dysfunction in primary human fibroblasts triggers an adaptive cell survival program that requires AMPK-alpha. Biochim Biophys Acta 1852, 529-540.

Drose S, Zwicker K, Brandt U (2002). Full recovery of the NADH:ubiquinone activity of complex I (NADH:ubiquinone oxidoreductase) from *Yarrowia lipolytica* by the addition of phospholipids. Biochim Biophys Acta 1556, 65-72.

Dudkina NV, Heinemeyer J, Sunderhaus S, Boekema EJ, Braun HP (2006). Respiratory chain supercomplexes in the plant mitochondrial membrane. Trends Plant Sci 11, 232-240.

Dudkina NV, Kudryashev M, Stahlberg H, Boekema EJ (2011). Interaction of complexes I, III, and IV within the bovine respirasome by single particle cryoelectron tomography. Proc Natl Acad Sci USA 108, 15196-15200.

Dykens JA, Will Y (2007) The significance of mitochondrial toxicity testing in drug development. Drug Discov Today 12, 777-785

Eble KS, Coleman WB, Hantgan RR, Cunningham CC (1990). Tightly associated cardiolipin in the bovine heart mitochondrial ATP synthase as analyzed by ^{31}P nuclear magnetic resonance spectroscopy. J Biol Chem 265, 19434-19440.

Eisenberg T, Abdellatif M, Schroeder S, Primessnig U, Stekovic S, Pendl T, Harger A, Schipke J, Zimmermann A, Schmidt A et al. (2016). Cardioprotection and lifespan extension by the natural polyamine spermidine. Nat Med 22, 1428-1438.

Ejsing CS, Sampaio JL, Surendranath V, Duchoslav E, Ekroos K, Klemm RW, Simons K, Shevchenko, A (2009). Global analysis of the yeast lipidome by quantitative shotgun mass spectrometry. Proc Natl Acad Sci USA 106, 2136-2141.

Elbaz-Alon Y, Rosenfeld-Gur E, Shinder V, Futerman AH, Geiger T, Schuldiner M (2014). A dynamic interface between vacuoles and mitochondria in yeast. Dev Cell 30, 95-102.

Ersoy BA, Tarun A, D'Aquino K, Hancer NJ, Ukomadu C, White MF, Michel T,

Manning BD, Cohen DE (2013). Phosphatidylcholine transfer protein interacts with thioesterase superfamily member 2 to attenuate insulin signaling. Sci Signal 6, 64-67.

Fernández-Murray JP, Ngo MH, McMaster CR (2013). Choline transport activity regulates phosphatidylcholine synthesis through choline transporter Hnm1 stability. J Biol Chem 288, 36106-36115.

Ferreira AK, Meneguelo R, Pereira A, Mendonca Filho O, Chierice GO, Maria DA (2012). Anticancer effects of synthetic phosphoethanolamine on Ehrlich ascites tumor: an experimental study. Anticancer Res 32, 95-104

Folch J, Lees M, Sloane Stanley GH, (1956). A simple method for the isolation and purification of total lipids from animal tissues. J Biol Chem 226, 497-509

Foriel S, Willems P, Smeitink J, Schenck A, Beyrath J (2015). Mitochondrial diseases: Drosophila melanogaster as a model to evaluate potential therapeutics. Int J Biochem Cell Biol 63, 60-65.

Forkink M, Basit F, Teixeira J, Swarts HG, Koopman WJ, Willems PH (2015). Complex I and complex III inhibition specifically increase cytosolic hydrogen peroxide levels without inducing oxidative stress in HEK293 cells. Redox Biol 6, 607-616.

Forkink M, Willems PH, Koopman WJ, Grefte S (2015). Live-cell assessment of mitochondrial reactive oxygen species using dihydroethidine. Methods Mol Biol 1264, 161-169.

Fry M, Green DE (1981). Cardiolipin requirement for electron transfer in complex I and III of the mitochondrial respiratory chain. J Biol Chem 256, 1874-1880.

Fullerton MD, Hakimuddin F, Bonen A, Bakovic M (2009). The development of a metabolic disease phenotype in CTP:phosphoethanolamine cytidylyltransferase-deficient mice. J Biol Chem 284, 25704-25713.

Genova ML, Baracca A, Biondi A, Casalena G, Faccioli M, Falasca AI, Formiggini G, Sgarbi G, Solaini G, Lenaz G (2008). Is supercomplex organization of the respiratory chain required for optimal electron transfer activity? Biochim Biophys Acta 1777, 740-746.

Genova ML, Lenaz G (2014). Functional role of mitochondrial respiratory supercomplexes. Biochim Biophys Acta 1837, 427-443.

Gibellini F, Hunter WN, Smith TK (2009). The ethanolamine branch of the Kennedy pathway is essential in the bloodstream form of *Trypanosoma brucei*. Mol Microbiol 73, 826-843.

Gibellini F, Smith TK (2010). The Kennedy pathway - De novo synthesis of phosphatidylethanolamine and phosphatidylcholine. IUBMB Life 62, 414-428.

Gohil VM, Greenberg ML (2009). Mitochondrial membrane biogenesis: phospholipids and proteins go hand in hand. J Cell Biol 184, 469-472.

Gohil VM, Nilsson R, Belcher-Timme CA, Luo B, Root DE, Mootha VK (2010). Mitochondrial and nuclear genomic responses to loss of LRPPRC expression. J Biol Chem 285, 13742-13747.

Gohil VM, Offner N, Walker JA, Sheth SA, Fossale E, Gusella JF, MacDonald ME, Neri C, Mootha VK (2011). Meclizine is neuroprotective in models of Huntington's disease. Hum Mol Genet 20, 294-300.

Gohil VM, Sheth SA, Nilsson R, Wojtovich AP, Lee JH, Perocchi F, Chen W, Clish CB, Ayata C, Brookes PS, Mootha VK (2010). Nutrient-sensitized screening for drugs that shift energy metabolism from mitochondrial respiration to glycolysis. Nat Biotechnol 28, 249-255.

Gohil VM, Thompson MN, Greenberg ML (2005). Synthetic lethal interaction of the mitochondrial phosphatidylethanolamine and cardiolipin biosynthetic pathways in *Saccharomyces cerevisiae*. J Biol Chem 280, 35410-35416.

Gohil VM, Zhu L, Baker CD, Cracan V, Yaseen A, Jain M, Clish CB, Brookes PS, Bakovic M, Mootha VK (2013). Meclizine inhibits mitochondrial respiration through direct targeting of cytosolic phosphoethanolamine metabolism. J Biol Chem 288, 35387-35395.

Gomez B Jr, Robinson NC (1999). Phospholipase digestion of bound cardiolipin reversibly inactivates bovine cytochrome bc1. Biochemistry 38, 9031-9038.

Gonzalvez F, Gottlieb E (2007). Cardiolipin: setting the beat of apoptosis. Apoptosis 12, 877-885.

Gu Z, Valianpour F, Chen S, Vaz FM, Hakkaart GA, Wanders RJ, Greenberg ML (2004). Aberrant cardiolipin metabolism in the yeast *taz1Δ* mutant: a model for Barth syndrome. Mol Microbiol 51, 149-158.

Guan XL, Wenk MR (2006). Mass spectrometry-based profiling of phospholipids and sphingolipids in extracts from *Saccharomyces cerevisiae*. Yeast 23, 465-477.

Gulshan K, Shahi P, Moye-Rowley WS (2010). Compartment-specific synthesis of phosphatidylethanolamine is required for normal heavy metal resistance. Mol Biol Cell 21, 443-455.

Hanahan D, Weinberg RA (2011). Hallmarks of cancer: the next generation. Cell 144, 646-674.

Henry SA, Kohlwein SD, Carman GM (2012). Metabolism and regulation of glycerolipids in the yeast *Saccharomyces cerevisiae*. Genetics 190, 317-349.

Holthuis JC, Menon AK (2014). Lipid landscapes and pipelines in membrane homeostasis. Nature 510, 48–57.

Horvath SE, Andrea Wagner A, Steyrer E, Daum G (2011). Metabolic link between phosphatidylethanolamine and triacylglycerol metabolism in the yeast *Saccharomyces cerevisiae*. Biochim Biophys Acta 1811, 1030-1037.

Horvath SE, Daum G (2013). Lipids of Mitochondria. Prog Lipid Res 52, 590-614.

Hsu P, Liu X, Zhang J, Wang HG, Ye JM, Shi Y (2015). Cardiolipin remodeling by TAZ/tafazzin is selectively required for the initiation of mitophagy. Autophagy 11, 643-652.

Huang W, Zhang J, Wei P, Schrader, WT, Moore DD (2004). Meclizine is an agonist ligand for mouse constitutive androstane receptor (CAR) and an inverse agonist for human CAR. Mol Endocrinol 18, 2402-2408.

Huss JM, Kelly PD (2005). Mitochondrial energy metabolism in heart failure: a question of balance. J Clin Invest 115, 547-555.

Huttemann M, Pecina P, Rainbolt M, Sanderson TH, Kagan VE, Samavati L, Doan JW, Lee I (2011). The multiple functions of cytochrome c and their regulation in life and death decisions of the mammalian cell: From respiration to apoptosis. Mitochondrion 11, 369-381.

Iannetti EF, Willems PH, Pellegrini M, Beyrath J, Smeitink JA, Blanchet L, Koopman WJ (2015). Toward high-content screening of mitochondrial morphology and membrane potential in living cells. Int J Biochem Cell Biol 63, 66-70.

Ichimura Y, Kirisako T, Takao T, Satomi Y, Shimonishi Y, Ishihara N, Mizushima N, Tanida I, Kominami E, Ohsumi M, Noda T, Ohsumi Y (2000). A ubiquitin-like system mediates protein lipidation. Nature 408, 488-492.

Indiveri C, Tonazzi A, Prezioso G, Palmieri F (1991). Kinetic characterization of the reconstituted carnitine carrier from rat liver mitochondria. Biochim Biophys Acta

1065, 231-238.

Jacobs RL, Zhao Y, Koonen DP, Sletten T, Su B, Lingrell S, Cao G, Peake DA, Kuo MS, Proctor SD et al. (2010). Impaired de novo choline synthesis explains why phosphatidylethanolamine N-methyltransferase-deficient mice are protected from diet-induced obesity. J Biol Chem 285, 22403-22413.

Jacque N, Ronchetti AM, Larrue C, Meunier G, Birsen R, Willems L, Saland E, Decroocq J, Maciel TT et al. (2015). Targeting glutaminolysis has antileukemic activity in acute myeloid leukemia and synergizes with BCL-2 inhibition. Blood 126, 1346-1356.

Janke C, Magiera MM, Rathfelder N, Taxis C, Reber S, Maekawa H, Moreno-Borchart A, Doenges G, Schwob E, Schiebel E et al. (2004). A versatile toolbox for PCR-based tagging of yeast genes: new fluorescent proteins, more markers and promoter substitution cassettes. Yeast 21, 947–962.

Jiang F, Ryan MT, Schlame M, Zhao M, Gu Z, Klingenberg M, Pfanner N, Greenberg ML (2000). Absence of cardiolipin in the crd1 null mutant results in decreased mitochondrial membrane potential and reduced mitochondrial function. J Biol Chem 275, 22387-22394.

Joseph-Horne T, Hollomon DW, Wood PM (2001). Fungal respiration: a fusion of standard and alternative components. Biochim Biophys Acta 1504, 179-195.

Joshi AS, Thompson MN, Fei N, Huttemann M, Greenberg ML (2012). Cardiolipin and mitochondrial phosphatidylethanolamine have overlapping functions in mitochondrial fusion in *Saccharomyces cerevisiae*. J Biol Chem 287, 17589-17597.

Joshi AS, Zhou J, Gohil VM, Chen S, Greenberg ML (2009). Cellular functions of cardiolipin in yeast. Biochim Biophys Acta 1793, 212-218.

Kadenbach B, Mende P, Kolbe HV, Stipani I, Palmieri F (1982). The mitochondrial phosphate carrier has an essential requirement for cardiolipin. FEBS Lett 139, 109-112.

Kagan VE, Tyurin VA, Jiang J, Tyurina YY, Ritov VB, Amoscato AA, Osipov AN, Belikova NA, Kapralov AA, Kini V et al. (2005). Cytochrome c acts as a cardiolipin oxygenase required for release of proapoptotic factors. Nat Chem Biol 1, 223-232.

Kelly RF, Lamont KT, Somers S, Hacking D, Lacerda L, Thomas P, Opie LH, Lecour S (2010). Ethanolamine is a novel STAT-3 dependent cardioprotective agent. Basic Res Cardiol 105, 763-770.

Kennedy EP, Weiss SB (1956). The function of cytidine coenzymes in the biosynthesis

of phospholipides. J Biol Chem 222, 193-214.

Kersten S (2014). Physiological regulation of lipoprotein lipase. Biochim Biophys Acta 1841, 919-933.

Kim K, Kim KH, Storey MK, Voelker DR, Carman GM (1999). Isolation and characterization of the *Saccharomyces cerevisiae* EKI1 gene encoding ethanolamine kinase. J Biol Chem 274, 14857-14866.

Kishi S, Campanholle G, Gohil VM, Perocchi F, Brooks CR, Morizane R, Sabbisetti V, Ichimura T, Mootha VK, Bonventre JV (2015). Meclizine preconditioning protects the kidney against ischemia-reperfusion injury. Ebiomedicine 2, 1090-1101.

Koopman WJ, Willems PH, Smeitink JA (2012). Monogenic mitochondrial disorders. N Engl J Med 366, 1132-1141.

Kornmann B, Currie E, Collins SR, Schuldiner M, Nunnari J, Weissman JS, Walter P (2009). An ER-mitochondria tethering complex revealed by a synthetic biology screen. Science 325, 477-481.

Koshkin V, Greenberg ML (2000). Oxidative phosphorylation in cardiolipin-lacking yeast mitochondria. Biochem J 347, 687-691.

Koshkin V, Greenberg ML (2002). Cardiolipin prevents rate-dependent uncoupling and provides osmotic stability in yeast mitochondria. Biochem J 364, 317-322.

Kramer RM, Deykin D (1983). Arachidonoyl transacylase in human platelets: Coenzyme A-independent transfer of arachidonate from phosphatidylcholine to lysoplasmenylethanolamine. J Biol Chem 258, 13806-13811.

Kubo N, Shirakawa O, Kuno T, Tanaka C (1987). Antimuscarinic effects of antihistamines: quantitative evaluation by receptor-binding assay. Jpn J Pharmacol 43, 277-282.

Kume H, Sasaki H, Kano-Sueoka T (2006). Serum ethanolamine and hepatocyte proliferation in perinatal and partially hepatectomized rats. Life Sci 79, 1764-1772.

Kuroda T, Tani M, Moriguchi A, Tokunaga S, Higuchi T, Kitada S (2011). FMP30 is required for the maintenance of a normal cardiolipin level and mitochondrial morphology in the absence of mitochondrial phosphatidylethanolamine synthesis. Mol Microbiol 80, 284-265.

Lahiri S, Toulmay A, Prinz WA (2015). Membrane contact sites, gateways for lipid homeostasis. Curr Opin Cell Biol 33, 82-87.

Lange C, Nett JH, Trumpower BL, Hunte C (2001). Specific roles of protein-

phospholipid interactions in the yeast cytochrome bc1 complex structure. EMBO J 20, 6591-6600.

Lee JM, Lee YK, Mamrosh JL, Busby SA, Griffin PR, Pathak MC, Ortlund EA, Moore DD (2011). A nuclear-receptor-dependent phosphatidylcholine pathway with antidiabetic effects. Nature 474, 506-510.

Lenaz G, Baracca A, Barbero G, Bergamini C, Dalmonte ME, Del Sole M, Faccioli M, Falasca A, Fato R, Genova ML et al. (2010). Mitochondrial respiratory chain super-complex I-III in physiology and pathology. Biochim Biophys Acta 1797, 633-640.

Letts JA, Fiedorczuk K, Sazanov LA (2016). The architecture of respiratory supercomplexes. Nature 537, 644-648.

Li L, Storm P, Karlsson OP, Berg S, Wieslander A (2003). Irreversible binding and activity control of the 1,2-diacylglycerol 3-glucosyltransferase from Acholeplasma laidlawii at an anionic lipid bilayer surface. Biochemistry 42, 9677-9686.

Liemburg-Apers DC, Schirris TJ, Russel FG, Willems PH, Koopman WJ (2015). Mitoenergetic Dysfunction Triggers a Rapid Compensatory Increase in Steady-State Glucose Flux. Biophys J 109, 1372-1386.

Liemburg-Apers DC, Willems PH, Koopman WJ, Grefte S (2015). Interactions between mitochondrial reactive oxygen species and cellular glucose metabolism. Arch Toxicol 89, 1209-1226.

Lu YW, Claypool SM (2015). Disorders of phospholipid metabolism: an emerging class of mitochondrial disease due to defects in nuclear genes. Front Genet 6, 1-27.

Maheshwari S, Lavigne M, Contet A, Alberge B, Pihan E, Kocken C, Wengelnik K, Douguet D, Vial H, Cerdan R (2013). Biochemical characterization of *Plasmodium falciparum* CTP:phosphoethanolamine cytidylyltransferase shows that only one of the two cytidylyltransferase domains is active. Biochem J 450, 159-167

Manjeri GR, Rodenburg RJ, Blanchet L, Roelofs S, Nijtmans LG, Smeitink JA, Driessen JJ, Koopman WJ, Willems PH (2016). Increased mitochondrial ATP production capacity in brain of healthy mice and a mouse model of isolated complex I deficiency after isoflurane anesthesia. J Inherit Metab Dis 39, 59-65.

Maranzana E, Barbero G, Falasca AI, Lenaz G, Genova ML (2013). Mitochondrial respiratory supercomplex association limits production of reactive oxygen species from complex I. Antioxid Redox Signal 19, 1469-1480.

McKenzie M, Lazarou M, Thorburn DR, Ryan MT (2006). Mitochondrial respiratory chain supercomplexes are destabilized in Barth Syndrome patients. J Mol Biol 361, 462-469.

Meisinger C, Pfanner N, Truscott KN (2006). Isolation of yeast mitochondria. Methods Mol Biol 313, 33–39.

Merkel O, Schmid PC, Paltauf F, Schmid HH (2005). Presence and potential signaling function of N-acylethanolamines and their phospholipid precursors in the yeast *Saccharomyces cerevisiae*. Biochim Biophys Acta 1734, 215–219.

Mileykovskaya E, Dowhan W (2014). Cardiolipin-dependent formation of mitochondrial respiratory supercomplexes. Chem Phys Lipids 179, 42-48.

Modica-Napolitano JS, Renshaw PF (2004). Ethanolamine and phosphoethanolamine inhibit mitochondrial function in vitro: implications for mitochondrial dysfunction hypothesis in depression and bipolar disorder. Biol Psychiatry 55, 273-277.

Moffat J, Grueneberg DA, Yang X, Kim SY, Kloepfer AM, Hinkle G, Piqani B, Eisenhaure TM, Luo B, Grenier JK et al. (2006). A lentiviral RNAi library for human and mouse genes applied to an arrayed viral high-content screen. Cell 124, 1283-1298.

Morein S, Andersson A, Rilfors L, Lindblom G (1996). Wild-type *Escherichia coli* cells regulate the membrane lipid composition in a "window" between gel and non-lamellar structures. J Biol Chem 271, 6801-6809.

Nalecz KA, Bolli R, Wojtczak L, Azzi A (1986). The monocarboxylate carrier from bovine heart mitochondria: partial purification and its substrate-transporting properties in a reconstituted system. Biochim Biophys Acta 851, 29-37.

Nunnari J, Suomalainen A (2012). Mitochondria: in sickness and in health. Cell 148, 1145-1159.

Osman C, Haag M, Potting C, Rodenfels J, Dip PV, Wieland FT, Brugger B, Westermann B, Langer T (2009). The genetic interactome of prohibitins: coordinated control of cardiolipin and phosphatidylethanolamine by conserved regulators in mitochondria. J Cell Biol 184, 583-596.

Osman C, Voelker DR, Langer T (2011). Making heads or tails of phospholipids in mitochondria. J Cell Biol 192, 7-16.

Ozawa T, Tanaka M, Wakabayashi T (1982). Crystallization of mitochondrial cytochrome oxidase. Proc Natl Acad Sci USA 79, 7175-7179.

Paradies G, Paradies V, De Benedictis V, Ruggiero FM, Petrosillo G (2014). Functional role of cardiolipin in mitochondrial bioenergetics. Biochim Biophys Acta 1837, 408-417.

Paradies G, Petrosillo G, Pistolese M, Ruggiero FM (2000). The effect of reactive oxygen species generated from the mitochondrial electron transport chain on the cytochrome c oxidase activity and on the cardiolipin content in bovine heart submitochondrial particles. FEBS Lett 466, 323-326.

Paradies G, Petrosillo G, Pistolese M, Ruggiero FM (2001). Reactive oxygen species generated by the mitochondrial respiratory chain affect the complex III activity via cardiolipin peroxidation in beef-heart submitochondrial particles. Mitochondrion 1, 151-159.

Paradies G, Petrosillo G, Pistolese M, Ruggiero FM (2002). Reactive oxygen species affect mitochondrial electron transport complex I activity through oxidative cardiolipin damage. Gene 286, 135-141.

Pavlovic Z, Bakovic M (2013). Regulation of Phosphatidylethanolamine Homeostasis - The Critical Role of CTP:Phosphoethanolamine Cytidylyltransferase (Pcyt2). Int J Mol Sci 14, 2529-2550

Petrosillo G, Ruggiero FM, Pistolese M, Paradies G (2001). Reactive oxygen species generated from the mitochondrial electron transport chain induce cytochrome c dissociation from beef-heart submitochondrial particles via cardiolipin peroxidation. Possible role in the apoptosis. FEBS Lett 509, 435-438.

Pfeiffer K, Gohil V, Stuart RA, Hunte C, Brandt U, Greenberg ML, Schagger H (2003). Cardiolipin stabilizes respiratory chain supercomplexes. J Biol Chem 278, 52873-52880.

Ren M, Phoon CK, Schlame M (2014). Metabolism and function of mitochondrial cardiolipin. Prog Lipid Res 55, 1-16.

Reznick AZ, Packer L (1994). Oxidative damage to proteins: spectrophotometric method for carbonyl assay. Methods Enzymol 233, 357-363.

Riekhof WR, Voelker DR (2006). Uptake and utilization of lyso-phosphatidylethanolamine by *Saccharomyces cerevisiae*. J Biol Chem 281, 36588–36596.

Rietveld AG, Killian JA, Dowhan W, de Kruijff B (1993). Polymorphic regulation of membrane phospholipid composition in *Escherichia coli*. J Biol Chem 268, 12427-12433.

Roberts LD, Souza AL, Gerszten RE, Clish CB (2012). Targeted Metabolomics. Curr Protoc Mol Biol 30.2, 1-34

Robinson NC (1993). Functional binding of cardiolipin to cytochrome c oxidase. J Bioenerg Biomembr 25, 153-163.

Rockenfeller P, Koska M, Pietrocola F, Minois N, Knittelfelder O, Sica V, Franz J, Carmona-Gutierrez D, Kroemer G, Madeo F (2015). Phosphatidylethanolamine positively regulates autophagy and longevity. Cell Death Differ 22, 499-508.

Sakai H, Kado S, Taketomi A, Sakane F (2014). Diacylglycerol kinase delta phosphorylates phosphatidylcholine-specific phospholipase C-dependent, palmitic acid-containing diacylglycerol species in response to high glucose levels. J Biol Chem 289, 26607-26617.

Sampaio JL, Gerl MJ, Klose C, Ejsing CS, Beug H, Simons K, Shevchenko A (2011). Membrane lipidome of an epithelial cell line. Proc Natl Acad Sci USA 108, 1903-1907.

Santos AX, Riezman H (2012). Yeast as a model system for studying lipid homeostasis and function. FEBS Lett 18, 2858-2867.

Scarpulla RC (2008). Transcriptional paradigms in mammalian mitochondrial biogenesis and function. Physiol Rev 88, 611-638.

Schagger H, Pfeiffer K (2000). Supercomplexes in the respiratory chains of yeast and mammalian mitochondria. EMBO J 19, 1777-1783.

Scharwey M, Tatsuta T, Langer T (2013). Mitochondrial lipid transport at a glance. J Cell Sci 126, 5317-5323.

Schirris TJ, Renkema GH, Ritschel T, Voermans NC, Bilos A, van Engelen BG, Brandt U, Koopman WJ, Beyrath JD, Rodenburg RJ et al. (2015). Statin-induced myopathy is associated with mitochondrial complex III inhibition. Cell Metab 22, 399-407.

Schirris TJ, Ritschel T, Herma Renkema G, Willems PH, Smeitink JA, Russel FG (2015). Mitochondrial ADP/ATP exchange inhibition: a novel off-target mechanism underlying ibipinabant-induced myotoxicity. Sci Rep 5, 14533-14539.

Schlame M (2013). Cardiolipin remodeling and the function of tafazzin. Biochim Biophys Acta 1831, 582-588.

Schlame M, Kelley RI, Feigenbaum A, Towbin JA, Heerdt PM, Schieble T, Wanders RJ, DiMauro S, Blanck TJ (2003). Phospholipid abnormalities in children with Barth syndrome. J Am Coll Cardiol 42, 1994-1999.

Schlame M, Ren M (2006). Barth syndrome, a human disorder of cardiolipin metabolism. FEBS Lett 580, 5450-5455.

Schockel L, Glasauer A, Basit F, Bitschar K, Truong H, Erdmann G, Algire C, Hagebarth A, Willems PH, Kopitz C, Koopman WJ, Heroult M (2015). Targeting mitochondrial complex I using BAY reduces melanoma tumor growth. Cancer Metab 3, 2243-2247.

Schug ZT, Frezza C, Galbraith LC, Gottlieb E (2012). The music of lipids: how lipid composition orchestrates cellular behaviour. Acta Oncol 51, 301-310.

Schuler MH, Di Bartolomeo F, Böttinger L, Horvath SE, Wenz LS, Daum G, Becker T (2015). Phosphatidylcholine affects the role of the sorting and assembly machinery in the biogenesis of mitochondrial β-barrel proteins. J Biol Chem 290, 26523-26532.

Schwarz D, Kisselev P, Pfeil W, Pisch S, Bornscheuer U, Schmid RD (1997). Evidence that nonbilayer phase propensity of the membrane is important for the side chain cleavage activity of cytochrome P450SCC. Biochemistry 36, 14262-14270.

Shaham O, Slate NG, Goldberger O, Xu Q, Ramanathan A, Souza AL, Clish CB, Sims KB, Mootha VK (2010). A plasma signature of human mitochondrial disease revealed through metabolic profiling of spent media from cultured muscle cells. Proc Natl Acad Sci USA 107, 1571-1575.

Sieprath T, Corne TD, Nooteboom M, Grootaert C, Rajkovic A, Buysschaert B, Robijns J, Broers JL, Ramaekers FC, Koopman WJ, Willems PH, De Vos WH (2015). Sustained accumulation of prelamin A and depletion of lamin A/C both cause oxidative stress and mitochondrial dysfunction but induce different cell fates. Nucleus 6, 236-246.

Slater SJ, Kelly MB, Yeager MD, Larkin J, Ho C, Stubbs CD (1996). Polyunsaturation in cell membranes and lipid bilayers and its effects on membrane proteins. Lipids 31, 189-192.

Steenbergen R, Nanowski TS, Beigneux A, Kulinski A, Young SG, Vance JE (2005). Disruption of the phosphatidylserine decarboxylase gene in mice causes embryonic lethality and mitochondrial defects. J Biol Chem 280, 40032-40040.

Storey MK, Clay KL, Kutateladze T, Murphy RC, Overduin M, Voelker DR (2001). Phosphatidylethanolamine has an essential role in *Saccharomyces cerevisiae* that is independent of its ability to form hexagonal phase structures. J Biol Chem 276, 48539-48548.

Strogolova V, Furness A, Robb-McGrath M, Garlich J, Stuart RA (2012). Rcf1 and Rcf2, members of the hypoxia-induced gene 1 protein family, are critical components of the mitochondrial cytochrome bc1-cytochrome c oxidase supercomplex. Mol Cell Biol 32, 1363-1373.

Szendroedi J, Phielix E, Roden M (2011). The role of mitochondria in insulin resistance and type 2 diabetes mellitus. Nat Rev Endocrinol 8, 92-103.

Tamura Y, Sesaki H, Endo T (2014). Phospholipid transport via mitochondria. Traffic 15, 933-945.

Tasseva G, Bai HD, Davidescu M, Haromy A, Michelakis E, Vance JE (2013). Phosphatidylethanolamine deficiency in Mammalian mitochondria impairs oxidative phosphorylation and alters mitochondrial morphology. J Biol Chem 288, 4158-4173.

Tie A, Bakovic, M (2007). Alternative splicing of CTP:phosphoethanolamine cytidylyltransferase produces two isoforms that differ in catalytic properties. J Lipid Res 48, 2172-2181

Toninello A, Dalla Via L, Siliprandi D, Garlid KD (1992). Evidence that spermine, spermidine, and putrescine are transported electrophoretically in mitochondria by a specific polyamine uniporter. J Biol Chem 267, 18393-18397.

Trouillard M, Meunier B, Rappaport F (2011). Questioning the functional relevance of mitochondrial supercomplexes by time-resolved analysis of the respiratory chain. Proc Natl Acad Sci USA 108, 1027-1034.

Tuller G, Hrastnik C, Achleitner G, Schiefthaler U, Klein F, Daum G (1998). YDL142c encodes cardiolipin synthase (Cls1p) and is non-essential for aerobic growth of *Saccharomyces cerevisiae*. FEBS Lett 421, 15-18.

Tuller G, Nemec T, Hrastnik C, Daum G (1999). Lipid composition of subcellular membranes of an FY1679-derived haploid yeast wild-type strain grown on different carbon sources. Yeast 15, 1555-1564.

Tyurina YY, Lou W, Qu F, Tyurin VA, Mohammadyani D, Liu J, Huttemann M, Frasso MA, Wipf P, Bayir H, Greenberg ML, Kagan VE (2017). Lipidomics Characterization of Biosynthetic and Remodeling Pathways of Cardiolipins in Genetically and Nutritionally Manipulated Yeast Cells. ACS Chem Biol 12, 265-281.

Vafai SB, Mootha VK (2012). Mitochondrial disorders as windows into an ancient organelle. Nature 491, 374-383.

Valianpour F, Mitsakos V, Schlemmer D, Towbin JA, Taylor JM, Ekert PG, Thorburn DR, Munnich A, Wanders RJ, Barth PG et al. (2005). Monolysocardiolipins accumulate in Barth syndrome but do not lead to enhanced apoptosis. J Lipid Res 46, 1182-1195.

van den Brink-van der Laan E, Killian JA, de Kruijff B (2004). Nonbilayer lipids affect peripheral and integral membrane proteins via changes in the lateral pressure profile. Biochim Biophys Acta 1666, 275-288.

van der Does C, Swaving J, van Klompenburg W, Driessen AJ (2000). Non-bilayer lipids stimulate the activity of the reconstituted bacterial protein translocase. J Biol Chem 275, 2472-2478.

van der Veen JN, Lingrell S, da Silva RP, Jacobs RL, Vance DE (2014). The concentration of phosphatidylethanolamine in mitochondria can modulate ATP production and glucose metabolism in mice. Diabetes 63, 2620-2630.

van Meer G, Voelker DR, Feigenson GW (2008). Membrane lipids: where they are and how they behave. Nat Rev Mol Cell Biol 9, 112-124.

Van Rhijn I, van Berlo T, Hilmenyuk T, Cheng TY, Wolf BJ, Tatituri RV, Uldrich AP, Napolitani G, Cerundolo V, Altman JD et al. (2016). Human autoreactive T cells recognize CD1b and phospholipids. Proc Natl Acad Sci USA 113, 380-385.

Vance DE, Vance JE (2009). Physiological consequences of disruption of mammalian phospholipid biosynthetic genes. J Lipid Res 50, 132-137.

Vance JE (2008). Phosphatidylserine and phosphatidylethanolamine in mammalian cells: two metabolically related aminophospholipids. J Lipid Res 49, 1377-1387.

Vance JE (2015). Phospholipid synthesis and transport in mammalian cells. Traffic 16, 1-18.

Verkleij AJ, Leunissen-Bijvelt J, de Kruijff B, Hope M, Cullis PR (1984). Non-bilayer structures in membrane fusion. Ciba Found Symp 103, 45-59.

Vreken P, Valianpour F, Nijtmans LG, Grivell LA, Plecko B, Wanders RJ, Barth PG (2000). Defective remodeling of cardiolipin and phosphatidylglycerol in Barth syndrome. Biochem Biophys Res Commun 279, 378-382.

Vukotic M, Oeljeklaus S, Wiese S, Vögtle FN, Meisinger C, Meyer HE, Zieseniss A, Katschinski DM, Jans DC, Jakobs S et al. (2012). Rcf1 mediates cytochrome oxidase assembly and respirasome formation, revealing heterogeneity of the enzyme complex. Cell Metab 15, 336-347.

Wallace DC (2012). Mitochondria and cancer. Nat Rev Cancer 12, 685-698.

Walters AM, Porter GA Jr., Brookes PS (2012). Mitochondria as a drug target in ischemic heart disease and cardiomyopathy. Circ Res 111, 1222-1236.

Wang G, McCain ML, Yang L, He A, Pasqualini FS, Agarwal A, Yuan H, Jiang D, Zhang D, Zangi L et al. (2014). Modeling the mitochondrial cardiomyopathy of Barth syndrome with induced pluripotent stem cell and heart-on-chip technologies. Nat Med 20, 616-623.

Wang S, Zhang S, Liou LC, Ren Q, Zhang Z, Caldwell GA, Caldwell KA, Witt SN (2014). Phosphatidylethanolamine deficiency disrupts α-synuclein homeostasis in yeast and worm models of Parkinson disease. Proc Natl Acad Sci USA 111, 3976-3985.

Wang Z, Lee B, Pearce D, Qian S, Wang Y, Zhang Q, Chow MSS (2012). Meclizine Metabolism and pharmacokinetics: formulation on its absorption. J Clin Pharmacol 52, 1343-1349

Watanabe Y, Tamura Y, Kawano S, Endo T (2015). Structural and mechanistic insights into phospholipid transfer by Ups1-Mdm35 in mitochondria. Nat Commun 6, 7922-7926.

Watkins SM, German JB (2002). Metabolomics and biochemical profiling in drug discovery and development. Curr Opin Mol Ther 4, 224-228.

Webhofer C, Gormanns P, Tolstikov V, Zieglgansberger W, Sillaber I, Holsboer F, Turck CW (2011). Metabolite profiling of antidepressant drug action reveals novel drug targets beyond monoamine elevation. Transl Psychiatry 1, 58-61.

Weinberg SE, Chandel NS (2015). Targeting mitochondria metabolism for cancer therapy. Nat Chem Biol 11, 9-15.

Weiss WA, Taylor SS, Shokat KM (2007). Recognizing and exploiting differences between RNAi and small-molecule inhibitors. Nat Chem Biol 3, 739-744.

Wenz T, Hielscher R, Hellwig P, Schägger H, Richers S, Hunte C (2009). Role of phospholipids in respiratory cytochrome bc(1) complex catalysis and supercomplex formation. Biochim Biophys Acta 1787, 609-616.

Will Y, Hynes J, Ogurtsov VI, Papkovsky DB (2006). Analysis of mitochondrial function using phosphorescent oxygen-sensitive probes. Nat Protoc 1, 2563-2572.

Willems PH, Rossignol R, Dieteren CE, Murphy MP, Koopman WJ (2015). Redox Homeostasis and Mitochondrial Dynamics. Cell Metab 22, 207-218.

Wittig I, Braun HP, Schagger H (2006). Blue native PAGE. Nat Protoc 1, 418–428.

Wittig I, Karas M, Schagger H (2007). High resolution clear native electrophoresis for in-gel functional assays and fluorescence studies of membrane protein complexes. Mol Cell Proteomics 6, 1215–1225.

Wu M, Gu J, Guo R, Huang Y, Yang M (2016). Structure of Mammalian Respiratory Supercomplex $I_1III_2IV_1$. Cell 167, 1598-1609.

Xu Y, Kelley RI, Blanck TJ, Schlame M (2003). Remodeling of cardiolipin by phospholipid transacylation. J Biol Chem 278, 51380-51385.

Xu Y, Malhotra A, Ren M, Schlame M (2006). The enzymatic function of tafazzin. J Biol Chem 281, 39217-39224.

Xu Y, Phoon CK, Berno B, D'Souza K, Hoedt E, Zhang G, Neubert TA, Epand RM, Ren M, Schlame M (2016). Loss of protein association causes cardiolipin degradation in Barth syndrome. Nat Chem Biol 12, 641-647.

Ye C, Lou W, Li Y, Chatzispyrou IA, Huttemann M, Lee I, Houtkooper RH, Vaz FM, Chen S, Greenberg ML (2014). Deletion of the cardiolipin-specific phospholipase Cld1 rescues growth and life span defects in the tafazzin mutant: implications for Barth syndrome. J Biol Chem 289, 3114-3125.

Yetukuri L, Ekroos K, Vidal-Puig A, Oresic, M (2008). Informatics and computational strategies for the study of lipids. Mol Biosyst 4, 121-127.

Zhang M, Mileykovskaya E, Dowhan W (2002). Gluing the respiratory chain together: Cardiolipin is required for supercomplex formation in the inner mitochondrial membrane. J Biol Chem 277, 43553–43556.

Zhong Q, Gohil VM, Ma L, Greenberg ML (2004). Absence of cardiolipin results in temperature sensitivity, respiratory defects, and mitochondrial DNA instability independent of pet56. J Biol Chem 279, 32294-32300.

Zhu L, Johnson C, Bakovic M (2008). Stimulation of the human CTP:phosphoethanolamine cytidylyltransferase gene by early growth response protein 1. J Lipid Res 49, 2197-2211.

Ziboh VA, Lord JT (1979). Phospholipase A activity in the skin: Modulators of arachidonic acid release from phosphatidylcholine. Biochem J 184, 283-290.

Zinser E, Sperka-Gottlieb CD, Fasch EV, Kohlwein SD, Paltauf F, Daum G (1991). Phospholipid synthesis and lipid composition of subcellular membranes in the unicellular eukaryote *Saccharomyces cerevisiae*. J Bacteriol 173, 2026-2034.

APPENDIX A

ETHANOLAMINE-MEDIATED RESCUE OF CL DEPLETED CELLS

I showed that Etn supplementation rescues the mitochondrial defects observed in CL depleted cells independent of its incorporation into PE. The mechanism underlying Etn-mediated rescue remains elusive. One possible candidate that contains the Etn moiety is N-acyl phosphatidylethanolamine (NAPE). NAPE is formed by acylation of PE and is and proposed to have a cytoprotective effects in yeast cells (Merkel et al., 2005). Two enzymes believed to be required for NAPE metabolism are Fmp30, a phospholipase D, and Amd2, a putative amidase. In order to determine if these enzymes were involved in the Etn-mediated rescue of CL depleted cells, I constructed the double knockouts *taz1Δamd2Δ* and *taz1Δfmp30Δ* and tested for a rescue of growth with Etn supplementation. These strains were both rescued by Etn, suggesting that NAPE is not required for Etn-mediated rescue (Fig. A-1).

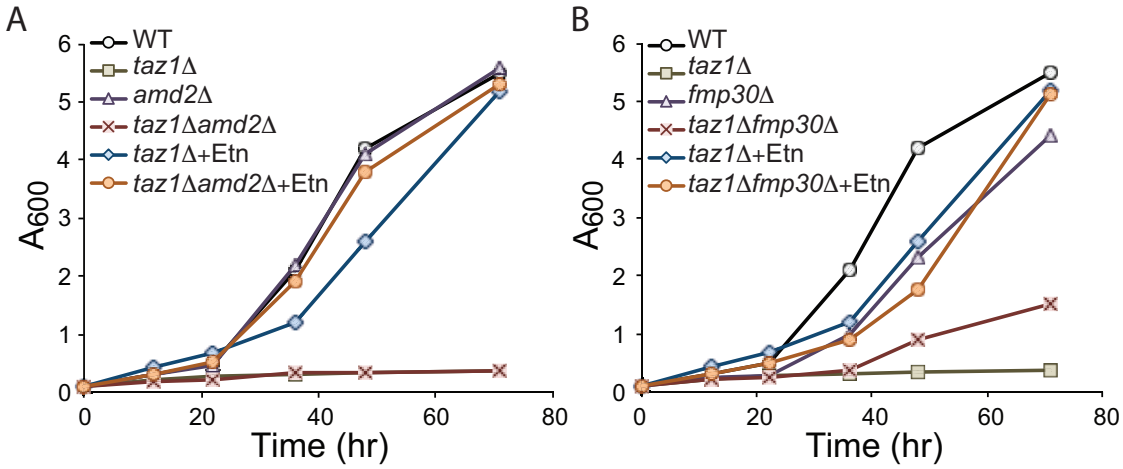

Figure A-1 Amd2 and Fmp30 are not required for the Etn-mediated rescue of CL deficiency.

(A) The growth of WT, *taz1Δ*, *amd2Δ*, *taz1Δamd2Δ* and (B) *taz1Δ*, *fmp30Δ*, *taz1Δfmp30Δ* cells at 37°C in SC ethanol and SC ethanol + 2 mM Etn media was monitored by measuring absorbance at 600 nm. Data are representative of at least two independent measurements.

The polyamine spermidine is an abundant cellular metabolite that contains amine groups (Fig. A-2A). The biosynthetic enzyme responsible for synthesizing spermidine in yeast is Spe3. In order to determine if Etn mediated its rescue by incorporation into spermidine via Spe3, I monitored the ability of Etn to rescue of *taz1Δspe3Δ* cells. Etn rescued the growth of these cells, suggesting that Spe3 does not mediate the rescue of CL deficient cells (Fig. A-2B). Interestingly, spermidine has been shown to be imported into the mitochondria (Toninello et al., 1992) and has been found to enhance mitophagy and mitochondrial respiration (Eisenberg et al., 2016). I examined the ability of spermidine to rescue CL deficient cells and found that this polyamine rescued respiratory growth similar to Etn (Fig. A-2C). It is possible that these amine-containing molecules utilize the same underlying mechanism to mediate the rescue of CL deficiency.

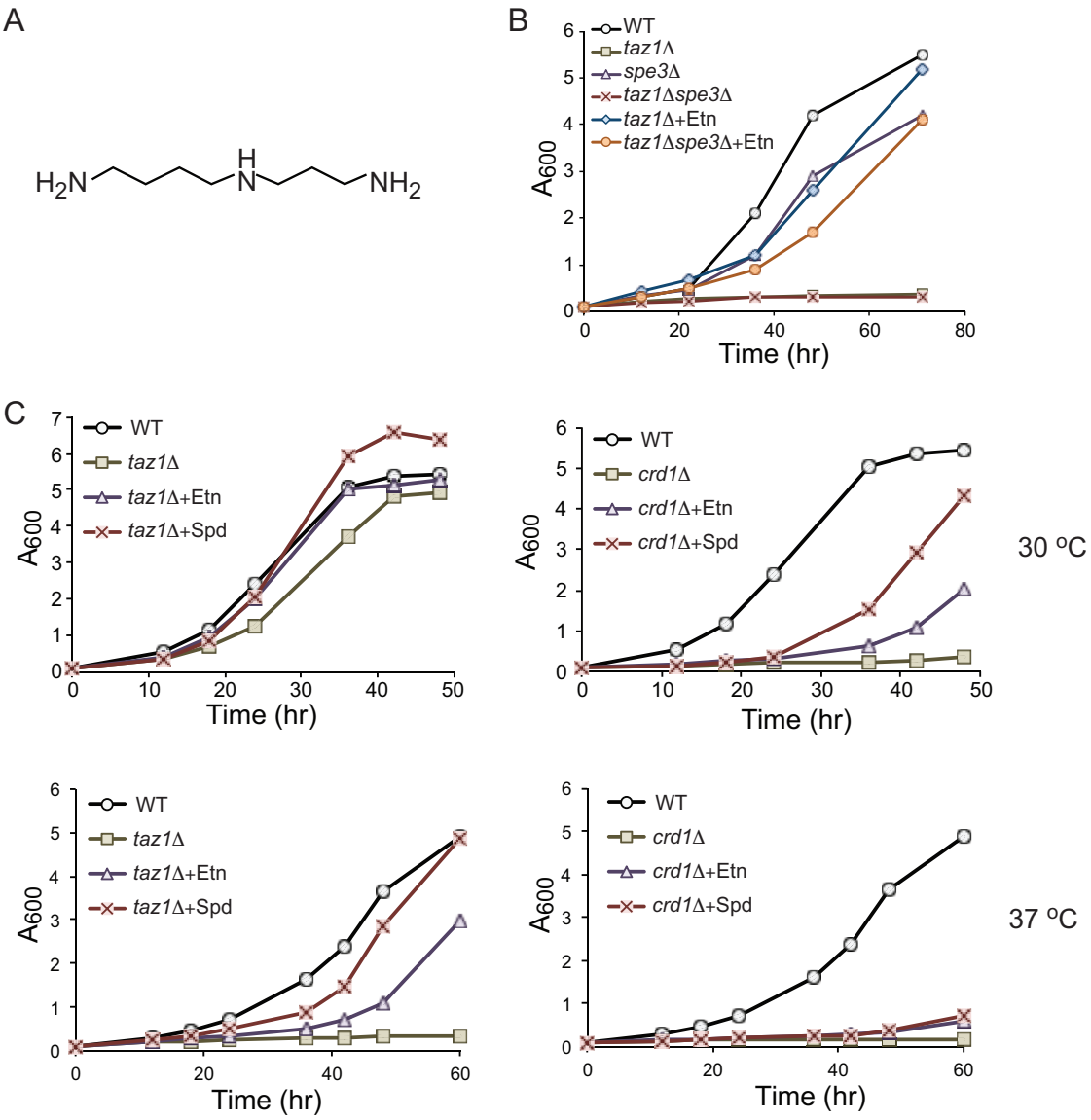

Figure A-2 Spermidine rescues the growth of CL deficient cells.

(A) The molecular structure of spermidine. (B) The growth of WT, *taz1Δ*, *spe3Δ*, *taz1Δspe3Δ* cells cultured at 37°C in SC ethanol and SC ethanol + 2 mM Etn media was monitored by measuring absorbance at 600 nm. Data are representative of at least two independent measurements. (C) The growth of WT, *taz1Δ*, and *crd1Δ* cells cultured at 30°C (upper panel) and 37°C (lower panel) in SC ethanol, SC ethanol + 2 mM Etn and SC ethanol + 2 mM spermidine (Spd) media was monitored by measuring absorbance at 600 nm. Data are representative of at least three independent measurements.

APPENDIX B

MECLIZINE-MEDIATED RESPIRATORY INHIBITION IN *SACCHAROMYCES CEREVISIAE*

I showed that meclizine inhibits respiratory growth in *S. cerevisiae*, suggesting that attenuation of respiration by meclizine is conserved from mammals to yeast. Meclizine inhibited the growth of yeast cells in non-fermentable, synthetic lactate medium, without affecting growth in glucose-containing medium (Fig. B-1A). Interestingly, stimulation of the Kennedy pathway by Etn supplementation further enhanced the growth defect (Fig. B-1A), suggesting that the effect of meclizine on mitochondrial energy metabolism is mediated by phosphoethanolamine build-up due to the inhibition of the Etn branch of the Kennedy pathway. Similar to our observations in *PCYT2* knockdown cells, we found that *ect1Δ* cells do not phenocopy the effect of meclizine on respiratory growth (Fig. B-1B), suggesting that meclizine may attenuate MRC function independent of PEtn build-up.

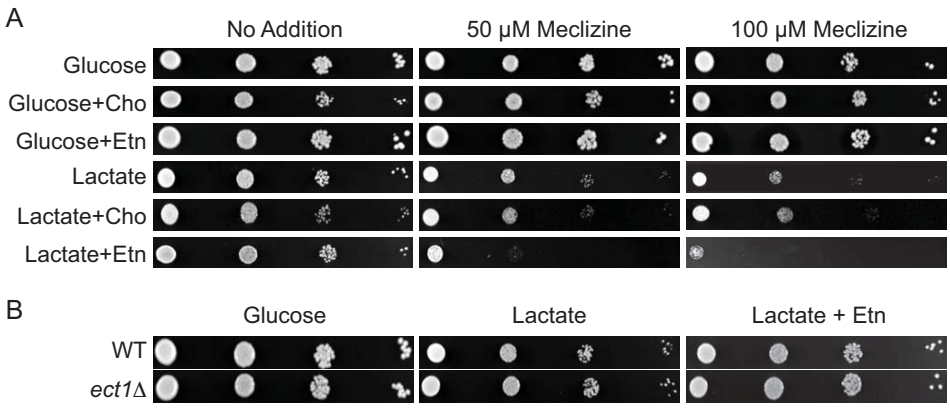

Figure B-1 Meclizine-mediated respiratory inhibition is conserved in yeast.
(A) Growth of *S. cerevisiae* in the presence of indicated dose of meclizine, 5 mM choline (Cho) and 5 mM ethanolamine (Etn) was monitored for 4 days before the images were captured. (B) Growth of *Ect1Δ* cells in the indicated media was monitored for 4 days.